J. Mech. Phys. Solids 166 (2022) 104930

Contents lists available at ScienceDirect

Journal of the Mechanics and Physics of Solids

journal homepage: www.elsevier.com/locate/jmps

Elastomers filled with liquid inclusions: Theory, numerical implementation, and some basic results

Kamalendu Ghosh [a], Oscar Lopez-Pamies [a,b,*]

[a] Department of Civil and Environmental Engineering, University of Illinois, Urbana–Champaign, IL 61801, USA
[b] Département de Mécanique, École Polytechnique, 91128 Palaiseau, France

ARTICLE INFO

Keywords:
Elastomers
Fillers
Finite deformation
Homogenization
Size effects

ABSTRACT

Experimental and theoretical results of late have pointed to elastomers filled with various types of liquid inclusions as a promising new class of materials with unprecedented properties. Motivated by these findings, the first of two objectives of this paper is to formulate the homogenization problem that describes the macroscopic mechanical response of elastomers filled with liquid inclusions under finite quasistatic deformations. The focus is on the non-dissipative case when the elastomer is a hyperelastic solid, the liquid making up the inclusions is a hyperelastic fluid, the interfaces separating the solid elastomer from the liquid inclusions feature their own hyperelastic behavior (which includes surface tension as a special case), and the inclusions are initially spherical in shape. The macroscopic behavior of such filled elastomers turns out to be that of a hyperelastic solid, albeit one that depends directly on the size of the inclusions and the constitutive behavior of the interfaces. It is hence characterized by an effective stored-energy function $\overline{W}(\overline{\mathbf{F}})$ of the macroscopic deformation gradient $\overline{\mathbf{F}}$. Strikingly, in spite of the fact that there are local residual stresses within the inclusions (due to the presence of initial interfacial forces), the resulting macroscopic behavior is free of residual stresses, that is, $\partial\overline{W}(\mathbf{I})/\partial\overline{\mathbf{F}} = \mathbf{0}$. What is more, in spite of the fact that the local moduli of elasticity in the bulk and the interfaces in the small-deformation limit do not possess minor symmetries (due to the presence of residual stresses and initial interfacial forces), the resulting effective modulus of elasticity does possess the standard minor symmetries, that is, $\overline{L}_{ijkl} = \overline{L}_{jikl} = \overline{L}_{ijlk}$, where $\overline{L}_{ijkl} := \partial^2\overline{W}(\mathbf{I})/\partial\overline{F}_{ij}\partial\overline{F}_{kl}$. The second objective of this paper is to implement and deploy a finite-element scheme to numerically generate solutions for the macroscopic response of a basic class of elastomers filled with liquid inclusions, that of isotropic suspensions of incompressible liquid inclusions of monodisperse size embedded in incompressible Neo-Hookean elastomers wherein the interfaces feature a constant surface tension. With guidance from the numerical solutions, the last part of this paper is devoted to proposing a simple explicit approximation for the effective stored-energy function $\overline{W}(\overline{\mathbf{F}})$.

1. Introduction

Over the past few years, a series of experimental and theoretical investigations have pointed to elastomers filled with liquid inclusions – ranging from ionic liquids, to liquid metals, to ferrofluids – as a promising new class of materials with unique combinations of mechanical and physical properties; see, e.g., the works of Lopez-Pamies (2014), Style et al. (2015a), Bartlett et al. (2017), Lefèvre et al. (2017), and Yun et al. (2019). The reason behind such novel properties is twofold.

* Corresponding author at: Department of Civil and Environmental Engineering, University of Illinois, Urbana–Champaign, IL 61801, USA.
E-mail addresses: kg5@illinois.edu (K. Ghosh), pamies@illinois.edu (O. Lopez-Pamies).

https://doi.org/10.1016/j.jmps.2022.104930
Received 28 January 2022; Received in revised form 8 May 2022; Accepted 8 May 2022
Available online 16 May 2022

On one hand, the addition of liquid inclusions to elastomers increases the overall deformability. This is in contrast to the addition of conventional fillers, which, being typically made of stiff solids, decreases deformability. Magnetorheological elastomers (MREs) are a class of materials that distinctly exemplifies this dichotomy. For instance, while MREs filled with iron particles are able to undergo very modest deformations even when subjected to large magnetic fields, MREs filled with ferrofluid inclusions are able to undergo significant deformations when subjected to modest magnetic fields thanks to the increased deformability afforded by the ferrofluid inclusions compared to that of iron particles (Lefèvre et al., 2017).

On the other hand, the mechanics and physics of the interfaces separating a solid elastomer from embedded liquid inclusions, while negligible when the inclusions are "large", may have a significant and even dominant impact on the macroscopic response of the material when the inclusions are "small". The experiments of Style et al. (2015a) on silicone elastomers filled with glycerol droplets provide a beautiful example of this size-dependent phenomenon. These authors showed – via indentation experiments with a cylindrical indenter – that the addition of glycerol droplets of approximately monodisperse radius $A \approx 1$ μm to a silicone elastomer with initial shear modulus $\mu_{\rm m} = 33$ kPa led to a macroscopic response of the resulting composite material that was *softer* than that of the silicone elastomer itself. By contrast, the same addition of droplets to a softer silicone elastomer with initial shear modulus $\mu_{\rm m} = 1$ kPa led to a macroscopic response that was *stiffer* than that of the elastomer without inclusions. Given that Style et al. (2015a) estimated the initial surface tension $\widehat{\gamma}_0 = 0.014$ N/m at the silicone/glycerol interfaces to be approximately the same for both types of filled elastomers, the drastically different macroscopic responses can be explained qualitatively as follows. The interface stiffness $\widehat{\gamma}_0/2A \approx 7$ kPa is significantly smaller than the bulk stiffness $\mu_{\rm m} = 33$ kPa of the stiffer elastomer, but larger than the bulk stiffness $\mu_{\rm m} = 1$ kPa of the softer one. As a result, the inclusions embedded in the stiffer silicone elastomer pose little resistance to deformation and hence lead to the softening of the macroscopic response. By contrast, the inclusions embedded in the softer silicone elastomer pose significant resistance to deformation, behave effectively as stiff inclusions, and hence lead to the stiffening of the macroscopic response. This type of competition between interface and bulk stiffnesses is commonly referred to as elasto-capillarity; see, e.g., Andreotti et al. (2016), Bico et al. (2018), and references therein.

In this paper, we strive to gain insight into the above-outlined phenomena by constructing a general framework, alongside some basic results, that describes the macroscopic mechanical behavior of elastomers filled with liquid inclusions directly in terms of their microscopic behavior.

We begin in Section 2 by formulating the homogenization problem that describes the macroscopic mechanical response of such filled elastomers under finite quasistatic deformations. The focus is on the non-dissipative case when the elastomer is a hyperelastic solid, the liquid making up the inclusions is a hyperelastic fluid, the interfaces separating the solid elastomer from the liquid inclusions feature their own hyperelastic behavior, which may possibly include the presence of initial interfacial forces such as surface tension, and the inclusions are initially spherical in shape. For clarity of presentation, prior to the formulation of the homogenization problem *per se* in Section 2.6, we devote Sections 2.1 through 2.3 to spelling out separately the relevant ingredients of:

- bulk and interface kinematics,
- bulk, surface, and interface forces, and
- bulk and interface hyperelastic constitutive behaviors.

The combination of these ingredients leads to the governing equations at large – not just those of homogenization – for elastomers filled with liquid inclusions undergoing finite quasistatic deformations. These equations are presented in Section 2.4. In Section Section 2.5, we discuss the key roles that the residual stresses in the bulk resulting from the presence of initial interfacial forces (in particular, an initial surface tension) as well as the initial shape of the inclusions play in the formulation. All the material in Sections 2.1–2.5 follows in the footstep of the pioneering work of Gurtin and Murdoch (1975a,b) on elastic material surfaces.

We proceed in Section 3 by presenting the specialization of the general homogenization problem formulated in Section 2 to the limit of small deformations, where some analytical treatment is possible. There, in Remark 15, we also introduce a number of explicit solutions for special classes of microstructures. In Section 4, we present a finite-element (FE) scheme to solve numerically the homogenization problem at finite deformations. We deploy the scheme in Sections 5 and 6 to generate solutions for a basic class of elastomers filled with liquid inclusions, that of isotropic suspensions of incompressible liquid inclusions of identical or monodisperse size embedded in incompressible Neo-Hookean elastomers wherein the interfaces feature a constant surface tension. The results in Section 5 pertain to suspensions with a dilute volume fraction $c \searrow 0$ of inclusions, while Section 6 presents results for suspensions with finite volume fractions in the range $c \in [0, 0.25]$. Both sections include comparisons with the experiments of Style et al. (2015a) whenever possible. They include as well a simple explicit approximation of the numerical solutions. We conclude in Section 7 by summarizing the main contributions of this work and by recording a number of final comments.

At the close of this introduction, it is fitting to make explicit mention of a number of related investigations on the macroscopic manifestation of interfaces on the mechanics of heterogeneous materials at large. This has been an active research topic for decades now, albeit one that has been mostly focused on solid–solid – as opposed to solid–liquid – interfaces and on asymptotically small – as opposed to finite – deformations.

Among the first related works in the context of asymptotically small deformations, Sharma et al. (2003), Sharma and Ganti (2004), and Duan et al. (2005a) revisited the fundamental Eshelby matrix/single-inclusion problem and accounted for an interface that features its own elasticity, this in the absence of surface tension. Duan et al. (2005b) exploited their generalized Eshelby analysis to formally define the effective modulus of elasticity of particulate composites with elastic matrix/inclusions interfaces. Their definition applies strictly to material systems wherein, again, there is no surface tension at the interfaces and hence no residual stresses in the bulk. Later, motivated by the experiments of Style et al. (2015a,b) worked out the solution for the Eshelby problem

incorporating now the presence of an initial surface tension at the matrix/inclusion interface. In an effort to consider the finite volume fraction of inclusions in the experiments of Style et al. (2015a), Mancarella et al. (2016) generalized the classical solution of Christensen and Lo (1979) to also account for the presence of an interfacial surface tension. Both of these solutions apply strictly to the case when the inclusions are made of an incompressible liquid and their initial shape is spherical, which imply a hydrostatic residual stress within the inclusions. Recently, Krichen et al. (2019) have presented a more general analysis of the macroscopic response of particulate composites containing initially spherical inclusions with interfaces that feature their own elasticity as well as an initial surface tension.

In the context of finite deformations, we are aware of only two related works, those of Wang and Henann (2016) and Zafar and Basu (2022). The former considers the problem of a unit cell, comprised of a nearly incompressible Neo-Hookean matrix embedding either one or two monodisperse spherical cavities whose boundaries are endowed with tangential and normal tractions that model the presence of a constant surface tension and the effect of a pressurized liquid, subjected to periodic boundary conditions with a prescribed average deformation gradient. The latter considers an analogous unit-cell problem in 2D with circular cavities whose boundaries feature tangential tractions that model the presence of a constant surface tension as well as interfacial elasticity. Both works present FE solutions for such problems and appear to identify the average of the stress in the bulk as the macroscopic measure of stress. Section 2.6 below deals in depth with this topic and shows that the macroscopic measure of stress for elastomers filled with liquid inclusions is actually more involved, as it contains contributions from the averages of the bulk stresses as well as from the interface stresses.

2. The problem

2.1. Initial configuration and kinematics

Consider a body made of M liquid inclusions fully embedded in an elastomeric matrix that in its initial configuration occupies the open domain[1] $\Omega_0 \subset \mathbb{R}^3$, with boundary $\partial\Omega_0$ and outward unit normal $\mathbf{N}$. Denote by $\Omega_0^{\mathtt{m}}$ the subdomain occupied by the matrix and by $\Omega_0^{\mathtt{i},j}$ $j = 1, 2, \dots, M$ that occupied by the jth inclusion. The inclusions are separated from the matrix by smooth interfaces, denoted by Γ_0^j for the jth inclusion, with unit normal $\widehat{\mathbf{N}}$ pointing outwards from the inclusions towards the matrix, so that $\Omega_0 = \Omega_0^{\mathtt{m}} \bigcup \Gamma_0 \bigcup \Omega_0^{\mathtt{i}}$, where $\Gamma_0 = \bigcup_{j=1}^M \Gamma_0^j$ and $\Omega_0^{\mathtt{i}} = \bigcup_{j=1}^M \Omega_0^{\mathtt{i},j}$. We identify material points in the body by their initial position vector

$$\mathbf{X} \in \Omega_0$$

and denote by $\theta_0^{\mathtt{i},j}(\mathbf{X})$ and $\theta_0^{\mathtt{i}}(\mathbf{X})$ the characteristic or indicator functions describing the individual and collective spatial locations occupied by the inclusions in Ω_0, that is,

$$\theta_0^{\mathtt{i},j}(\mathbf{X}) = \begin{cases} 1 & \text{if } \mathbf{X} \in \Omega_0^{\mathtt{i},j} \\ 0 & \text{otherwise} \end{cases} \qquad j = 1, 2, \dots, M \qquad \text{and} \qquad \theta_0^{\mathtt{i}}(\mathbf{X}) = \sum_{j=1}^{M} \theta_0^{\mathtt{i},j}(\mathbf{X}). \tag{1}$$

As will become apparent below, it is convenient to single out the material points on the interfaces with their own labeling. We write

$$\widehat{\mathbf{X}} = \mathbf{X} \quad \text{when} \quad \mathbf{X} \in \Gamma_0.$$

Fig. 1(a) shows a schematic of the body in its initial configuration with all the pertinent geometric quantities depicted.

In response to the body, surface, and interfacial forces to be described below, the position vector $\mathbf{X}$ of a material point may occupy a new position $\mathbf{x}$ specified by a continuous,[2] invertible, orientation-preserving mapping $\mathbf{y}$ from Ω_0 to the current configuration $\Omega = \Omega^{\mathtt{m}} \bigcup \Gamma \bigcup \Omega^{\mathtt{i}} \subset \mathbb{R}^3$, where, in direct analogy with their initial counterparts, $\Omega^{\mathtt{m}}$, $\Omega^{\mathtt{i}}$, and Γ denote the subdomains occupied by the matrix and the inclusions and the interfaces separating them; by the same token, the notation $\hat{\mathbf{n}}$, $\theta^{\mathtt{i},j}$, and $\theta^{\mathtt{i}}$ is used to denote the counterparts of $\widehat{\mathbf{N}}$, $\theta_0^{\mathtt{i},j}$, and $\theta_0^{\mathtt{i}}$ in the current configuration. We write

$$\mathbf{x} = \mathbf{y}(\mathbf{X}).$$

Singling out again the material points on the interfaces with their own labeling, we also write

$$\hat{\mathbf{x}} = \mathbf{y}(\widehat{\mathbf{X}}).$$

We denote the deformation gradient at $\mathbf{X} \in \Omega_0$ by

$$\mathbf{F}(\mathbf{X}) = \nabla \mathbf{y}(\mathbf{X}) = \frac{\partial \mathbf{y}}{\partial \mathbf{X}}(\mathbf{X})$$

[1] For notational simplicity, we present the problem in the setting of $n = 3$ space dimensions. However, as elaborated in the companion paper (Ghosh et al., 2022), the problem in $n \geq 2$ space dimensions is not fundamentally different and the pertinent formulation can be inferred form the formulation presented here.

[2] The assumption of continuity at Γ corresponds physically to a no-slip condition at the matrix/inclusions interfaces. The fact that we also assume continuity of deformation in $\Omega_0^{\mathtt{i}}$ is inconsequential from a physical point of view while, at the same time, is convenient from a mathematical one. This is because the focus of this work in on quasi-static deformations and for those the only aspect that matters within the inclusions is their pressure, which only depends on the volumetric part of their deformation.

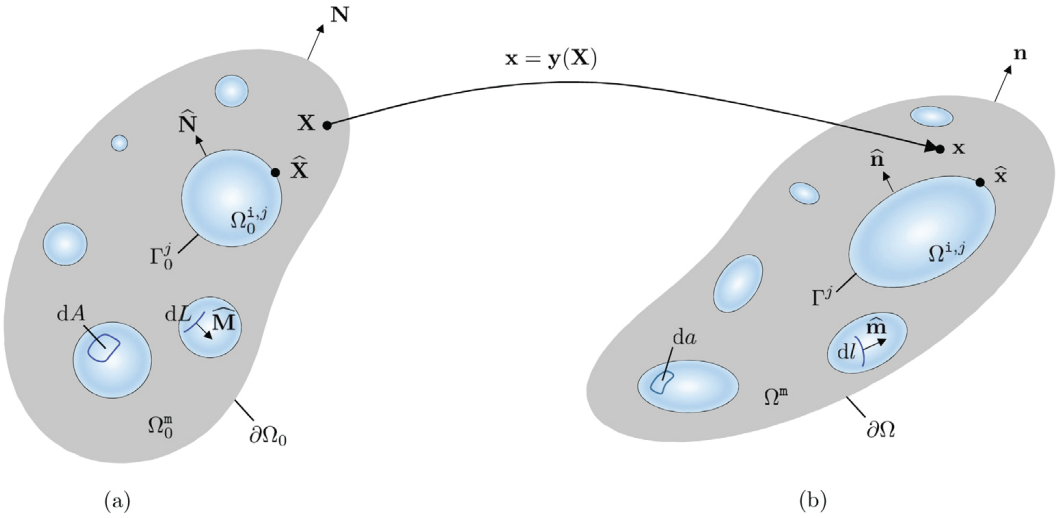

Fig. 1. Schematics of (a) the initial and (b) the current configurations of a body made of an elastomeric matrix filled with liquid inclusions.

and the *interface deformation gradient* at $\widehat{\mathbf{X}} \in \Gamma_0$ by

$$\widehat{\mathbf{F}}(\widehat{\mathbf{X}}) = \widehat{\nabla}\mathbf{y}(\widehat{\mathbf{X}}) = \mathbf{F}(\widehat{\mathbf{X}})\widehat{\mathbf{I}}, \tag{2}$$

where $\widehat{\mathbf{I}}$ stands for the projection tensor

$$\widehat{\mathbf{I}} = \mathbf{I} - \widehat{\mathbf{N}} \otimes \widehat{\mathbf{N}}.$$

The notation (2) merits some clarification. Assuming sufficient regularity away from the interfaces, the requirement that the deformation field $\mathbf{y}(\mathbf{X})$ be continuous implies the Hadamard jump condition

$$[\![\mathbf{F}(\widehat{\mathbf{X}})]\!]\widehat{\mathbf{I}} = \mathbf{0} \quad \text{with} \qquad [\![\mathbf{F}(\widehat{\mathbf{X}})]\!] := \mathbf{F}^{\mathtt{i}}(\widehat{\mathbf{X}}) - \mathbf{F}^{\mathtt{m}}(\widehat{\mathbf{X}}), \tag{3}$$

where $\mathbf{F}^{\mathtt{i}}$ ($\mathbf{F}^{\mathtt{m}}$) denotes the limit of $\mathbf{F}$ when approaching Γ_0 from $\Omega_0^{\mathtt{i}}$ ($\Omega_0^{\mathtt{m}}$). Although $\mathbf{F}^{\mathtt{i}} \neq \mathbf{F}^{\mathtt{m}}$ at Γ_0, $\mathbf{F}^{\mathtt{i}}\widehat{\mathbf{I}} = \mathbf{F}^{\mathtt{m}}\widehat{\mathbf{I}}$, and it is for this reason that, with some abuse of notation, we do not include the label '$\mathtt{i}$' or '$\mathtt{m}$' in the right-hand side of (2).

The interested reader is referred to, for instance, do Carmo (2016), Weatherburn (2016), Gurtin et al. (1998), and Javili et al. (2013) for a thorough description of differential operators defined on surfaces embedded in $\mathbb{R}^3$ and of the kinematics of interfaces. For our purposes here, it suffices to make explicit mention of some of the properties of the interface deformation gradient (2). In direct analogy with the transformation rules for material line elements $\mathrm{d}\mathbf{X}$ in the bulk, material line elements $\mathrm{d}\widehat{\mathbf{X}}$ on the interfaces transform according to the rules

$$\mathrm{d}\widehat{\mathbf{x}} = \widehat{\mathbf{F}}\mathrm{d}\widehat{\mathbf{X}} \qquad \text{and} \qquad \mathrm{d}\widehat{\mathbf{X}} = \widehat{\mathbf{F}}^{-1}\mathrm{d}\widehat{\mathbf{x}}.$$

Owing to its rank deficiency, the inverse $\widehat{\mathbf{F}}^{-1}$ of the interface gradient deformation $\widehat{\mathbf{F}}$ is defined implicitly by the relations

$$\widehat{\mathbf{F}}^{-1}\widehat{\mathbf{F}} = \widehat{\mathbf{I}} \qquad \text{and} \qquad \widehat{\mathbf{F}}\widehat{\mathbf{F}}^{-1} = \widehat{\mathbf{i}}.$$

where

$$\widehat{\mathbf{i}} = \mathbf{I} - \widehat{\mathbf{n}} \otimes \widehat{\mathbf{n}} \qquad \text{with} \qquad \widehat{\mathbf{n}} = \frac{1}{|J\mathbf{F}^{-T}\widehat{\mathbf{N}}|} J\mathbf{F}^{-T}\widehat{\mathbf{N}}.$$

That is

$$\widehat{\mathbf{F}}^{-1} = \mathbf{F}^{-1}\widehat{\mathbf{i}}.$$

In these last expressions, we have made use of the standard notation $J = \det \mathbf{F}$ for the determinant of the deformation gradient $\mathbf{F}$ and exploited the facts that $J^{\mathtt{i}}\mathbf{F}^{\mathtt{i}-T}\widehat{\mathbf{N}} = J^{\mathtt{m}}\mathbf{F}^{\mathtt{m}-T}\widehat{\mathbf{N}}$ and $\mathbf{F}^{\mathtt{i}-1}\widehat{\mathbf{i}} = \mathbf{F}^{\mathtt{m}-1}\widehat{\mathbf{i}}$, thanks to (3), to simply write, with the same abuse of notation as in (2), $J\mathbf{F}^{-T}\widehat{\mathbf{N}}$ and $\mathbf{F}^{-1}\widehat{\mathbf{i}}$ without the label '$\mathtt{i}$' or '$\mathtt{m}$'. Furthermore, the area $\mathrm{d}A$ of material surface elements $\widehat{\mathbf{N}}\mathrm{d}A$ on the interfaces transforms according to the rule

$$\mathrm{d}a = \widehat{J}\mathrm{d}A \qquad \text{with} \qquad \widehat{J} = |J\mathbf{F}^{-T}\widehat{\mathbf{N}}|.$$

This transformation rule also serves to define the interface determinant operator $\widehat{\det}\,\widehat{\mathbf{F}} = \widehat{J}$. Finally, we note that material curve elements $\widehat{\mathbf{M}}\,\mathrm{d}L$ on the interfaces transform according to the rule

$$\widehat{\mathbf{m}}\,\mathrm{d}l = \widehat{J}\widehat{\mathbf{F}}^{-T}\widehat{\mathbf{M}}\,\mathrm{d}L,$$

where $\widehat{\mathbf{M}}$ is a unit vector that is tangential to Γ_0 and normal to the curve $\mathrm{d}L$. Fig. 1(b) provides a schematic of the body in its current configuration with all the above geometric quantities depicted.

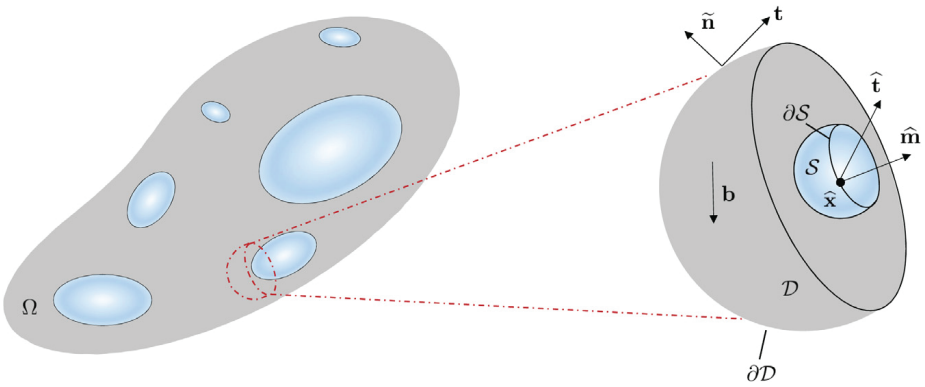

Fig. 2. Schematic of a subdomain of the current configuration $\mathcal{D} \subset \Omega$, with boundary $\partial\mathcal{D}$ and outward unit normal $\tilde{\mathbf{n}}$, indicating the body force $\mathbf{b}(\mathbf{x})$, surface force $\mathbf{t}(\mathbf{x}, \tilde{\mathbf{n}})$, and interfacial force $\hat{\mathbf{t}}(\hat{\mathbf{x}}, \hat{\mathbf{m}})$ that is subjected to.

2.2. Equilibrium equations and the concepts of bulk and interface stresses

In any given subdomain of the current configuration $\mathcal{D} \subset \Omega$, with boundary $\partial\mathcal{D}$ and outward unit normal[3] $\tilde{\mathbf{n}}$, we consider that there may be three types of forces present, to wit, a *body force* per unit current volume

$$\mathbf{b}(\mathbf{x}), \quad \mathbf{x} \in \mathcal{D},$$

a *surface force* per unit current area, or surface traction,

$$\mathbf{t}(\mathbf{x}, \tilde{\mathbf{n}}), \quad \mathbf{x} \in \partial\mathcal{D},$$

and an *interfacial force* per unit current length, or interfacial traction,

$$\hat{\mathbf{t}}(\hat{\mathbf{x}}, \hat{\mathbf{m}}), \quad \hat{\mathbf{x}} \in \partial\mathcal{S},$$

acting on the boundary $\partial\mathcal{S}$ of any subsurfaces of the interfaces $\mathcal{S} \subset \Gamma$ that the subdomain $\mathcal{D}$ may contain. The first two of these forces are standard. The third one accounts for the possibility of additional forces at the matrix/inclusions interfaces, such as, for instance, surface tension and Marangoni forces; see, e.g., Popinet (2018) and references therein. Within such interfacial forces, we shall restrict attention to *tangential* forces in the sense that

$$\hat{\mathbf{i}}\hat{\mathbf{t}} = \hat{\mathbf{t}}. \tag{4}$$

Note that Cauchy's fundamental postulate has been tacitly assumed to apply, thus the dependencies of the surface traction $\mathbf{t}$ on $\tilde{\mathbf{n}}$ and of the interfacial traction $\hat{\mathbf{t}}$ on $\hat{\mathbf{m}}$, which, again, stands for the outward unit normal to $\partial\mathcal{S}$. Fig. 2 shows a schematic of a generic subdomain $\mathcal{D}$ with all three types of forces depicted.

Absent inertia, granted the above-described types of forces, balance of linear momentum reads

$$\int_{\mathcal{D}} \mathbf{b}(\mathbf{x}) \, \mathrm{d}\mathbf{x} + \int_{\partial\mathcal{D}} \mathbf{t}(\mathbf{x}, \tilde{\mathbf{n}}) \, \mathrm{d}\mathbf{x} + \int_{\partial\mathcal{S}} \hat{\mathbf{t}}(\hat{\mathbf{x}}, \hat{\mathbf{m}}) \, \mathrm{d}\hat{\mathbf{x}} = \mathbf{0}. \tag{5}$$

Assuming that $\mathbf{t}$ and $\hat{\mathbf{t}}$ are continuous in $\partial\mathcal{D} \setminus \partial\mathcal{S}$ and $\partial\mathcal{S}$, respectively, if follows from (5) that

$$\mathbf{t}(\mathbf{x}, \tilde{\mathbf{n}}) = \mathbf{T}(\mathbf{x})\tilde{\mathbf{n}}, \quad \mathbf{x} \in \mathcal{D} \setminus \mathcal{S}, \qquad \hat{\mathbf{t}}(\hat{\mathbf{x}}, \hat{\mathbf{m}}) = \hat{\mathbf{T}}(\hat{\mathbf{x}})\hat{\mathbf{m}}, \quad \hat{\mathbf{x}} \in \mathcal{S}, \tag{6}$$

where $\mathbf{T}$ is the standard Cauchy stress tensor in the bulk while $\hat{\mathbf{T}}$ is the *interface Cauchy stress* tensor. The former is continuous in $\mathcal{D} \setminus \mathcal{S}$ but may have a jump at $\mathcal{S}$, while the latter is continuous on $\mathcal{S}$ and, by virtue of (4), is a *tangential* tensor in the sense that $\hat{\mathbf{i}}\hat{\mathbf{T}}\hat{\mathbf{i}} = \hat{\mathbf{T}}$. Making use of relations (6), the bulk and interface divergence theorems,[4] and the fact that $\hat{\mathbf{T}}$ is a *superficial* tensor in the sense that $\hat{\mathbf{T}}\hat{\mathbf{i}} = \hat{\mathbf{T}}$, the balance of linear momentum (5) can be rewritten as

$$\int_{\mathcal{D}} \mathbf{b}(\mathbf{x}) \, \mathrm{d}\mathbf{x} + \int_{\mathcal{D}\setminus\mathcal{S}} \operatorname{div} \mathbf{T} \, \mathrm{d}\mathbf{x} - \int_{\mathcal{S}} [\![\mathbf{T}]\!]\hat{\mathbf{n}} \, \mathrm{d}\hat{\mathbf{x}} + \int_{\mathcal{S}} \widehat{\operatorname{div}} \hat{\mathbf{T}} \, \mathrm{d}\hat{\mathbf{x}} = \mathbf{0},$$

[3] For clarity, we make use of the notation $\tilde{\cdot}$ (in contrast to the notation $\hat{\cdot}$ used for interfacial quantities) to refer to quantities on the boundary $\partial\mathcal{D}$ of arbitrary subdomains $\mathcal{D} \subset \Omega$, which may or may not contain interfaces.

[4] For convenience, we recall here that the bulk divergence theorem for a second-order tensor $\mathbf{A}$ (smooth in $\mathcal{D}$ except possibly at $\mathcal{S}$) reads, in indicial notation with respect to a Cartesian frame of reference, $\int_{\mathcal{D}\setminus\mathcal{S}} \partial A_{ij}/\partial x_k \, \mathrm{d}\mathbf{x} = \int_{\partial\mathcal{D}} A_{ij} n_k \, \mathrm{d}\mathbf{x} + \int_{\mathcal{S}} [\![A_{ij}]\!]\hat{n}_k \, \mathrm{d}\mathbf{x}$, while the interface divergence theorem for a second-order tensor $\hat{\mathbf{A}}$ (smooth in $\mathcal{S}$ but not necessarily superficial) reads $\int_{\mathcal{S}} (\partial\hat{A}_{ij}/\partial x_l)\hat{i}_{kl} \, \mathrm{d}\mathbf{x} = \int_{\partial\mathcal{S}} \hat{A}_{ij}\hat{m}_k \, \mathrm{d}\mathbf{x} + \int_{\mathcal{S}} (\partial\hat{n}_p/\partial x_q)\hat{i}_{pq}\hat{A}_{ij}\hat{n}_k \, \mathrm{d}\mathbf{x}$.

from which one can readily determine the localized form

$$\begin{cases} \operatorname{div}\mathbf{T}+\mathbf{b}=\mathbf{0}, & \mathbf{x}\in\Omega\setminus\Gamma \\ \widehat{\operatorname{div}}\,\widehat{\mathbf{T}}-[\![\mathbf{T}]\!]\widehat{\mathbf{n}}=\mathbf{0}, & \mathbf{x}\in\Gamma \end{cases}. \tag{7}$$

In these expressions, $[\![\mathbf{T}(\widehat{\mathbf{x}})]\!]=\mathbf{T}^{\mathrm{i}}(\widehat{\mathbf{x}})-\mathbf{T}^{\mathrm{m}}(\widehat{\mathbf{x}})$, where $\mathbf{T}^{\mathrm{i}}$ ($\mathbf{T}^{\mathrm{m}}$) denotes the limit of $\mathbf{T}$ when approaching Γ from Ω^{i} (Ω^{m}), div is the standard divergence operator in the bulk, and $\widehat{\operatorname{div}}$ stands for the interface divergence operator, that is, $\operatorname{div}\mathbf{T}=\partial\mathbf{T}/\partial\mathbf{x}\cdot\mathbf{I}$ and $\widehat{\operatorname{div}}\,\widehat{\mathbf{T}}=\partial\widehat{\mathbf{T}}/\partial\mathbf{x}\cdot\widehat{\mathbf{i}}$ (in indicial notation, $\partial T_{ij}/\partial x_k\,\delta_{jk}$ and $\partial\widehat{T}_{ij}/\partial x_k\,\widehat{i}_{jk}$).

In turn, balance of angular momentum reads

$$\int_D \mathbf{x}\wedge\mathbf{b}(\mathbf{x})\;\mathrm{d}\mathbf{x}+\int_{\partial\mathcal{D}}\mathbf{x}\wedge\mathbf{t}\left(\mathbf{x},\widetilde{\mathbf{n}}\right)\;\mathrm{d}\mathbf{x}+\int_{\partial\mathcal{S}}\widehat{\mathbf{x}}\wedge\widehat{\mathbf{t}}\left(\widehat{\mathbf{x}},\widehat{\mathbf{m}}\right)\;\mathrm{d}\widehat{\mathbf{x}}=\mathbf{0},$$

from which, making use of (6) and (7), one can deduce the localized form

$$\begin{cases} \mathbf{T}^T=\mathbf{T}, & \mathbf{x}\in\Omega\setminus\Gamma \\ \widehat{\mathbf{T}}^T=\widehat{\mathbf{T}}, & \mathbf{x}\in\Gamma \end{cases}. \tag{8}$$

Eqs. (7) and (8) constitute the equilibrium equations for the body in Eulerian (spatial) form. For computational purposes, we shall find it more convenient to deal with them in their Lagrangian (material) form

$$\begin{cases} \operatorname{Div}\mathbf{S}+\mathbf{B}=\mathbf{0}, & \mathbf{X}\in\Omega_0\setminus\Gamma_0 \\ \widehat{\operatorname{Div}}\,\widehat{\mathbf{S}}-[\![\mathbf{S}]\!]\widehat{\mathbf{N}}=\mathbf{0}, & \mathbf{X}\in\Gamma_0 \end{cases} \tag{9}$$

and

$$\begin{cases} \mathbf{S}\mathbf{F}^T=\mathbf{F}\mathbf{S}^T, & \mathbf{X}\in\Omega_0\setminus\Gamma_0 \\ \widehat{\mathbf{S}}\widehat{\mathbf{F}}^T=\widehat{\mathbf{F}}\widehat{\mathbf{S}}^T, & \mathbf{X}\in\Gamma_0 \end{cases}, \tag{10}$$

where $\mathbf{S}=J\mathbf{T}\mathbf{F}^{-T}$ is the standard first Piola–Kirchhoff stress tensor in the bulk, $\mathbf{B}=J\mathbf{b}$, and $\widehat{\mathbf{S}}=\widehat{J}\widehat{\mathbf{T}}\widehat{\mathbf{F}}^{-T}$ stands for the *interface first Piola–Kirchhoff stress* tensor. It follows from the connection $\widehat{\mathbf{F}}^{-T}=\widehat{\mathbf{i}}\widehat{\mathbf{F}}^{-T}\widehat{\mathbf{I}}$ that the interface first Piola–Kirchhoff stress $\widehat{\mathbf{S}}$ is a *superficial* tensor in the sense that $\widehat{\mathbf{S}}\widehat{\mathbf{I}}=\widehat{\mathbf{S}}$. Contrary to $\widehat{\mathbf{T}}$, however, $\widehat{\mathbf{S}}$ is *not* a *tangential* tensor since, in general, $\widehat{\mathbf{I}}\widehat{\mathbf{S}}\widehat{\mathbf{I}}\neq\widehat{\mathbf{S}}$. The notation utilized here for the bulk divergence, interface divergence, and jump operators is entirely analogous to that employed in (7) and (8), that is, $\operatorname{Div}\mathbf{S}=\partial\mathbf{S}/\partial\mathbf{X}\cdot\mathbf{I}$ ($\partial S_{ij}/\partial X_k\,\delta_{jk}$), $\widehat{\operatorname{Div}}\,\widehat{\mathbf{S}}=\partial\widehat{\mathbf{S}}/\partial\mathbf{X}\cdot\widehat{\mathbf{I}}$ ($\partial\widehat{S}_{ij}/\partial X_k\,\widehat{I}_{jk}$), and $[\![\mathbf{S}(\widehat{\mathbf{X}})]\!]=\mathbf{S}^{\mathrm{i}}(\widehat{\mathbf{X}})-\mathbf{S}^{\mathrm{m}}(\widehat{\mathbf{X}})$. A direct derivation of (9) and (10) starting from (7)–(8) is included in Appendix A for completeness.

2.3. Constitutive behaviors of the bulk and the interfaces

Constitutive behavior of the elastomeric matrix. The focus of this work is on material systems wherein the underlying elastomeric matrix is presumed to behave mechanically as an isotropic hyperelastic solid. In particular, we consider that the mechanical behavior of the elastomeric matrix is characterized by a stored-energy function

$$W_{\mathrm{m}}=W_{\mathrm{m}}(\mathbf{F})\geq 0 \tag{11}$$

that satisfies the standard constraints of objectivity and material isotropy $W_{\mathrm{m}}(\mathbf{Q}\mathbf{F}\mathbf{K})=W_{\mathrm{m}}(\mathbf{F})$ for all $\mathbf{Q},\mathbf{K}\in SO(3)$ and linearizes according to

$$W_{\mathrm{m}}(\mathbf{F})=\mu_{\mathrm{m}}\operatorname{tr}\mathbf{E}^2+\frac{\Lambda_{\mathrm{m}}}{2}(\operatorname{tr}\mathbf{E})^2+O(\|\mathbf{F}-\mathbf{I}\|^3) \tag{12}$$

in the limit of small deformations as $\mathbf{F}\to\mathbf{I}$, where $\mathbf{E}=(\mathbf{H}+\mathbf{H}^T)/2$ with $\mathbf{H}=\mathbf{F}-\mathbf{I}$. The material constants $\mu_{\mathrm{m}}>0$ and $\Lambda_{\mathrm{m}}>0$ in the linearized expression (12) denote the initial shear modulus and first Lamé constant of the elastomer. In the sequel, for definiteness and clarity of presentation, we will begin by restriction attention to the basic Neo-Hookean stored-energy function

$$W_{\mathrm{m}}(\mathbf{F})=\frac{\mu_{\mathrm{m}}}{2}[\,\mathbf{F}\cdot\mathbf{F}-3]-\mu_{\mathrm{m}}\ln J+\frac{\Lambda_{\mathrm{m}}}{2}(J-1)^2. \tag{13}$$

Remark 1. Here, it is important to emphasize that the use of stored-energy functions (11) with (12) implies that, in its initial configuration, the elastomeric matrix is stress free. In other words, we are assuming that there are *no* pre-stresses or residual stresses in the elastomeric matrix. Depending on the fabrication process of the filled elastomer of interest, however, this assumption may not be appropriate. As elaborated below in Section 2.5, this assumption is indeed appropriate for the prototypical case when the liquid inclusions are initially *spherical* in shape. In this work, we shall focus on elastomers filled with initially spherical liquid inclusions.

Constitutive behavior of the liquid inclusions. Granted the absence of inertia, the liquid making up the inclusions is presumed to behave as a hyperelastic fluid; see, e.g., Wang and Truesdell (1973). Precisely, we consider that the mechanical behavior of the liquid inclusions is characterized by the stored-energy functions

$$W_{\mathrm{i}}^j(\mathbf{X},J)=r_{\mathrm{i}}^j(\mathbf{X})J+\frac{\Lambda_{\mathrm{i}}}{2}(J-1)^2\quad j=1,2,\ldots,M, \tag{14}$$

where, as will become apparent below in Section 2.5, $r_{\mathrm{i}}^{j}(\mathbf{X})$ shall stand for the pressure – which is *not* necessarily zero due to the possible presence of initial interfacial forces – that the liquid within the jth inclusion is subjected to in the initial configuration, when $\mathbf{F}=\mathbf{I}$, and $\Lambda_{\mathrm{i}}\geq 0$ denotes the initial first Lamé constant of the liquid and thus serves to quantify its compressibility. The case of an incompressible liquid is recovered by setting $\Lambda_{\mathrm{i}}=+\infty$.

Remark 2. All M inclusions are assumed to be made of the same liquid, thus the unique value of Λ_{i} in (14). However, because each inclusion is allowed to have its own initial geometry, and thus its own initial size, the term $r_{\mathrm{i}}^{j}(\mathbf{X})$ in (14) describing the residual stress within the inclusions may be different for each inclusion. As explained below in Section 2.5, such a residual stress is not arbitrary but it must comply with the governing equations of equilibrium.

Pointwise constitutive behavior of the bulk. Given the indicator functions (1) for the inclusions and the stored-energy functions (13) and (14) for the elastomeric matrix and the inclusions, the pointwise stored-energy function for the bulk of the body can be compactly written as

$$W(\mathbf{X},\mathbf{F})=r_{\mathrm{i}}(\mathbf{X})J+\frac{\mu(\mathbf{X})}{2}\left[\mathbf{F}\cdot\mathbf{F}-3\right]-\mu(\mathbf{X})\ln J+\frac{\Lambda(\mathbf{X})}{2}\left(J-1\right)^{2}, \tag{15}$$

where

$$r_{\mathrm{i}}(\mathbf{X})=\sum_{j=1}^{M}\theta_{0}^{\mathrm{i},j}(\mathbf{X})r_{\mathrm{i}}^{j}(\mathbf{X}),\qquad \mu(\mathbf{X})=\left(1-\theta_{0}^{\mathrm{i}}(\mathbf{X})\right)\mu_{\mathrm{m}},\qquad \Lambda(\mathbf{X})=\left(1-\theta_{0}^{\mathrm{i}}(\mathbf{X})\right)\Lambda_{\mathrm{m}}+\theta_{0}^{\mathrm{i}}(\mathbf{X})\Lambda_{\mathrm{i}}. \tag{16}$$

It then follows that the first Piola–Kirchhoff stress tensor $\mathbf{S}$ at any material point in the bulk reads

$$\mathbf{S}(\mathbf{X})=\frac{\partial W}{\partial\mathbf{F}}(\mathbf{X},\mathbf{F})=r_{\mathrm{i}}(\mathbf{X})J\mathbf{F}^{-T}+\mu(\mathbf{X})\left(\mathbf{F}-\mathbf{F}^{-T}\right)+\Lambda(\mathbf{X})(J-1)J\mathbf{F}^{-T},\quad \mathbf{X}\in\Omega_{0}\setminus\Gamma_{0}. \tag{17}$$

Remark 3. In the limit of small deformations as $\mathbf{F}\to\mathbf{I}$, granted the linearized behavior (12) of the elastomer, the constitutive response (17) reduces asymptotically to

$$\mathbf{S}(\mathbf{X})=r_{\mathrm{i}}(\mathbf{X})\mathbf{I}-r_{\mathrm{i}}(\mathbf{X})\mathbf{H}^{T}+r_{\mathrm{i}}(\mathbf{X})(\mathrm{tr}\,\mathbf{E})\mathbf{I}+2\mu(\mathbf{X})\mathbf{E}+\Lambda(\mathbf{X})(\mathrm{tr}\,\mathbf{E})\mathbf{I}+O(\|\mathbf{F}-\mathbf{I}\|^{2}), \tag{18}$$

where, again, $\mathbf{H}=\mathbf{F}-\mathbf{I}$ and $\mathbf{E}=(\mathbf{H}+\mathbf{H}^{T})/2$ is the infinitesimal strain tensor. The corresponding Cauchy stress tensor $\mathbf{T}=J^{-1}\mathbf{S}\mathbf{F}^{T}$ is given by

$$\mathbf{T}(\mathbf{x})=r_{\mathrm{i}}(\mathbf{x})\mathbf{I}+2\mu(\mathbf{x})\mathbf{E}+\Lambda(\mathbf{x})(\mathrm{tr}\,\mathbf{E})\mathbf{I}+O(\|\mathbf{F}-\mathbf{I}\|^{2}). \tag{19}$$

Three key features are now immediate. First, in the initial configuration, when $\mathbf{x}=\mathbf{X}$, $\mathbf{F}=\mathbf{I}$, and $\mathbf{H}=\mathbf{E}=\mathbf{0}$, the stress measures (18) and (19) reduce to

$$\mathbf{S}(\mathbf{X})=r_{\mathrm{i}}(\mathbf{X})\mathbf{I}\qquad\text{and}\qquad\mathbf{T}(\mathbf{x})=r_{\mathrm{i}}(\mathbf{x})\mathbf{I},$$

which indicate that the inclusions, but *not* the matrix, have a hydrostatic residual stress. Second, the stress (18) is *not* symmetric as it does not depend only on the symmetric part $\mathbf{E}$ of $\mathbf{H}$, but also on $\mathbf{H}$ itself. Third, the first Piola–Kirchhoff stress (18) does *not* coincide with the Cauchy stress (19) to $O(\|\mathbf{F}-\mathbf{I}\|)$. As elaborated below, these three non-standard features are direct consequences of the presence of a residual stress, which in turn is a direct consequence of the presence of interfacial forces.

Remark 4. The bulk constitutive response (18) in the limit of small deformations can be rewritten as

$$\mathbf{S}(\mathbf{X})=r_{\mathrm{i}}(\mathbf{X})\mathbf{I}+\mathbf{L}(\mathbf{X})\mathbf{H}+O(\|\mathbf{F}-\mathbf{I}\|^{2})$$

with

$$\mathbf{L}(\mathbf{X})=r_{\mathrm{i}}(\mathbf{X})\boldsymbol{\mathcal{A}}+\left(2\mu(\mathbf{X})-r_{\mathrm{i}}(\mathbf{X})\right)\boldsymbol{\mathcal{K}}+\left(2\mu(\mathbf{X})+2r_{\mathrm{i}}(\mathbf{X})+3\Lambda(\mathbf{X})\right)\boldsymbol{\mathcal{J}}, \tag{20}$$

where

$$\mathcal{A}_{ijkl}=\frac{1}{2}(\delta_{ik}\delta_{jl}-\delta_{il}\delta_{jk}),\quad \mathcal{K}_{ijkl}=\frac{1}{2}\left(\delta_{ik}\delta_{jl}+\delta_{il}\delta_{jk}-\frac{2}{3}\delta_{ij}\delta_{kl}\right),\quad \mathcal{J}_{ijkl}=\frac{1}{3}\delta_{ij}\delta_{kl}. \tag{21}$$

From these, it is straightforward to verify that $L_{ijkl}(\mathbf{X})$ exhibits major symmetry, $L_{ijkl}(\mathbf{X})=L_{klij}(\mathbf{X})$, but *not* minor symmetries, $L_{ijkl}(\mathbf{X})\neq L_{jikl}(\mathbf{X})\neq L_{ijlk}(\mathbf{X})$. It is also a simple matter to verify that the tensors $\boldsymbol{\mathcal{A}}$, $\boldsymbol{\mathcal{K}}$, and $\boldsymbol{\mathcal{J}}$ satisfy the orthonormality properties

$$\boldsymbol{\mathcal{A}}\boldsymbol{\mathcal{K}}=\boldsymbol{\mathcal{K}}\boldsymbol{\mathcal{A}}=\boldsymbol{\mathcal{A}}\boldsymbol{\mathcal{J}}=\boldsymbol{\mathcal{J}}\boldsymbol{\mathcal{A}}=\boldsymbol{\mathcal{K}}\boldsymbol{\mathcal{J}}=\boldsymbol{\mathcal{J}}\boldsymbol{\mathcal{K}}=\mathbf{0},\quad \boldsymbol{\mathcal{A}}\boldsymbol{\mathcal{A}}=\boldsymbol{\mathcal{A}},\quad \boldsymbol{\mathcal{K}}\boldsymbol{\mathcal{K}}=\boldsymbol{\mathcal{K}},\quad \boldsymbol{\mathcal{J}}\boldsymbol{\mathcal{J}}=\boldsymbol{\mathcal{J}},$$

and hence that (20) is the spectral representation of the initial modulus of elasticity $\mathbf{L}(\mathbf{X})$ for the bulk. Due to the lack of minor symmetry of $\boldsymbol{\mathcal{A}}$, the tensor (20) does *not* posses the typical pointwise positive definiteness of the initial modulus of elasticity of standard elastic materials. We will come back to this important point in Remark 14.

Remark 5. Thanks to the objectivity of the stored-energy functions (13) and (14), the constitutive relation (17) satisfies automatically the balance of angular momentum $(10)_{1}$ in the bulk.

Pointwise constitutive behavior of the interfaces. We now turn to the constitutive description of the interfaces. Similar to the elastomeric matrix and liquid inclusions, we also consider that under the quasistatic deformations of interest here any interfacial dissipative phenomena is negligible and presume the interfaces to exhibit an isotropic hyperelastic behavior. Specifically, we consider that the interface first Piola–Kirchhoff stress tensor $\widehat{\mathbf{S}}$ is given by a relation of the form

$$\widehat{\mathbf{S}}(\mathbf{X}) = \frac{\partial \widehat{W}}{\partial \widehat{\mathbf{F}}}(\widehat{\mathbf{F}}), \quad \mathbf{X} \in \Gamma_0 \tag{22}$$

in terms of a suitably well-behaved interface stored-energy function $\widehat{W}(\widehat{\mathbf{F}})$. In the sequel, for definiteness and clarity of presentation, we will begin by making use of the Neo-Hookean-type stored-energy function

$$\widehat{W}(\widehat{\mathbf{F}}) = \widehat{\gamma}_0\, \widehat{J} + \frac{\widehat{\mu}}{2}\left[\widehat{\mathbf{F}}\cdot\widehat{\mathbf{F}} - 2\right] - \widehat{\mu}\ln\widehat{J} + \frac{\widehat{\Lambda}}{2}(\widehat{J}-1)^2. \tag{23}$$

Here, as elaborated in the next remark, the material constant $\widehat{\gamma}_0 \geq 0$ describes the *surface tension* on the interfaces in the initial configuration. On the other hand, $\widehat{\mu} \geq 0$ and $\widehat{\Lambda} \geq 0$ can be viewed as the *interface Lamé constants* in the same initial configuration. All three material constants $\widehat{\gamma}_0$, $\widehat{\mu}$, $\widehat{\Lambda}$ have units of $force/length$. Making use of the relations $\partial\widehat{J}/\partial\widehat{\mathbf{F}} = \widehat{J}\widehat{\mathbf{F}}^{-T}$ and $\partial(\widehat{\mathbf{F}}\cdot\widehat{\mathbf{F}})/\partial\widehat{\mathbf{F}} = 2\widehat{\mathbf{F}}$, it is straightforward to show that the interface first Piola–Kirchhoff stress tensor (22) associated with the stored-energy function (23) is given by

$$\widehat{\mathbf{S}}(\mathbf{X}) = \widehat{\gamma}_0\, \widehat{J}\widehat{\mathbf{F}}^{-T} + \widehat{\mu}(\widehat{\mathbf{F}} - \widehat{\mathbf{F}}^{-T}) + \widehat{\Lambda}(\widehat{J}-1)\widehat{J}\widehat{\mathbf{F}}^{-T}, \quad \mathbf{X} \in \Gamma_0. \tag{24}$$

Remark 6. The interface Cauchy stress tensor $\widehat{\mathbf{T}} = \widehat{J}^{-1}\widehat{\mathbf{S}}\widehat{\mathbf{F}}^T$ associated with the stored-energy function (23) reads

$$\widehat{\mathbf{T}}(\mathbf{x}) = \widehat{\gamma}_0\,\widehat{\mathbf{i}} + \widehat{\mu}(\widehat{J}^{-1}\widehat{\mathbf{F}}\widehat{\mathbf{F}}^T - \widehat{\mathbf{i}}) + \widehat{\Lambda}(\widehat{J}-1)\widehat{\mathbf{i}}, \quad \mathbf{x} \in \Gamma. \tag{25}$$

This expression makes it plain that the constitutive relation (24) utilized here to describe the mechanical behavior of the interfaces generalizes in two counts the basic constitutive relation of constant surface-tension stress

$$\widehat{\mathbf{T}}(\mathbf{x}) = \widehat{\gamma}_0\widehat{\mathbf{i}}.$$

Specifically, the constitutive relation (25) includes Neo-Hookean-type deviatoric elasticity, via the term $\widehat{\mu}(\widehat{J}^{-1}\widehat{\mathbf{F}}\widehat{\mathbf{F}}^T - \widehat{\mathbf{i}})$, and not just surface tension. It also accounts for a surface tension that is not necessarily a constant but instead one that depends on the deformation of the interface via the term $\widehat{\Lambda}(\widehat{J}-1)\widehat{\mathbf{i}}$. At present, very little is known from direct observations about what the mechanical behavior of interfaces between elastomers and liquids looks like, especially at finite deformations. The constitutive relation (24) should be hence regarded as a simple plausible generalization of the basic concept of constant surface tension. We will introduce another generalization in the latter part of Section 7.

Remark 7. In the limit of small deformations as $\mathbf{F} \to \mathbf{I}$, so that $\widehat{\mathbf{F}} \to \widehat{\mathbf{I}}$, the constitutive response (24) reduces asymptotically to

$$\widehat{\mathbf{S}}(\mathbf{X}) = \widehat{\gamma}_0\widehat{\mathbf{I}} + \widehat{\gamma}_0\widehat{\mathbf{H}} + 2(\widehat{\mu} - \widehat{\gamma}_0)\widehat{\mathbf{E}} + (\widehat{\Lambda} + \widehat{\gamma}_0)(\mathrm{tr}\widehat{\mathbf{E}})\widehat{\mathbf{I}} + O(\|\mathbf{F}-\mathbf{I}\|^2), \tag{26}$$

where $\widehat{\mathbf{E}} = (\widehat{\mathbf{I}}\widehat{\mathbf{H}} + \widehat{\mathbf{H}}^T\widehat{\mathbf{I}})/2$ with $\widehat{\mathbf{H}} = \widehat{\mathbf{F}} - \widehat{\mathbf{I}}$. The corresponding interface Cauchy stress tensor (25) reduces in turn to

$$\widehat{\mathbf{T}}(\mathbf{x}) = \widehat{\gamma}_0\widehat{\mathbf{I}} + 2\widehat{\mu}\widehat{\mathbf{E}} + \widehat{\Lambda}(\mathrm{tr}\widehat{\mathbf{E}})\widehat{\mathbf{I}} + O(\|\mathbf{F}-\mathbf{I}\|^2). \tag{27}$$

The asymptotic results (26) and (27) were originally introduced by Gurtin and Murdoch (1975a,b). Of note here is that, in the presence of an initial surface tension when $\widehat{\gamma}_0 > 0$, the interface first Piola–Kirchhoff stress (26) is not symmetric and does *not* coincide with the interface Cauchy stress (27) to $O(\|\mathbf{F}-\mathbf{I}\|)$.

Remark 8. The interface constitutive response (26) in the limit of small deformations can be rewritten as

$$\widehat{\mathbf{S}}(\mathbf{X}) = \widehat{\gamma}_0\widehat{\mathbf{I}} + \widehat{\mathbf{L}}\widehat{\mathbf{H}} + O(\|\mathbf{F}-\mathbf{I}\|^2)$$

with

$$\widehat{\mathbf{L}} = \widehat{\gamma}_0\widehat{\boldsymbol{\mathcal{A}}} + \left(2\widehat{\mu} - \widehat{\gamma}_0\right)\widehat{\boldsymbol{\mathcal{K}}} + \left(2\widehat{\mu} + \widehat{\gamma}_0 + 2\widehat{\Lambda}\right)\widehat{\boldsymbol{\mathcal{J}}}, \tag{28}$$

where

$$\widehat{\mathcal{A}}_{ijkl} = \delta_{ik}\widehat{I}_{jl} - \frac{1}{2}\left(\widehat{I}_{ik}\widehat{I}_{jl} + \widehat{I}_{il}\widehat{I}_{jk}\right), \quad \widehat{\mathcal{K}}_{ijkl} = \frac{1}{2}\left(\widehat{I}_{ik}\widehat{I}_{jl} + \widehat{I}_{il}\widehat{I}_{jk} - \widehat{I}_{ij}\widehat{I}_{kl}\right), \quad \widehat{\mathcal{J}}_{ijkl} = \frac{1}{2}\widehat{I}_{ij}\widehat{I}_{kl}.$$

In complete analogy to its bulk counterpart (20), $\widehat{L}_{ijkl} = \widehat{L}_{klij}$ but $\widehat{L}_{ijkl} \neq \widehat{L}_{jikl} \neq \widehat{L}_{ijlk}$, the tensors $\widehat{\boldsymbol{\mathcal{A}}}$, $\widehat{\boldsymbol{\mathcal{K}}}$, and $\widehat{\boldsymbol{\mathcal{J}}}$ satisfy the orthonormality properties

$$\widehat{\boldsymbol{\mathcal{A}}}\widehat{\boldsymbol{\mathcal{K}}} = \widehat{\boldsymbol{\mathcal{K}}}\widehat{\boldsymbol{\mathcal{A}}} = \widehat{\boldsymbol{\mathcal{A}}}\widehat{\boldsymbol{\mathcal{J}}} = \widehat{\boldsymbol{\mathcal{J}}}\widehat{\boldsymbol{\mathcal{A}}} = \widehat{\boldsymbol{\mathcal{K}}}\widehat{\boldsymbol{\mathcal{J}}} = \widehat{\boldsymbol{\mathcal{J}}}\widehat{\boldsymbol{\mathcal{K}}} = \mathbf{0}, \quad \widehat{\boldsymbol{\mathcal{A}}}\widehat{\boldsymbol{\mathcal{A}}} = \widehat{\boldsymbol{\mathcal{A}}}, \quad \widehat{\boldsymbol{\mathcal{K}}}\widehat{\boldsymbol{\mathcal{K}}} = \widehat{\boldsymbol{\mathcal{K}}}, \quad \widehat{\boldsymbol{\mathcal{J}}}\widehat{\boldsymbol{\mathcal{J}}} = \widehat{\boldsymbol{\mathcal{J}}},$$

and hence (28) is the spectral representation of the initial modulus of elasticity $\widehat{\mathbf{L}}$ for the interfaces. In this regard, note that (28) is *not* positive definite (as a fourth-order tensor acting on superficial second-order tensors $\widehat{\mathbf{H}} = \widehat{\mathbf{H}}\,\widehat{\mathbf{I}}$) when $\widehat{\gamma}_0 > \widehat{\mu}$.

Remark 9. Thanks to the objectivity of the interface stored-energy function (23), the constitutive relation (24) satisfies automatically the balance of angular momentum $(10)_2$ on the interfaces.

2.4. Governing equations

We are now in a position to write down the governing equations for our problem by combining the above deformation, force, and constitutive ingredients. Considering that $\bar{\mathbf{y}}(\mathbf{X})$ is the given deformation applied on the part of the boundary $\partial\Omega_0^D$ and that $\bar{\mathbf{s}}(\mathbf{X})$ is the given nominal traction applied on the complementary part of the boundary $\partial\Omega_0^{\mathcal{N}} = \partial\Omega_0 \setminus \partial\Omega_0^D$, substitution of the constitutive relations (17) and (24) for the bulk and interfaces in the equilibrium equations (9) yields the following governing equations

$$\left\{\begin{array}{l} \mathrm{Div}\left[r_{\mathrm{i}}(\mathbf{X})J\nabla\mathbf{y}^{-T} + \mu(\mathbf{X})\left(\nabla\mathbf{y} - \nabla\mathbf{y}^{-T}\right) + \Lambda(\mathbf{X})(J-1)J\nabla\mathbf{y}^{-T}\right] + \mathbf{B} = \mathbf{0}, \quad \mathbf{X} \in \Omega_0 \setminus \Gamma_0 \\ \widehat{\mathrm{Div}}\left[\hat{\gamma}_0\,\hat{J}\hat{\nabla}\mathbf{y}^{-T} + \hat{\mu}(\hat{\nabla}\mathbf{y} - \hat{\nabla}\mathbf{y}^{-T}) + \hat{\Lambda}(\hat{J}-1)\hat{J}\hat{\nabla}\mathbf{y}^{-T}\right] - \\ \left[\!\left[r_{\mathrm{i}}(\mathbf{X})J\nabla\mathbf{y}^{-T} + \mu(\mathbf{X})\left(\nabla\mathbf{y} - \nabla\mathbf{y}^{-T}\right) + \Lambda(\mathbf{X})(J-1)J\nabla\mathbf{y}^{-T}\right]\!\right]\hat{\mathbf{N}} = \mathbf{0}, \quad \mathbf{X} \in \Gamma_0 \\ \mathbf{y}(\mathbf{X}) = \bar{\mathbf{y}}(\mathbf{X}), \quad \mathbf{X} \in \partial\Omega_0^D \\ \left[\mu_{\mathrm{m}}\left(\nabla\mathbf{y} - \nabla\mathbf{y}^{-T}\right) + \Lambda_{\mathrm{m}}(J-1)J\nabla\mathbf{y}^{-T}\right]\mathbf{N} = \bar{\mathbf{s}}(\mathbf{X}), \quad \mathbf{X} \in \partial\Omega_0^{\mathcal{N}} \end{array}\right. \tag{29}$$

for the deformation field $\mathbf{y}(\mathbf{X})$; recall that the balance of angular momentum (10) is automatically satisfied. These equations constitute a generalization of the classical elastostatics equations for heterogeneous Neo-Hookean materials that accounts for: (*i*) the presence of residual stresses (in the inclusions) and (*ii*) a jump condition across material (matrix/inclusions) interfaces that is not simply given by the continuity of tractions but by a more complex condition due to the presence of interfacial forces. At present, as is the case for the simpler classical elastostatics equations (Lefèvre et al., 2022), there is still no existence theorem of solutions for (29). Be that as it may, for suitably well-behaved residual stresses $r_{\mathrm{i}}(\mathbf{X})$, body forces $\mathbf{B}(\mathbf{X})$, and boundary data $\bar{\mathbf{y}}(\mathbf{X})$ and $\bar{\mathbf{s}}(\mathbf{X})$, the expectation is that a unique solution for $\mathbf{y}(\mathbf{X})$ exists[5] in the limit of small deformations, which may bifurcate into multiple solutions at sufficiently large deformations (Healey and Simpson, 1998).

2.5. Residual stresses

In the initial configuration, prior to the application of the external body force $\mathbf{B}(\mathbf{X})$ in the bulk and the boundary data $\bar{\mathbf{y}}(\mathbf{X})$ and $\bar{\mathbf{s}}(\mathbf{X})$, the deformation field $\mathbf{y}(\mathbf{X}) = \mathbf{X}$ and hence the governing equations (29) reduce to

$$\left\{\begin{array}{l} \mathrm{Div}\left[r_{\mathrm{i}}(\mathbf{X})\mathbf{I}\right] = \mathbf{0}, \quad \mathbf{X} \in \Omega_0 \setminus \Gamma_0 \\ \hat{\gamma}_0\,\widehat{\mathrm{Div}}\,\hat{\mathbf{I}} - \left[\!\left[r_{\mathrm{i}}(\mathbf{X})\right]\!\right]\hat{\mathbf{N}} = \mathbf{0}, \quad \mathbf{X} \in \Gamma_0 \end{array}\right. , \tag{30}$$

which can be viewed as the definition of the hydrostatic residual stress $r_{\mathrm{i}}(\mathbf{X})$ within the inclusions required to balance out the interfacial forces. Recognizing that $\left[\!\left[r_{\mathrm{i}}(\mathbf{X})\right]\!\right] = r_{\mathrm{i}}(\mathbf{X})$ and that

$$\widehat{\mathrm{Div}}\,\hat{\mathbf{I}} = -\nabla(\hat{\mathbf{N}} \otimes \hat{\mathbf{N}}) \cdot \hat{\mathbf{I}} = -(\hat{\mathbf{I}} \cdot \nabla\hat{\mathbf{N}})\hat{\mathbf{N}} = -(\mathrm{tr}\,\hat{\nabla}\hat{\mathbf{N}})\hat{\mathbf{N}} = 2\kappa\hat{\mathbf{N}}$$

in terms of the mean curvature $\kappa = -\mathrm{tr}\,\hat{\nabla}\hat{\mathbf{N}}/2$ of the interfaces, Eqs. (30) can be rewritten more explicitly as

$$\left\{\begin{array}{l} \nabla r_{\mathrm{i}}(\mathbf{X}) = \mathbf{0}, \quad \mathbf{X} \in \Omega_0 \setminus \Gamma_0 \\ r_{\mathrm{i}}(\mathbf{X}) = 2\kappa\hat{\gamma}_0, \quad \mathbf{X} \in \Gamma_0 \end{array}\right. . \tag{31}$$

Now, the PDE $(31)_1$ states that the hydrostatic residual stress $r_{\mathrm{i}}(\mathbf{X})$ must be *constant* – possibly a different constant – within each inclusion. In view of the boundary condition $(31)_2$, which is nothing more than the standard Young–Laplace equation, a solution to the boundary-value problem (31) then only exists for the case when all M inclusions have shapes of *constant mean curvature* (Kenmotsu, 2003), for only then $(31)_2$ is consistent with $(31)_1$. Physically, as alluded to in Remark 1, this result implies that to deal with liquid inclusions of general initial shape, one would have to account for residual stresses in the elastomeric matrix and not just within the inclusions.

Henceforth, we shall restrict attention to the prototypical case of elastomers filled with liquid inclusions that are initially *spherical* in shape and thus have constant mean curvature. For these, the solution to (31) simply reads

$$r_{\mathrm{i}}(\mathbf{X}) = -\sum_{j=1}^{M} \theta_0^{\mathrm{i},j}(\mathbf{X})\frac{2\hat{\gamma}_0}{A_j}, \tag{32}$$

where A_j denotes the initial radius of the jth inclusion. The more general case of elastomers filled with liquid inclusions of arbitrary initial shape will be considered in future work.

2.6. Macroscopic or homogenized response of elastomers filled with spherical liquid inclusions

The governing equations (29) with (32) apply to elastomers filled with any arbitrary number of spherical liquid inclusions of any size and spatial distribution. In this work, we wish to restrict attention to elastomers filled with liquid inclusions wherein the latter are not only initially spherical in shape but they are also of much smaller size than the size of the body and are as well distributed uniformly in space.

[5] In point of fact, explicit solutions can be readily worked out in terms of spherical harmonics for some special cases; see, for instance, Sharma et al. (2003), Duan et al. (2005a), Style et al. (2015b), and Appendix D.

2.6.1. The formal view

Based on elementary intuition, and more so on experimental observations (Style et al., 2015a), the expectation is that elastomers filled with a statistically uniform spatial distribution of liquid inclusions that are of much smaller size than Ω_0 behave macroscopically as homogeneous nonlinear elastic materials, their elasticity being characterized by the relation between the macroscopic first Piola–Kirchhoff stress

$$\overline{\mathbf{S}} := \frac{1}{|\Omega_0|}\int_{\partial\Omega_0} \mathbf{S}\mathbf{N}\otimes\mathbf{X}\,\mathrm{d}\mathbf{X} \tag{33}$$

and the macroscopic deformation gradient tensor

$$\overline{\mathbf{F}} := \frac{1}{|\Omega_0|}\int_{\partial\Omega_0} \mathbf{y}\otimes\mathbf{N}\,\mathrm{d}\mathbf{X} \tag{34}$$

when, neglecting body forces, they are subjected to affine boundary conditions (Hill, 1972).

Remark 10. Granted the continuity of the deformation field $\mathbf{y}(\mathbf{X})$, it follows from the bulk divergence theorem that

$$\overline{\mathbf{F}} = \frac{1}{|\Omega_0|}\int_{\Omega_0} \mathbf{F}(\mathbf{X})\,\mathrm{d}\mathbf{X}. \tag{35}$$

On the other hand, granted the balance of linear momentum (9) with body force $\mathbf{B}=0$ and the fact that $\widehat{\mathbf{S}}$ is a superficial tensor, it follows from the bulk and interface divergence theorems that

$$\overline{\mathbf{S}} = \frac{1}{|\Omega_0|}\left(\int_{\Omega_0} \mathbf{S}(\mathbf{X})\,\mathrm{d}\mathbf{X} + \int_{\Gamma_0} \widehat{\mathbf{S}}(\mathbf{X})\,\mathrm{d}\mathbf{X}\right). \tag{36}$$

In contrast to the macroscopic deformation gradient tensor (34), which turns out to be equal to the volume average (35) of the local deformation gradient tensor $\mathbf{F}(\mathbf{X})$, the macroscopic stress (33) is *not* equal to the volume average of the local first Piola–Kirchhoff stress $\mathbf{S}(\mathbf{X})$. Instead, as indicated by relation (36), it contains an additional contribution given by the average of the interface stress $\widehat{\mathbf{S}}(\mathbf{X})$. The derivation of the results (35) and (36) is presented in Appendix B.

For affine deformations, when $\overline{\mathbf{F}}$ is prescribed, the problem amounts to solving the boundary-value problem

$$\begin{cases} \mathrm{Div}\left[r_{\mathrm{i}}(\mathbf{X})J\nabla\mathbf{y}^{-T} + \mu(\mathbf{X})\left(\nabla\mathbf{y}-\nabla\mathbf{y}^{-T}\right) + \Lambda(\mathbf{X})(J-1)J\nabla\mathbf{y}^{-T}\right] = \mathbf{0}, \quad \mathbf{X}\in\Omega_0\setminus\Gamma_0 \\ \widehat{\mathrm{Div}}\left[\hat{\gamma}_0\,\hat{J}\hat{\nabla}\mathbf{y}^{-T} + \hat{\mu}(\hat{\nabla}\mathbf{y}-\hat{\nabla}\mathbf{y}^{-T}) + \hat{\Lambda}(\hat{J}-1)\hat{J}\hat{\nabla}\mathbf{y}^{-T}\right] - \\ \left[\!\left[r_{\mathrm{i}}(\mathbf{X})J\nabla\mathbf{y}^{-T} + \mu(\mathbf{X})\left(\nabla\mathbf{y}-\nabla\mathbf{y}^{-T}\right) + \Lambda(\mathbf{X})(J-1)J\nabla\mathbf{y}^{-T}\right]\!\right]\widehat{\mathbf{N}} = \mathbf{0}, \quad \mathbf{X}\in\Gamma_0 \\ \mathbf{y}(\mathbf{X}) = \overline{\mathbf{F}}\mathbf{X}, \quad \mathbf{X}\in\partial\Omega_0 \end{cases} \tag{37}$$

for the deformation field $\mathbf{y}(\mathbf{X})$ and then computing the resulting average (33), or equivalently (36), for the macroscopic first Piola–Kirchhoff stress; in these equations, recall that the material parameters $\mu(\mathbf{X})$ and $\Lambda(\mathbf{X})$ are given by $(16)_{2,3}$ and the residual stress $r_{\mathrm{i}}(\mathbf{X})$ by (32). Akin to the classical case when there are no residual stresses nor interfacial forces (Ogden, 1974), the constitutive relationship between (33) and (34) turns out to be hyperelastic. That is, there is an effective stored-energy function, $\overline{W} = \overline{W}(\overline{\mathbf{F}})$ say, whose derivative with respect to the macroscopic deformation gradient $\overline{\mathbf{F}}$ yields the macroscopic first Piola–Kirchhoff stress $\overline{\mathbf{S}}$. Precisely, as elaborated in Appendix C to avoid loss of continuity,

$$\overline{\mathbf{S}} = \frac{\partial\overline{W}}{\partial\overline{\mathbf{F}}}(\overline{\mathbf{F}}) \qquad \text{with} \qquad \overline{W}(\overline{\mathbf{F}}) = \overline{W}_0 + \frac{1}{|\Omega_0|}\left(\int_{\Omega_0} W(\mathbf{X},\nabla\mathbf{y})\,\mathrm{d}\mathbf{X} + \int_{\Gamma_0}\widehat{W}(\hat{\nabla}\mathbf{y})\,\mathrm{d}\mathbf{X}\right). \tag{38}$$

In this last expression, the constant

$$\overline{W}_0 = -\frac{1}{|\Omega_0|}\left(\int_{\Omega_0} W(\mathbf{X},\mathbf{I})\,\mathrm{d}\mathbf{X} + \int_{\Gamma_0}\widehat{W}(\hat{\mathbf{I}})\,\mathrm{d}\mathbf{X}\right)$$

is introduced for the convenience of having $\overline{W}(\mathbf{I}) = 0$, the deformation field $\mathbf{y}(\mathbf{X})$ is solution[6] to (37), and we recall that the local stored-energy functions for the bulk W and the interfaces $\widehat{W}$ are given by (15) and (23). A simple change of variables $(\mathbf{y},\overline{\mathbf{F}}) \mapsto (\overline{\mathbf{Q}}^T\mathbf{y}, \overline{\mathbf{Q}}\,\overline{\mathbf{F}})$ in (37) suffices to establish that the effective stored-energy function $(38)_2$ satisfies the condition

$$\overline{W}(\overline{\mathbf{Q}}\,\overline{\mathbf{F}}) = \overline{W}(\overline{\mathbf{F}}) \qquad \text{for all } \overline{\mathbf{Q}}\in\mathrm{SO}(3) \tag{39}$$

and hence that it satisfies macroscopic material frame indifference. As a result, the macroscopic stress (33) and deformation gradient tensor (34) automatically satisfy the macroscopic balance of angular momentum

$$\overline{\mathbf{S}}\,\overline{\mathbf{F}}^T = \overline{\mathbf{F}}\,\overline{\mathbf{S}}^T. \tag{40}$$

[6] As already pointed out in the context of the general governing equations (29) above, at sufficiently large deformations, Eqs. (37) may admit multiple solutions $\mathbf{y}(\mathbf{X})$. The evaluation of $(38)_2$ should be carried out for the solution $\mathbf{y}(\mathbf{X})$ that is realized physically, which typically corresponds to the solution with lowest energy.

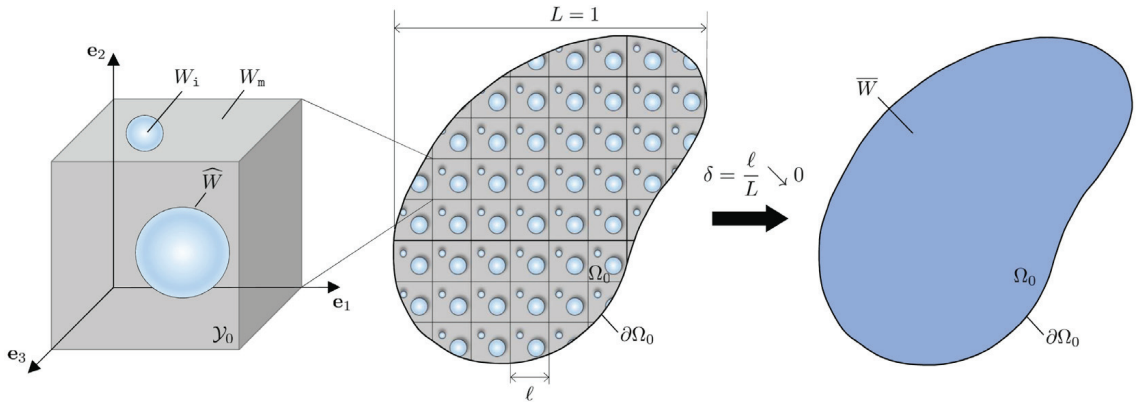

Fig. 3. Schematics of an elastomer filled with a periodic distribution of spherical liquid inclusions in the initial configuration Ω_0, of size $L = 1$, its defining unit cell $\mathcal{Y}_0 = (0, \ell)^3$, and the homogenization limit $\delta = \ell/L \searrow 0$. For simplicity, the schematic shown here is for a unit cell that contains only $M^\sharp = 2$ inclusions. Fig. 8 shows one of the actual unit cells, wherein $M^\sharp = 30$, that is used to generate the results presented in Section 6.

2.6.2. *The rigorous view*

The above definition of homogenized response is purely formal. To make it precise, consider elastomers filled with liquid inclusions that, as schematically depicted by Fig. 3, are periodically distributed over periods of size ℓ in the initial configuration Ω_0. Denote the length scale of Ω_0 by L, define the ratio of length scales $\delta = \ell/L$, and, for convenience, choose units so that $L = 1$ and hence $\delta = \ell$. In this setting, the collective indicator function $(1)_2$ for the inclusions is taken to be of the form

$$\theta_0^{\mathrm{i}}(\mathbf{X}) = \theta_0^{\sharp\mathrm{i}}(\delta^{-1}\mathbf{X}),$$

where $\theta_0^{\sharp\mathrm{i},j}(\mathbf{Y})$ is a $\mathcal{Y}_0$-periodic function with $\mathcal{Y}_0 = (0, \ell)^3$, that is, $\theta_0^{\sharp\mathrm{i}}(\mathbf{Y} + \ell\,\mathbf{Z}) = \theta_0^{\sharp\mathrm{i}}(\mathbf{Y})$ for all $\mathbf{Y} \in \mathcal{Y}_0$ and any $\mathbf{Z} \in \mathbb{Z}^3$. It follows that the material parameters $(16)_{2,3}$ and the residual stress (32) are also $\mathcal{Y}_0$-periodic. We write

$$\begin{cases} \mu(\mathbf{X}) = \mu^\sharp(\delta^{-1}\mathbf{X}) \quad \text{with} \quad \mu^\sharp(\delta^{-1}\mathbf{X}) = \left(1 - \theta_0^{\sharp\mathrm{i}}(\delta^{-1}\mathbf{X})\right)\mu_{\mathrm{m}} \\ \Lambda(\mathbf{X}) = \Lambda^\sharp(\delta^{-1}\mathbf{X}) \quad \text{with} \quad \Lambda^\sharp(\delta^{-1}\mathbf{X}) = \left(1 - \theta_0^{\sharp\mathrm{i}}(\delta^{-1}\mathbf{X})\right)\Lambda_{\mathrm{m}} + \theta_0^{\sharp\mathrm{i}}(\delta^{-1}\mathbf{X})\Lambda_{\mathrm{i}} \\ r_{\mathrm{i}}(\mathbf{X}) = r_{\mathrm{i}}^\sharp(\delta^{-1}\mathbf{X}) \quad \text{with} \quad r_{\mathrm{i}}^\sharp(\delta^{-1}\mathbf{X}) = -\displaystyle\sum_{j=1}^{M^\sharp} \theta_0^{\sharp\mathrm{i},j}(\delta^{-1}\mathbf{X})\frac{2\widehat{\gamma}_0}{A_j} \end{cases}, \tag{41}$$

where $M^\sharp$ stands for the number of inclusions within the unit cell $\mathcal{Y}_0$ while $\theta_0^{\sharp\mathrm{i},j}(\mathbf{Y})$ denotes the indicator function describing the initial spatial locations that they occupy in $\mathcal{Y}_0$.

For a fixed value of the ratio of length scales δ, neglecting body forces and using a superscript δ to denote dependence on this parameter explicitly, the general governing equations (29) specialize to

$$\begin{cases} \mathrm{Div}\left[r_{\mathrm{i}}^\sharp(\delta^{-1}\mathbf{X})J^\delta\nabla\mathbf{y}^{\delta-T} + \mu^\sharp(\delta^{-1}\mathbf{X})\left(\nabla\mathbf{y}^\delta - \nabla\mathbf{y}^{\delta-T}\right) + \Lambda^\sharp(\delta^{-1}\mathbf{X})(J^\delta - 1)J^\delta\nabla\mathbf{y}^{\delta-T}\right] = \mathbf{0}, \quad \mathbf{X} \in \Omega_0 \setminus \Gamma_0 \\ \widehat{\mathrm{Div}}\left[\widehat{\gamma}_0\,\widehat{J}^\delta\widehat{\nabla}\mathbf{y}^{\delta-T} + \widehat{\mu}(\widehat{\nabla}\mathbf{y}^\delta - \widehat{\nabla}\mathbf{y}^{\delta-T}) + \widehat{\Lambda}(\widehat{J}^\delta - 1)\widehat{J}^\delta\widehat{\nabla}\mathbf{y}^{\delta-T}\right] - \\ \left[\!\left[r_{\mathrm{i}}^\sharp(\delta^{-1}\mathbf{X})J^\delta\nabla\mathbf{y}^{\delta-T} + \mu^\sharp(\delta^{-1}\mathbf{X})\left(\nabla\mathbf{y}^\delta - \nabla\mathbf{y}^{\delta-T}\right) + \Lambda^\sharp(\delta^{-1}\mathbf{X})(J^\delta - 1)J^\delta\nabla\mathbf{y}^{\delta-T}\right]\!\right]\widehat{\mathbf{N}} = \mathbf{0}, \quad \mathbf{X} \in \Gamma_0 \\ \mathbf{y}^\delta(\mathbf{X}) = \overline{\mathbf{y}}(\mathbf{X}), \quad \mathbf{X} \in \partial\Omega_0^D \\ \left[\mu_{\mathrm{m}}\left(\nabla\mathbf{y}^\delta - \nabla\mathbf{y}^{\delta-T}\right) + \Lambda_{\mathrm{m}}(J^\delta - 1)J^\delta\nabla\mathbf{y}^{\delta-T}\right]\mathbf{N} = \overline{\mathbf{s}}(\mathbf{X}), \quad \mathbf{X} \in \partial\Omega_0^{\mathcal{N}} \end{cases} \tag{42}$$

for the deformation field $\mathbf{y}^\delta(\mathbf{X})$. The expectation is that one can pass to the limit as $\delta \searrow 0$ in (42) and show that the deformation field $\mathbf{y}^\delta(\mathbf{X})$ converges to a macroscopic deformation field $\mathbf{y}(\mathbf{X})$ solution of the elastostatics equations

$$\begin{cases} \mathrm{Div}\left[\dfrac{\partial\overline{W}}{\partial\overline{\mathbf{F}}}(\nabla\mathbf{y})\right] = \mathbf{0}, \quad \mathbf{X} \in \Omega_0 \\ \mathbf{y}(\mathbf{X}) = \overline{\mathbf{y}}(\mathbf{X}), \quad \mathbf{X} \in \partial\Omega_0^D \\ \left[\dfrac{\partial\overline{W}}{\partial\overline{\mathbf{F}}}(\nabla\mathbf{y})\right]\mathbf{N} = \overline{\mathbf{s}}(\mathbf{X}), \quad \mathbf{X} \in \partial\Omega_0^{\mathcal{N}} \end{cases} \tag{43}$$

for a *homogeneous* hyperelastic solid.[7] Moreover, based on the classical homogenization result of Braides (1985) and Müller (1987) for hyperelastic solids without residual stresses and interfacial forces, the expectation is that the effective stored-energy function $\overline{W}$ in (43) is given by the formula

$$\overline{W}(\overline{\mathbf{F}}) = \overline{W}_0^\sharp + \frac{1}{|\mathcal{Y}_0^{\mathbf{k}}|}\left(\int_{\mathcal{Y}_0^{\mathbf{k}}} W^\sharp(\mathbf{Y},\nabla\chi)\,\mathrm{d}\mathbf{Y} + \int_{\mathcal{G}_0^{\mathbf{k}}} \widehat{W}(\widehat{\nabla}\chi)\,\mathrm{d}\mathbf{Y}\right), \tag{44}$$

where the constant

$$\overline{W}_0^\sharp = -\frac{1}{|\mathcal{Y}_0^{\mathbf{k}}|}\left(\int_{\mathcal{Y}_0^{\mathbf{k}}} W^\sharp(\mathbf{Y},\mathbf{I})\,\mathrm{d}\mathbf{Y} + \int_{\mathcal{G}_0^{\mathbf{k}}} \widehat{W}(\widehat{\mathbf{I}})\,\mathrm{d}\mathbf{Y}\right)$$

is introduced for the convenience of having $\overline{W}(\mathbf{I}) = 0$, and where

$$W^\sharp(\mathbf{Y},\mathbf{F}) = r_1^\sharp(\mathbf{Y})J + \frac{\mu^\sharp(\mathbf{Y})}{2}\left[\mathbf{F}\cdot\mathbf{F} - 3\right] - \mu^\sharp(\mathbf{Y})\ln J + \frac{\Lambda^\sharp(\mathbf{Y})}{2}(J-1)^2,$$

we recall that the material parameters $\mu^\sharp(\mathbf{Y})$ and $\Lambda^\sharp(\mathbf{Y})$ and the residual stress $r_1^\sharp(\mathbf{Y})$ are given by (41), the local stored-energy function for the interface $\widehat{W}$ is given by (23), $\mathbf{k}\in\mathbb{N}^3$, $\mathcal{Y}_0^{\mathbf{k}} := \mathbf{k}\mathcal{Y}_0$, $\mathcal{G}_0$ ($\mathcal{G}_0^{\mathbf{k}}$) denotes the domain occupied by the interfaces in the unit cell $\mathcal{Y}_0$ (super cell $\mathcal{Y}_0^{\mathbf{k}}$), and $\chi(\mathbf{Y})$ is the field

$$\chi(\mathbf{Y}) = \overline{\mathbf{F}}\mathbf{Y} + \mathbf{u}(\mathbf{Y}) \text{ with } \mathcal{Y}_0^{\mathbf{k}}\text{–periodic fluctuation } \mathbf{u}(\mathbf{Y}) \tag{45}$$

defined as the solution of the super-cell problem

$$\begin{cases} \mathrm{Div}\left[r_1^\sharp(\mathbf{Y})\mathcal{J}\nabla\chi^{-T} + \mu^\sharp(\mathbf{Y})\left(\nabla\chi - \nabla\chi^{-T}\right) + \Lambda^\sharp(\mathbf{Y})(\mathcal{J}-1)\mathcal{J}\nabla\chi^{-T}\right] = \mathbf{0}, \quad \mathbf{Y}\in\mathcal{Y}_0^{\mathbf{k}}\setminus\mathcal{G}_0^{\mathbf{k}} \\ \widehat{\mathrm{Div}}\left[\hat{\gamma}_0\,\widehat{\mathcal{J}}\widehat{\nabla}\chi^{-T} + \hat{\mu}(\widehat{\nabla}\chi - \widehat{\nabla}\chi^{-T}) + \hat{\Lambda}(\widehat{\mathcal{J}}-1)\widehat{\mathcal{J}}\widehat{\nabla}\chi^{-T}\right] - \\ \left[\!\left[r_1^\sharp(\mathbf{Y})\mathcal{J}\nabla\chi^{-T} + \mu^\sharp(\mathbf{Y})\left(\nabla\chi - \nabla\chi^{-T}\right) + \Lambda^\sharp(\mathbf{Y})(\mathcal{J}-1)\mathcal{J}\nabla\chi^{-T}\right]\!\right]\widehat{\mathbf{N}} = \mathbf{0}, \quad \mathbf{Y}\in\mathcal{G}_0^{\mathbf{k}} \end{cases} \tag{46}$$

with $\mathcal{J} = \det\nabla\chi$ and $\widehat{\mathcal{J}} = \widehat{\det}\,\widehat{\nabla}\chi$.

We emphasize that the size of the super cell in (44)–(46), as characterized by the vector $\mathbf{k}$, is *not* known a priori. Due to the possibility of bifurcations at sufficiently large deformations, one has to identify the period $\mathbf{k}\mathcal{Y}_0$ of the solution that is preferred by the filled elastomer at hand – typically, the solution with lowest energy – thereby determining the appropriate value of $\mathbf{k}$; see, e.g., Geymonat et al. (1993). In direct analogy with the average relation (36), as shown in Appendix C, we note that

$$\overline{\mathbf{S}} = \frac{\partial\overline{W}}{\partial\overline{\mathbf{F}}}(\overline{\mathbf{F}}) = \frac{1}{|\mathcal{Y}_0^{\mathbf{k}}|}\left(\int_{\mathcal{Y}_0^{\mathbf{k}}} \mathbf{S}^\sharp(\mathbf{Y})\,\mathrm{d}\mathbf{Y} + \int_{\mathcal{G}_0^{\mathbf{k}}} \widehat{\mathbf{S}}(\mathbf{Y})\,\mathrm{d}\mathbf{Y}\right), \tag{47}$$

where $\mathbf{S}^\sharp(\mathbf{Y}) = \partial W^\sharp(\mathbf{Y},\mathbf{F})/\partial\mathbf{F}$. In analogy with (39)–(40), we also note that the effective stored-energy function (44) satisfies the condition of macroscopic material frame indifference $\overline{W}(\overline{\mathbf{Q}}\,\overline{\mathbf{F}}) = \overline{W}(\overline{\mathbf{F}})$ for all $\overline{\mathbf{Q}}\in\mathrm{SO}(3)$ and that, as a result, the macroscopic stress (47) and macroscopic deformation gradient tensor $\overline{\mathbf{F}}$ automatically satisfy the macroscopic balance of angular momentum $\overline{\mathbf{S}}\,\overline{\mathbf{F}}^T = \overline{\mathbf{F}}\,\overline{\mathbf{S}}^T$.

The definition (44) for the effective stored-energy function $\overline{W}(\overline{\mathbf{F}})$ for filled elastomers with periodic microstructures is entirely consistent with the formal definition (38). Their computation amounts to solving the nonlinear boundary-value problem (37), or equivalently (46), and carrying out the appropriate averages. In general, these equations can only be solved numerically. As announced in the Introduction, one of the objectives of this work is to put forth a FE scheme to construct numerical solutions for such a type of equations. For definiteness, we focus on the Eqs. (46) for materials with periodic microstructures and present the corresponding FE scheme in Section 4. As elaborated prior to that in Section 3, nevertheless, Eqs. (46) admit great simplification in the limit of small deformations and thus permit further analytical treatment which is insightful spelling out.

3. The homogenized response in the small-deformation limit

In the limit of small deformations as $\|\overline{\mathbf{F}} - \mathbf{I}\| \to 0$, the nonlinear elastostatics super-cell problem (46) reduces asymptotically to a *linear* elastostatics unit-cell problem, albeit a non-standard one with residual stresses and a non-standard jump condition across material interfaces due to the presence of interfacial forces. It follows that the resulting macroscopic constitutive response (47) reduces to one of *linear elasticity*. The derivation of this asymptotic result goes as follows.

Introduce the macroscopic deformation measure $\overline{\mathbf{H}} = \overline{\mathbf{F}} - \mathbf{I}$ and consider solutions to (46) of the asymptotic form

$$\chi(\mathbf{Y}) = \mathbf{Y} + \overline{\mathbf{H}}\mathbf{Y} + \mathbf{u}(\mathbf{Y}) + O(\|\overline{\mathbf{H}}\|^2) \text{ with } u_i(\mathbf{Y}) = \omega_{ijk}(\mathbf{Y})\overline{H}_{jk} \text{ where } \boldsymbol{\omega}(\mathbf{Y}) \text{ is } \mathcal{Y}_0\text{–periodic}$$

[7] Passing to the limit rigorously in (42) is currently out of reach. In the more tractable asymptotic setting of small deformations, however, passing to the limit rigorously should be possible, as the companion two-scale asymptotic analysis of Ghosh et al. (2022) suggests.

in the limit as $\|\overline{\mathbf{H}}\| \to 0$. The tensor $\boldsymbol{\omega}$ quantifying the linearity of the displacement field $\mathbf{u}(\mathbf{Y})$ in $\overline{\mathbf{H}}$ is the so-called "concentration" tensor. By making explicit use of this ansatz, standard calculations show that the Eqs. (46) reduce to $O(\|\overline{\mathbf{H}}\|)$ to the unit-cell problem

$$\begin{cases} \mathrm{Div}\left[\mathbf{L}^\sharp(\mathbf{Y})(\overline{\mathbf{H}}+\nabla\mathbf{u})\right]=\mathbf{0}, \quad \mathbf{Y}\in\mathcal{Y}_0\setminus\mathcal{G}_0 \\ \widehat{\mathrm{Div}}\left[\widehat{\mathbf{L}}(\overline{\mathbf{H}}+\nabla\mathbf{u})\widehat{\mathbf{I}}\right]-\left[\!\left[\mathbf{L}^\sharp(\mathbf{Y})(\overline{\mathbf{H}}+\nabla\mathbf{u})\right]\!\right]\widehat{\mathbf{N}}=\mathbf{0}, \quad \mathbf{Y}\in\mathcal{G}_0 \end{cases} \tag{48}$$

for the displacement field $\mathbf{u}(\mathbf{Y})$. In these equations,

$$\mathbf{L}^\sharp(\mathbf{Y}) = r_{\mathrm{i}}^\sharp(\mathbf{Y})\boldsymbol{\mathcal{A}} + \left(2\mu^\sharp(\mathbf{Y}) - r_{\mathrm{i}}^\sharp(\mathbf{Y})\right)\boldsymbol{\mathcal{K}} + \left(2\mu^\sharp(\mathbf{Y}) + 2r_{\mathrm{i}}^\sharp(\mathbf{Y}) + 3\lambda^\sharp(\mathbf{Y})\right)\boldsymbol{\mathcal{J}}, \tag{49}$$

where we recall that $\boldsymbol{\mathcal{A}}$, $\boldsymbol{\mathcal{K}}$, $\boldsymbol{\mathcal{J}}$ are the orthonormal tensors (21), $\widehat{\mathbf{L}}$ is given by (28), and critical use has been made of the fact that the residual stress and the initial surface tension are self-equilibrated, that is, $\mathrm{Div}[r_{\mathrm{i}}^\sharp(\mathbf{Y})\mathbf{I}]=\mathbf{0}$ and $\widehat{\gamma}_0\widehat{\mathrm{Div}}\,\widehat{\mathbf{I}} - [\![r_{\mathrm{i}}^\sharp(\mathbf{Y})]\!]\widehat{\mathbf{N}}=\mathbf{0}$. When written explicitly in terms of the concentration tensor $\boldsymbol{\omega}(\mathbf{Y})$, upon removing the common factor $\overline{\mathbf{H}}$, the unit-cell problem (48) reads

$$\begin{cases} \dfrac{\partial}{\partial Y_j}\left[L^\sharp_{ijkl}(\mathbf{Y})\left(\delta_{km}\delta_{\ln}+\dfrac{\partial\omega_{kmn}}{\partial Y_l}(\mathbf{Y})\right)\right]=0, \quad \mathbf{Y}\in\mathcal{Y}_0\setminus\mathcal{G}_0 \\ \dfrac{\partial}{\partial Y_q}\left[\widehat{L}_{ijkl}\left(\delta_{km}\widehat{I}_{nl}+\widehat{I}_{pl}\dfrac{\partial\omega_{kmn}}{\partial Y_p}(\mathbf{Y})\right)\right]\widehat{I}_{qj}-\left[\!\left[L^\sharp_{ijkl}(\mathbf{Y})\left(\delta_{km}\delta_{\ln}+\dfrac{\partial\omega_{kmn}}{\partial Y_l}(\mathbf{Y})\right)\right]\!\right]\widehat{N}_j=0, \quad \mathbf{Y}\in\mathcal{G}_0 \end{cases} . \tag{50}$$

By the same token, it is not difficult to deduce that in the limit as $\|\overline{\mathbf{H}}\| \to 0$ the macroscopic constitutive response (47) reduces to $O(\|\overline{\mathbf{H}}\|)$ to the linear relation

$$\overline{\mathbf{S}} = \overline{\mathbf{L}}\,\overline{\mathbf{H}} + O(\|\overline{\mathbf{H}}\|^2) \tag{51}$$

with

$$\overline{L}_{ijkl} = \frac{1}{|\mathcal{Y}_0|}\left(\int_{\mathcal{Y}_0} L^\sharp_{ijmn}(\mathbf{Y})\left(\delta_{mk}\delta_{nl}+\frac{\partial\omega_{mkl}}{\partial Y_n}(\mathbf{Y})\right)\mathrm{d}\mathbf{Y} + \int_{\mathcal{G}_0}\widehat{L}_{ijmn}\left(\delta_{mk}\widehat{I}_{nl}+\widehat{I}_{pn}\frac{\partial\omega_{mkl}}{\partial Y_p}(\mathbf{Y})\right)\mathrm{d}\mathbf{Y}\right), \tag{52}$$

where $\boldsymbol{\omega}(\mathbf{Y})$ is the solution to the unit-cell problem (50). The following remarks are in order.

Remark 11 (*Existence of Solution for the Unit-Cell Problem* (50))**.** Given that the pointwise moduli of elasticity (49) and (28) for the bulk and the interfaces are *not* positive definite in general, the standard argument based on the Lax–Milgram theorem does *not* apply to prove existence of solution for the unit-cell problem (50). We are currently working on a proof of existence that we shall present elsewhere.

Remark 12 (*Absence of a Macroscopic Residual Stress*)**.** The macroscopic constitutive response (51) is free of residual stresses, this in spite of the fact that there is a local residual stress within the inclusions and an initial surface tension on the elastomer/inclusions interfaces. The reason behind this result is that the average of the local residual stress and initial surface tension cancel each other out. Precisely,

$$\int_{\mathcal{Y}_0} r_{\mathrm{i}}^\sharp(\mathbf{Y})\mathbf{I}\,\mathrm{d}\mathbf{Y} + \int_{\mathcal{G}_0}\widehat{\gamma}_0\widehat{\mathbf{I}}\,\mathrm{d}\mathbf{Y} = \sum_{j=1}^{M^\sharp}\left(-\frac{4}{3}\pi A_j^3\frac{2\widehat{\gamma}_0}{A_j}+4\pi A_j^2\widehat{\gamma}_0-\frac{4}{3}\pi A_j^3\frac{\widehat{\gamma}_0}{A_j}\right)\mathbf{I}=\mathbf{0}. \tag{53}$$

Remark 13 (*Symmetries of the Effective Modulus of Elasticity* $\overline{\mathbf{L}}$)**.** Remarkably, the effective modulus of elasticity (52) satisfies the major and minor symmetries

$$\overline{L}_{ijkl}=\overline{L}_{klij} \quad \text{and} \quad \overline{L}_{ijkl}=\overline{L}_{jikl}=\overline{L}_{ijlk}$$

of a conventional homogeneous elastic solid, this in spite of the fact that the local moduli of elasticity $\mathbf{L}^\sharp(\mathbf{Y})$ and $\widehat{\mathbf{L}}$ for the bulk and the interfaces do *not* possess minor symmetries.

The major symmetry $\overline{L}_{ijkl}=\overline{L}_{klij}$ is a direct consequence of the fact that the macroscopic constitutive response (51) is hyperelastic. Indeed, the formula (52) can be rewritten in the equivalent form

$$\overline{L}_{ijkl} = \frac{1}{|\mathcal{Y}_0|}\left(\int_{\mathcal{Y}_0}\left(\delta_{mi}\delta_{nj}+\frac{\partial\omega_{mij}}{\partial Y_n}(\mathbf{Y})\right)L^\sharp_{mnpq}(\mathbf{Y})\left(\delta_{pk}\delta_{ql}+\frac{\partial\omega_{pkl}}{\partial Y_q}(\mathbf{Y})\right)\mathrm{d}\mathbf{Y}+\right.$$
$$\left.\int_{\mathcal{G}_0}\left(\delta_{mi}\widehat{I}_{nj}+\widehat{I}_{rn}\frac{\partial\omega_{mij}}{\partial Y_r}(\mathbf{Y})\right)\widehat{L}_{mnpq}\left(\delta_{pk}\widehat{I}_{ql}+\widehat{I}_{sq}\frac{\partial\omega_{pkl}}{\partial Y_s}(\mathbf{Y})\right)\mathrm{d}\mathbf{Y}\right),$$

from which it is trivial to establish that $\overline{L}_{ijkl}=\overline{L}_{klij}$ since $L^\sharp_{mnpq}(\mathbf{Y})=L^\sharp_{pqmn}(\mathbf{Y})$ and $\widehat{L}_{mnpq}=\widehat{L}_{pqmn}$.

The minor symmetries $\overline{L}_{ijkl} = \overline{L}_{jikl}$ and $\overline{L}_{ijkl} = \overline{L}_{ijlk}$, on the other hand, are a direct consequence of the macroscopic material frame indifference of the effective stored-energy function (44), which implies macroscopic balance of angular momentum, and the absence (53) of a macroscopic residual stress. Indeed, after recognizing that

$$\int_{\mathcal{Y}_0} r_{\mathrm{i}}^{\sharp}(\mathbf{Y})\left(\delta_{il}\delta_{jk} + \frac{\partial \omega_{jkl}}{\partial Y_i}(\mathbf{Y})\right) \mathrm{d}\mathbf{Y} + \int_{\mathcal{C}_0} \widehat{\gamma}_0 \left(\delta_{jk}\widehat{I}_{il} + \widehat{I}_{ip}\frac{\partial \omega_{jkl}}{\partial Y_p}(\mathbf{Y})\right) \mathrm{d}\mathbf{Y} = 0,$$

it is straightforward to show that the formula (52) can be rewritten as

$$\overline{L}_{ijkl} = \frac{1}{|\mathcal{Y}_0|}\left(\int_{\mathcal{Y}_0}\left(L_{ijmn}^{\sharp}(\mathbf{Y}) + r_{\mathrm{i}}^{\sharp}(\mathbf{Y})\delta_{in}\delta_{jm}\right)\left(\delta_{mk}\delta_{nl} + \frac{\partial \omega_{mkl}}{\partial Y_n}(\mathbf{Y})\right)\mathrm{d}\mathbf{Y} + \right.$$
$$\left. \int_{\mathcal{C}_0}\left(\widehat{L}_{ijmn} + \widehat{\gamma}_0\delta_{jm}\widehat{I}_{in}\right)\left(\delta_{mk}\widehat{I}_{nl} + \widehat{I}_{pn}\frac{\partial \omega_{mkl}}{\partial Y_p}(\mathbf{Y})\right)\mathrm{d}\mathbf{Y}\right),$$

from which it is trivial to establish that $\overline{L}_{ijkl} = \overline{L}_{jikl}$ since $L_{ijmn}^{\sharp}(\mathbf{Y}) + r_{\mathrm{i}}^{\sharp}(\mathbf{Y})\delta_{in}\delta_{jm}$ and $\widehat{L}_{ijmn} + \widehat{\gamma}_0\delta_{jm}\widehat{I}_{in}$ possess minor symmetries. Minor symmetries in the last two indices $\overline{L}_{ijkl} = \overline{L}_{ijlk}$ can be established by exploiting the major symmetry $\overline{L}_{ijkl} = \overline{L}_{klij}$ and then following the same steps as above.

Remark 14 (*Positive Definiteness of* $\overline{\mathbf{L}}$)**.** Physically, for suitably well-behaved residual stresses $r_{\mathrm{i}}(\mathbf{X})$, the expectation is that the effective modulus of elasticity (52) be positive definite. However, given that the pointwise moduli of elasticity (49) and (28) for the bulk and the interfaces are *not* positive definite in general, the standard argument based on pointwise positive energy density (see, e.g., Section 2.3 of Chapter 1 in the monograph by Bensoussan et al., 2011) to prove so does *not* apply here. This difficulty is intimately related to the difficulty of proving existence for the unit-cell problem (50) noted in Remark 11. We shall address both of these issues in a future contribution.

Remark 15 (*Computation of* $\overline{\mathbf{L}}$)**.** In general, the solution to the unit-cell problem (50) for the concentration tensor $\boldsymbol{\omega}(\mathbf{Y})$ required to compute the effective modulus of elasticity (52) can only be generated numerically. In this work, as elaborated in the next section within the more general setting of finite deformations, we put forth a FE scheme to solve such a type of unit-cell problems.

Dilute microstructures. Nonetheless, there are classes of microstructures of practical interest that do admit analytical solutions for (50). The most fundamental among these is that of a dilute volume fraction of inclusions, when

$$c \searrow 0, \qquad c := \frac{1}{|\mathcal{Y}_0|}\int_{\mathcal{Y}_0} \theta_0^{\sharp \mathrm{i}}(\mathbf{Y})\,\mathrm{d}\mathbf{Y},$$

that are all of monodisperse size $A_j = A$, for which $\boldsymbol{\omega}(\mathbf{Y})$ can be explicitly determined in terms of spherical harmonics; see Appendix D. For instance, the resulting effective modulus of elasticity (52) for the physically relevant case of a dilute suspension of incompressible liquid inclusions with interfaces that only exhibit surface tension, when $\Lambda_{\mathrm{i}} = +\infty$ and $\widehat{\mu} = \widehat{\Lambda} = 0$, reads

$$\overline{\mathbf{L}} = 2\,\overline{\mu}^{\,\mathrm{dil}}\,\boldsymbol{\mathcal{K}} + \left(2\,\overline{\mu}^{\,\mathrm{dil}} + 3\overline{\Lambda}^{\,\mathrm{dil}}\right)\boldsymbol{\mathcal{J}} + O(c^2)$$

with

$$\overline{\mu}^{\,\mathrm{dil}} = \mu_{\mathrm{m}} + \frac{15\mu_{\mathrm{m}}(2\mu_{\mathrm{m}} + \Lambda_{\mathrm{m}})\left(\dfrac{\widehat{\gamma}_0}{2A} - \mu_{\mathrm{m}}\right)}{\mu_{\mathrm{m}}(14\mu_{\mathrm{m}} + 9\Lambda_{\mathrm{m}}) + \dfrac{\widehat{\gamma}_0}{2A}(34\mu_{\mathrm{m}} + 15\Lambda_{\mathrm{m}})}\,c \tag{54}$$

and

$$\overline{\Lambda}^{\,\mathrm{dil}} = \Lambda_{\mathrm{m}} + \frac{3(2\mu_{\mathrm{m}} + \Lambda_{\mathrm{m}})\left(\Lambda_{\mathrm{m}}\left(6\mu_{\mathrm{m}} + 5\dfrac{\widehat{\gamma}_0}{A}\right) + 8\mu_{\mathrm{m}}\left(2\mu_{\mathrm{m}} + \dfrac{\widehat{\gamma}_0}{A}\right)\right)}{2\mu_{\mathrm{m}}(14\mu_{\mathrm{m}} + 9\Lambda_{\mathrm{m}}) + \dfrac{\widehat{\gamma}_0}{A}(34\mu_{\mathrm{m}} + 15\Lambda_{\mathrm{m}})}\,c. \tag{55}$$

For incompressible elastomers, when $\Lambda_{\mathrm{m}} = +\infty$, the effective shear and first Lamé moduli (54)–(55) further specialize to

$$\overline{\mu}^{\,\mathrm{dil,inc}} = \mu_{\mathrm{m}} + \frac{5\left(\dfrac{\widehat{\gamma}_0}{2A} - \mu_{\mathrm{m}}\right)\mu_{\mathrm{m}}}{3\mu_{\mathrm{m}} + 5\dfrac{\widehat{\gamma}_0}{2A}}\,c \qquad \text{and} \qquad \overline{\Lambda}^{\,\mathrm{dil,inc}} = +\infty. \tag{56}$$

As first recognized by Style et al. (2015a), the simple result (56) serves to bring front and center the effect that interface mechanics can have in the macroscopic behavior of elastomers filled with liquid inclusions. For small surface-tension-to-inclusion-size ratio $\widehat{\gamma}_0/2A$ relative to the shear modulus of the matrix μ_{m}, the effective shear modulus $(56)_1$ reduces to the classical result of Eshelby and thus states that the presence of liquid inclusions leads to the *softening* of the response of the material in the sense that $\overline{\mu}^{\,\mathrm{dil,inc}} < \mu_{\mathrm{m}}$. For large $\widehat{\gamma}_0/2A$ relative to μ_{m}, on the other hand, the result $(56)_1$ indicates that $\overline{\mu}^{\,\mathrm{dil,inc}} > \mu_{\mathrm{m}}$. That is, the presence of liquid inclusions leads to the *stiffening* of the response of the material. This can be understood at once by recognizing that initially spherical liquid

inclusions with large $\widehat{\gamma}_0/2A$ pose great resistance to deformation and hence *de facto* behave like stiff inclusions. The transition from softening to stiffening occurs at the equality $\widehat{\gamma}_0/2A = \mu_{\rm m}$, which, rather interestingly, results in the presence of liquid inclusions going unnoticed[8] in the sense that $\overline{\mu}^{\rm dil,inc} = \mu_{\rm m}$. This transition prompts the definition of the *elasto-capillary number*

$$eCa := \frac{\widehat{\gamma}_0}{2\mu_{\rm m} A}, \tag{57}$$

in terms of which the effective shear modulus $(56)_1$ can be rewritten as

$$\overline{\mu}^{\rm dil,inc} = \mu_{\rm m} + \frac{5\,(eCa-1)}{3+5\,eCa}\,\mu_{\rm m}\,c. \tag{58}$$

Here, it is important to emphasize that the definition (57) is only meaningful as an elasto-capillary number within the asymptotic setting of infinitesimally small deformations. Another interesting observation is that, in the limit as $\widehat{\gamma}_0/2A \to +\infty$, the effective shear modulus $(56)_1$ reduces to $\overline{\mu}^{\rm dil,inc} = \mu_{\rm m} + \mu_{\rm m}\,c$, which is significantly smaller than the corresponding Einstein's result for spherical rigid inclusions $\overline{\mu}^{\rm dil,rig} = \mu_{\rm m} + (5/2)\mu_{\rm m}\,c$. The reason for this (factor of 2.5) difference is that the forces at a matrix/liquid-inclusion interface featuring surface tension are different from those at a matrix/rigid-inclusion interface, even in the limit as $\widehat{\gamma}_0/2A \to +\infty$.

Iterative microstructures. Other classes of microstructures that admit analytically tractable solutions beyond the dilute limit are those that can be constructed via iterative homogenization (Bruggeman, 1935; Norris, 1985; Avellaneda, 1987). For example, in the footstep of Christensen and Lo (1979), several authors (Duan et al., 2005b; Mancarella et al., 2016) have worked out solutions for the so-called differential-coated-sphere (DCS) assemblages; see also Krichen et al. (2019).

As recently discussed by Lefèvre and Lopez-Pamies (2022), many other iterative microstructures beyond DCS assemblages with different percolation thresholds allow for analytical solutions as well. The simplest among these is the one that results from the standard *differential scheme* (Bruggeman, 1935) for which the effective modulus of elasticity $\overline{\mathbf{L}} = \overline{\mathbf{L}}(c)$ is implicitly defined by the solution to the initial-value problem

$$\begin{cases} (1-c)\dfrac{{\rm d}\overline{\mathbf{L}}}{{\rm d}c}(c) - \boldsymbol{\mathcal{H}}\left\{\overline{\mathbf{L}};\mu_{\rm i},\Lambda_{\rm i},\widehat{\mathbf{L}}\right\} = 0 \\ \overline{\mathbf{L}}(0) = \mathbf{L}_{\rm m} = 2\mu_{\rm m}\boldsymbol{\mathcal{K}} + \left(2\,\mu_{\rm m} + 3\Lambda_{\rm m}\right)\boldsymbol{\mathcal{J}} \end{cases}, \tag{59}$$

where $\boldsymbol{\mathcal{H}}\{\overline{\mathbf{L}};\mu_{\rm i},\Lambda_{\rm i},\widehat{\mathbf{L}}\}$ is the tensor function such that $\overline{\mathbf{L}} = \mathbf{L}_{\rm m} + \boldsymbol{\mathcal{H}}\left\{\mathbf{L}_{\rm m};\mu_{\rm i},\Lambda_{\rm i},\widehat{\mathbf{L}}\right\}\,c + O(c^2)$ in the dilute limit of inclusions.

When considering the physically relevant case of suspensions of incompressible liquid inclusions embedded in an incompressible elastomer with interfaces that only exhibit surface tension, it follows immediately from (56) and (57) that the tensor function $\boldsymbol{\mathcal{H}}$ specializes to

$$\boldsymbol{\mathcal{H}}\left\{\mathbf{L}_{\rm m};0,+\infty,\widehat{\mathbf{L}}\right\} = \frac{5\,(eCa-1)}{3+5\,eCa}\,\mu_{\rm m}\,\boldsymbol{\mathcal{K}} + \infty\boldsymbol{\mathcal{J}}.$$

The resulting initial-value problem (59) for the effective modulus of elasticity can be readily solved in closed form yielding the simple formula

$$\overline{\mathbf{L}} = 2\,\overline{\mu}^{\rm DS}\,\boldsymbol{\mathcal{K}} + \left(2\,\overline{\mu}^{\rm DS} + 3\overline{\Lambda}^{\rm DS}\right)\boldsymbol{\mathcal{J}}$$

with

$$\overline{\mu}^{\rm DS} = \frac{\mu_{\rm m}}{(1-c)^{\frac{5(eCa-1)}{3+5eCa}}} \qquad \text{and} \qquad \overline{\Lambda}^{\rm DS} = +\infty. \tag{60}$$

By construction, the result (60) corresponds to the *exact* effective elastic constants of an incompressible elastomer filled with an isotropic distribution of initially spherical inclusions of infinitely many radii that are scaled in a manner such that they all have identical elasto-capillary number (57) and are distributed in a manner such that they can fill the entire space, thus their percolation at $c = 1$.

As revealed by the comparisons with the numerical solutions presented in Section 6 below, the formula $(60)_1$ has the added merit of being accurately descriptive of isotropic suspensions of liquid inclusions of monodisperse size for volume fractions in the small-to-moderate[9] range, up to roughly $c = 0.20$. It is also worth remarking that, much like its asymptotic counterpart (58) for dilute suspensions, $\overline{\mu}^{\rm DS} < \mu_{\rm m}$ for $eCa < 1$, $\overline{\mu}^{\rm DS} > \mu_{\rm m}$ for $eCa > 1$, and $\overline{\mu}^{\rm DS} = \mu_{\rm m}$ for $eCa = 1$. That is, irrespectively of their volume fraction c, inclusions with elasto-capillary number $eCa < 1$ lead to the softening of the response of the material, while those with $eCa > 1$ lead to stiffening. Precisely at $eCa = 1$, the presence of inclusions goes unnoticed in the sense that $\overline{\mu}^{\rm DS} = \mu_{\rm m}$. Moreover, in the limits as $eCa \searrow 0$ and $eCa \to +\infty$, the effective shear modulus (60) reduces to $\overline{\mu}^{\rm DS} = \mu_{\rm m}/(1-c)^{-5/3}$ and $\overline{\mu}^{\rm DS} = \mu_{\rm m}/(1-c)$, respectively. The former, of course, agrees identically with the classical differential-scheme result for suspensions of spherical incompressible liquid inclusions (Roscoe, 1973). The latter, interestingly, is significantly smaller than the corresponding result due to Brinkman

[8] In other words, the value $\widehat{\gamma}_0/2A = \mu_{\rm m}$ leads to the "cloaking" of the homogenized response; see, e.g., Yavari and Golgoon (2019) and references therein for a detailed account of cloaking phenomena in mechanics.

[9] In view of the recent work of Lefèvre and Lopez-Pamies (2022) on suspensions of monodisperse spherical rigid inclusions, the construction of an iterative-homogenization solution that remains accurately descriptive over the entire range of volume fractions of monodisperse spherical liquid inclusions – from the dilute limit $c \searrow 0$ to the percolation threshold $c \nearrow c_p \approx 0.64$ (Scott, 1960) – is most certainly viable.

(1952) and Roscoe (1952) for spherical rigid inclusions $\overline{\mu}^{\rm DS,rig} = \mu_{\rm m}/(1-c)^{5/2}$. Again, the reason for this significant difference is that the forces at a matrix/liquid-inclusion interface are different from those at a matrix/rigid-inclusion interface, even in the limit as $eCa \to +\infty$.

4. The homogenized response at finite deformations

When considering arbitrary macroscopic deformation gradients $\overline{\mathbf{F}}$, as already pointed out above, the super-cell problem (46) defining the macroscopic response (47) can only be solved numerically. In this section, we present a robust FE scheme to generate solutions for (46) that is specifically designed to deal with the inherent challenges of (*i*) large deformations, (*ii*) the typical near or complete incompressibility of the elastomeric matrix and liquid inclusions, and (*iii*) the coupling of the interface PDE $(46)_2$ with the bulk PDE $(46)_1$. We begin in Section 4.1 by reformulating the governing equations (46) into an equivalent hybrid set of equations wherein the deformation field and a pressure field – as opposed to just the deformation field – are the independent functions to be solved for. Subsequently, in Sections 4.2 and 4.3, we spell out the weak form of the these hybrid equations and their FE discretization.

4.1. A hybrid set of governing equations

We wish to be able to deal with compressible as well as with nearly or completely incompressible materials. For the latter group, to which typical elastomers and liquids pertain, Eqs. (46) cannot be utilized directly. This difficultly can be handled by reformulating (46) as an alternative equivalent set of equations wherein a pressure field – and not just the deformation field – is also an unknown. Much like in the simpler setting of hyperelasticity without residual stresses and interfacial forces, as elaborated in Appendix E, such a reformulation hinges on the introduction of an appropriate Legendre transform. The resulting alternative equivalent set of governing equations reduces to the super-cell problem

$$\begin{cases} \text{Div}\left[\mu^\sharp(\mathbf{Y})\nabla\chi + p\mathcal{J}\nabla\chi^{-T}\right] = \mathbf{0}, \quad \mathbf{Y}\in\mathcal{Y}_0^{\mathbf{k}}\setminus\mathcal{C}_0^{\mathbf{k}} \\ \det\nabla\chi - 1 + \dfrac{\Lambda^\sharp(\mathbf{Y}) + r_{\rm i}^\sharp(\mathbf{Y}) - p - \sqrt{4\Lambda^\sharp(\mathbf{Y})\mu^\sharp(\mathbf{Y}) + (\Lambda^\sharp(\mathbf{Y}) - r_{\rm i}^\sharp(\mathbf{Y}) + p)^2}}{2\Lambda^\sharp(\mathbf{Y})} = 0, \quad \mathbf{Y}\in\mathcal{Y}_0^{\mathbf{k}}\setminus\mathcal{C}_0^{\mathbf{k}} \\ \widehat{\text{Div}}\left[\hat{\gamma}_0\,\hat{\mathcal{J}}\hat{\nabla}\chi^{-T} + \hat{\mu}(\hat{\nabla}\chi - \hat{\nabla}\chi^{-T}) + \hat{\Lambda}(\hat{\mathcal{J}}-1)\hat{\mathcal{J}}\hat{\nabla}\chi^{-T}\right] - \left[\!\left[\mu^\sharp(\mathbf{Y})\nabla\chi + p\mathcal{J}\nabla\chi^{-T}\right]\!\right]\hat{\mathbf{N}} = \mathbf{0}, \quad \mathbf{Y}\in\mathcal{C}_0^{\mathbf{k}} \end{cases} \tag{61}$$

for the deformation field $\chi(\mathbf{Y})$, still of the form (45), and a $\mathcal{Y}_0^{\mathbf{k}}$-periodic pressure field $p(\mathbf{Y})$.

4.2. Weak form

When written in weak form, the hybrid set of governing equations (61) amount to finding $\chi(\mathbf{Y})\in\mathcal{K}$ and $p(\mathbf{Y})\in\mathcal{P}$ such that

$$\begin{cases} \displaystyle\int_{\mathcal{Y}_0^{\mathbf{k}}}\left[\mu^\sharp(\mathbf{Y})\nabla\chi + p\mathcal{J}\nabla\chi^{-T}\right]\cdot\nabla\mathbf{w}\,\mathrm{d}\mathbf{Y} + \\ \displaystyle\int_{\mathcal{C}_0^{\mathbf{k}}}\left[\hat{\gamma}_0\,\hat{\mathcal{J}}\hat{\nabla}\chi^{-T} + \hat{\mu}(\hat{\nabla}\chi - \hat{\nabla}\chi^{-T}) + \hat{\Lambda}(\hat{\mathcal{J}}-1)\hat{\mathcal{J}}\hat{\nabla}\chi^{-T}\right]\cdot\hat{\nabla}\mathbf{w}\,\mathrm{d}\mathbf{Y} = 0, \quad \forall\mathbf{w}\in\mathcal{K}_0 \\ \displaystyle\int_{\mathcal{Y}_0^{\mathbf{k}}}\left[\det\nabla\chi - 1 + \frac{\Lambda^\sharp(\mathbf{Y}) + r_{\rm i}^\sharp(\mathbf{Y}) - p - \sqrt{4\Lambda^\sharp(\mathbf{Y})\mu^\sharp(\mathbf{Y}) + (\Lambda^\sharp(\mathbf{Y}) - r_{\rm i}^\sharp(\mathbf{Y}) + p)^2}}{2\Lambda^\sharp(\mathbf{Y})}\right]q\,\mathrm{d}\mathbf{X} = 0, \quad \forall q\in\mathcal{P} \end{cases} . \tag{62}$$

In these expressions, $\mathcal{K}$ and $\mathcal{P}$ stand for sufficiently large sets of admissible deformation fields $\chi(\mathbf{Y})$ of the form (45) and pressure fields $p(\mathbf{Y})$ that are $\mathcal{Y}_0^{\mathbf{k}}$-periodic, respectively. Similarly, $\mathcal{K}_0$ stands for a sufficiently large space of vector fields $\mathbf{w}(\mathbf{Y})$ that are $\mathcal{Y}_0^{\mathbf{k}}$-periodic.

4.3. Discretization: conforming Crouzeix–Raviart finite elements

Having determined the weak form (62), we now turn to its discretization. To efficiently deal with the initial spherical shape of the inclusions and with the coupling between the bulk and interface terms in $(62)_1$, it is convenient to consider partitions ${}^h\mathcal{Y}_0^{\mathbf{k}} = \bigcup_{e=1}^{\mathtt{N}_e}\mathcal{E}^{(e)}$ of the super cell $\mathcal{Y}_0^{\mathbf{k}}$ that comprise $\mathtt{N}_e$ non-overlapping quadratic simplicial volume elements $\mathcal{E}^{(e)}$ that are exclusively contained either within the matrix or within the inclusions so as to have a space discretization that is entirely conforming with the microstructure.

Given this partition, we look for approximate solutions ${}^h\chi(\mathbf{Y})$ and ${}^hp(\mathbf{Y})$ of the deformation field $\chi(\mathbf{Y})$ and the pressure field $p(\mathbf{Y})$ in the finite dimensional subspace of quadratic Crouzeix–Raviart conforming finite elements; see, e.g., Chapter II in Girault and Raviart (1986), Chapter 8 in Boffi et al. (2012). These subspaces have been established – via extensive numerical studies (Lefèvre and Lopez-Pamies, 2017a,b; Lefèvre et al., 2017) – to be stable and convergent in nonlinear elastostatics, without the presence of interfacial forces, as well as in other related settings for material behaviors of arbitrary compressibility, including incompressible behaviors, thus their use here.

As detailed in the Appendix in Lefèvre and Lopez-Pamies (2017b) within the related setting of periodic homogenization of nonlinear electro-elastostatics, it follows that ${}^h\chi(\mathbf{Y})$ and ${}^hp(\mathbf{Y})$ admit the representations

$$ {}^h\chi(\mathbf{Y}) = \sum_{n=1}^{\mathtt{N}_n} {}^hN_{CR}^{(n)}(\mathbf{Y})\chi^{(n)} \qquad \text{and} \qquad {}^hp(\mathbf{Y}) = \sum_{l=0}^{4\mathtt{N}_e-1} {}^hN_{P}^{(l)}(\mathbf{Y})p^{(l)} \tag{63} $$

in terms of the global degrees of freedom $\chi^{(n)}$ and $p^{(l)}$ and associated global shape functions ${}^hN_{CR}^{(n)}(\mathbf{Y})$ and ${}^hN_{P}^{(l)}(\mathbf{Y})$ that result from the assembly process, where $\mathtt{N}_n$ stands for the total number of nodes in the partition ${}^h\mathcal{Y}_0^{\mathbf{k}}$ of the super cell $\mathcal{Y}_0^{\mathbf{k}}$. Here, it is important to emphasize that the assembly process – while algorithmically standard thanks to the use of a space discretization that is conforming with the microstructure – it includes the contributions from the interfacial forces described by the interface integral in $(62)_1$. Physically, $\chi^{(n)}$ corresponds to the deformation field ${}^h\chi(\mathbf{Y})$ at node (n), whereas $p^{(l)}$ corresponds to the value of the pressure ${}^hp(\mathbf{Y})$ at the barycenters of the elements and the three components of its gradient. Note hence that the interface integral in $(62)_1$ involves directly the nodal displacements $\chi^{(n)}$ at the matrix/inclusions interfaces. By contrast, it involves the entire FE discretization $(63)_2$ of the pressure field since the barycenters of the elements lie strictly within the volume of the elements and not on the matrix/inclusions interfaces.

By making use of the representation (63), analogous ones for the test functions $\mathbf{w}$ and q, and enforcing the pertinent periodicity conditions, Eqs. (62) reduce to a system of nonlinear algebraic equations for the degrees of freedom $\chi^{(n)}$ and $p^{(l)}$. These equations can be solved by means of a Newton-like nonlinear method together with direct or iterative solvers for the resulting saddle-point linear system of equations at each Newton iteration.

Application to isotropic suspensions of monodisperse liquid inclusions. In the next two sections, we deploy the above-outlined FE scheme to construct numerical solutions for the effective stored-energy function (44) and associated macroscopic stress-deformation response (47) of elastomers filled with *isotropic* distributions of spherical liquid inclusions of monodisperse size. In both sections, we restrict attention to the basic case of incompressible elastomers, incompressible liquid inclusions, and interfaces that only feature surface tension, to wit,

$$ A_j = A \quad j = 1, 2, \dots, M^\sharp, \qquad \Lambda_{\mathtt{m}} = \Lambda_{\mathtt{i}} = +\infty, \qquad \text{and} \qquad \widehat{\mu} = \widehat{\Lambda} = 0. \tag{64} $$

Consistent with the bifurcation analysis of Michel et al. (2010) for filled elastomers with *isotropic* microstructures, we have not encountered any evidence of bifurcations of short wavelength. Accordingly, all the results that are presented below correspond to solutions with $\mathbf{k} = (1, 1, 1)$, that is, solutions that are $\mathcal{Y}_0$-periodic. Complementary to the numerical solutions, we also put forth an explicit approximation for (44) and, whenever possible, present direct comparisons with the experimental results of Style et al. (2015a) on three types of soft silicone elastomers filled with either ionic-liquid or glycerol droplets.

5. Results for suspensions of monodisperse liquid inclusions at dilute volume fractions

We begin by presenting results for elastomers filled with liquid inclusions at dilute volume fractions in the limit as $c \searrow 0$. Because of the overall geometric isotropy and the overall constitutive incompressibility and isotropy of the problem, the resulting effective stored-energy function (44) admits the asymptotic representation

$$ \overline{W}(\overline{\mathbf{F}}) = \begin{cases} \overline{\Psi}^{\text{dil,inc}}(\overline{I}_1, \overline{I}_2) + O(c^2) & \text{if } \det\overline{\mathbf{F}} = 1 \\ +\infty & \text{otherwise} \end{cases} \qquad \text{with} \quad \overline{\Psi}^{\text{dil,inc}}(\overline{I}_1, \overline{I}_2) = \frac{\mu_{\mathtt{m}}}{2}\left[\overline{I}_1 - 3\right] + \mathcal{H}(\overline{I}_1, \overline{I}_2)c \tag{65} $$

in terms of the principal invariants $\overline{I}_1 = \text{tr}\,\overline{\mathbf{C}} = \overline{\mathbf{F}} \cdot \overline{\mathbf{F}}$ and $\overline{I}_2 = ((\text{tr}\,\overline{\mathbf{C}})^2 - \text{tr}\,\overline{\mathbf{C}}^2)/2 = \overline{\mathbf{F}}^{-1} \cdot \overline{\mathbf{F}}^{-1}$ of the macroscopic right Cauchy–Green deformation tensor $\overline{\mathbf{C}} = \overline{\mathbf{F}}^T\overline{\mathbf{F}}$. The problem thus amounts to computing the effective function $\mathcal{H}(\overline{I}_1, \overline{I}_2)$ in the term of $O(c)$ in (65).

5.1. Numerical results

The effective function $\mathcal{H}(\overline{I}_1, \overline{I}_2)$. In order to generate a numerical solution for the effective function $\mathcal{H}(\overline{I}_1, \overline{I}_2)$, we adopt the strategy followed by Lopez-Pamies et al. (2013a) for dilute suspensions of spherical rigid inclusions. Precisely, we first consider that the unit cell $\mathcal{Y}_0$ contains only one inclusion, $M^\sharp = 1$, located at its geometric center and that the volume fraction of the inclusions c is sufficiently small in the sense that the terms of $O(c^2)$ and of higher order in (65) can be neglected. For the problem at hand here, a parametric study indicates that the value

$$ c = \frac{4\pi A^3}{3\ell^3} = 10^{-3} $$

is sufficiently small in that sense. This implies that for a given radius A of the inclusions, the length of the unit cell $\ell \approx 16\,A$. As a second step, we parameterize the applied macroscopic deformation gradient in the form

$$ \overline{\mathbf{F}} = \overline{\lambda}_1\mathbf{e}_1 \otimes \mathbf{e}_1 + \overline{\lambda}_2\mathbf{e}_2 \otimes \mathbf{e}_2 + \frac{1}{\overline{\lambda}_1\overline{\lambda}_2}\mathbf{e}_3 \otimes \mathbf{e}_3 \quad \text{with} \quad \overline{\lambda}_1 = \lambda,\ \overline{\lambda}_2 = \lambda^m,\ \lambda \geq 1,\ m \in \left[-\frac{1}{2}, 1\right], \tag{66} $$

where $\overline{\lambda}_1$, $\overline{\lambda}_2$, $\overline{\lambda}_3 = (\overline{\lambda}_1\,\overline{\lambda}_2)^{-1}$ and $\{\mathbf{e}_1, \mathbf{e}_2, \mathbf{e}_3\}$ stand, respectively, for the macroscopic principal stretches and the Cartesian principal axes of the unit cell $\mathcal{Y}_0$; see Fig. 3. This parametrization is convenient because it fully exploits the overall incompressibility and

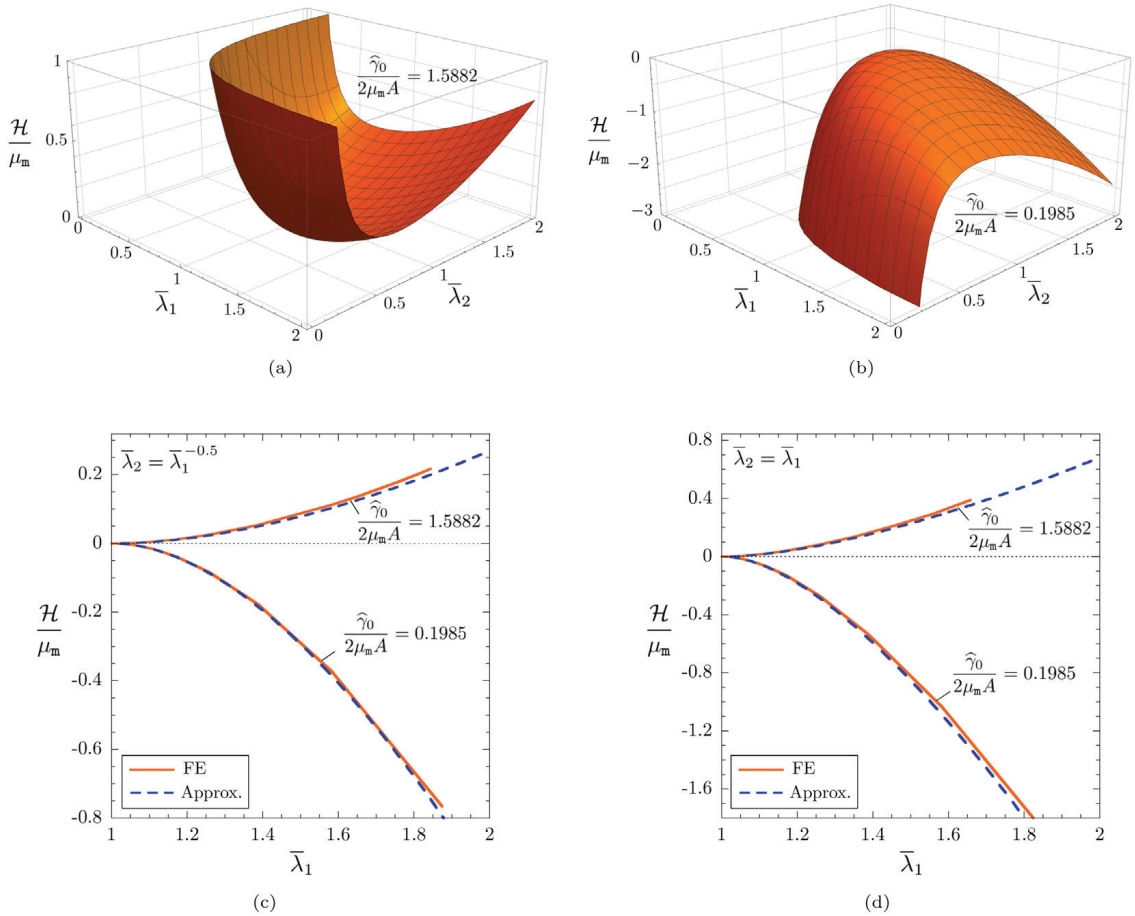

Fig. 4. The effective function $\mathcal{H}(\overline{I}_1, \overline{I}_2)$, normalized by the shear modulus of the elastomeric matrix μ_m, for dilute suspensions of monodisperse spherical liquid inclusions with two values of the dimensionless parameter $\widehat{\gamma}_0/2\mu_m A$. (a, b) 3D plots of $\mathcal{H}(\overline{I}_1, \overline{I}_2)/\mu_m$ in the entire space of principal stretches $(\overline{\lambda}_1, \overline{\lambda}_2)$. (c, d) Plots of $\mathcal{H}(\overline{I}_1, \overline{I}_2)/\mu_m$ as a function of $\overline{\lambda}_1$ for $\overline{\lambda}_2 = \overline{\lambda}_1^{-0.5}$ and $\overline{\lambda}_2 = \overline{\lambda}_1$. For direct comparison, the plots in (c, d) include the results (dashed lines) based on the approximation (69).

isotropy of the filled elastomer. To see this, recall the elementary identities $\overline{I}_1 = \overline{\lambda}_1^2 + \overline{\lambda}_2^2 + \overline{\lambda}_1^{-2}\overline{\lambda}_2^{-2}$ and $\overline{I}_2 = \overline{\lambda}_1^{-2} + \overline{\lambda}_2^{-2} + \overline{\lambda}_1^2\overline{\lambda}_2^2$, introduce $\breve{\mathcal{H}}(\overline{\lambda}_1, \overline{\lambda}_2) = \mathcal{H}(\overline{I}_1, \overline{I}_2)$, and note that the overall incompressibility and isotropy imply the symmetries $\breve{\mathcal{H}}(\overline{\lambda}_1, \overline{\lambda}_2) = \breve{\mathcal{H}}(\overline{\lambda}_2, \overline{\lambda}_1) = \breve{\mathcal{H}}(\overline{\lambda}_1, (\overline{\lambda}_1\,\overline{\lambda}_2)^{-1}) = \breve{\mathcal{H}}((\overline{\lambda}_1\,\overline{\lambda}_2)^{-1}, \overline{\lambda}_1) = \breve{\mathcal{H}}(\overline{\lambda}_2, (\overline{\lambda}_1\,\overline{\lambda}_2)^{-1}) = \breve{\mathcal{H}}((\overline{\lambda}_1\,\overline{\lambda}_2)^{-1}, \overline{\lambda}_2)$. It follows that macroscopic deformation gradients of the form (66) suffice to fully characterize the effective function $\mathcal{H}(\overline{I}_1, \overline{I}_2)$. Lastly, we solve numerically the governing equations (62) for applied macroscopic deformation gradients (66) with the discretized set of values $m \in \{-0.5, -0.25, 0, 0.25, 0.5, 0.75, 1\}$ and then compute the resulting effective stored-energy function $\overline{\Psi}^{\text{dil,inc}}(\overline{I}_1, \overline{I}_2)$ from which we finally determine the effective function $\mathcal{H}(\overline{I}_1, \overline{I}_2)$ by solving for it in (65), namely,

$$\mathcal{H}(\overline{I}_1, \overline{I}_2) = \frac{1}{c}\left(\overline{\Psi}^{\text{dil,inc}}(\overline{I}_1, \overline{I}_2) - \frac{\mu_m}{2}\left[\overline{I}_1 - 3\right]\right).$$

Fig. 4 shows the numerical results obtained for the effective function $\mathcal{H}(\overline{I}_1, \overline{I}_2)$, normalized by the shear modulus of the elastomeric matrix μ_m, for the two values of the dimensionless parameter, or *initial* elasto-capillary number, $\widehat{\gamma}_0/2\mu_m A = 1.5882$ and 0.1985. The reason behind these specific values is twofold. On one hand, they are consistent with two of the experimental measurements reported by Style et al. (2015a) on a silicone elastomer, with shear modulus $\mu_m = 566.67$ Pa, filled with ionic-liquid droplets of several initial radii including $A = 2$ and 16 μm, and silicone/ionic-liquid interfaces featuring an estimated initial surface tension of $\widehat{\gamma}_0 = 0.0036$ N/m. On the other hand, based on the formula $(56)_1$ for the effective shear modulus in the small-deformation limit, the value $\widehat{\gamma}_0/2\mu_m A = 1.5882 > 1$ is expected to be representative of a case where the presence of inclusions leads to *stiffening*, while the value $\widehat{\gamma}_0/2\mu_m A = 0.1985 < 1$ is expected to be representative of a case where the presence of inclusions leads to *softening*.

Specifically, Figs. 4(a) and 4(b) show the normalized effective function $\mathcal{H}(\overline{I}_1, \overline{I}_2)/\mu_m$ in the entire space of principal stretches $(\overline{\lambda}_1, \overline{\lambda}_2)$ for $\widehat{\gamma}_0/2\mu_m A = 1.5882$ and 0.1985, respectively. To aid the quantitative visualization, Figs. 4(c, d) show $\mathcal{H}(\overline{I}_1, \overline{I}_2)/\mu_m$ for both $\widehat{\gamma}_0/2\mu_m A = 1.5882$ and 0.1985 as a function of $\overline{\lambda}_1$ with $\overline{\lambda}_2 = \overline{\lambda}_1^{-0.5}$ in Fig. 4(c) and $\overline{\lambda}_2 = \overline{\lambda}_1$ in Fig. 4(d); note that the results with $\overline{\lambda}_2 = \overline{\lambda}_1^{-0.5}$ correspond to uniaxial tension, while those with $\overline{\lambda}_2 = \overline{\lambda}_1$ correspond to equibiaxial tension. For direct comparison, Figs. 4(c, d) also display the results based on the approximation (69) introduced in the next subsection.

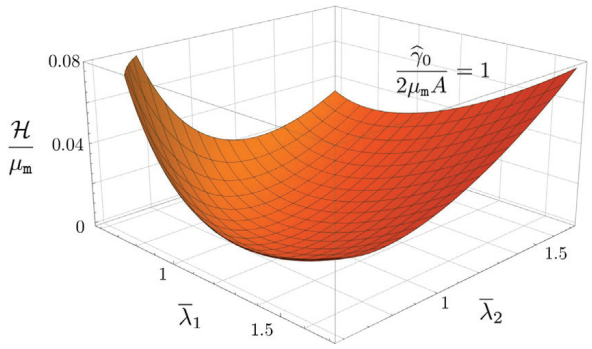

Fig. 5. The effective function $\mathcal{H}(\overline{I}_1, \overline{I}_2)$, normalized by the shear modulus of the elastomeric matrix μ_m, for dilute suspensions of monodisperse spherical liquid inclusions with dimensionless parameter $\widehat{\gamma}_0/2\mu_m A = 1$.

There are two main observations from Fig. 4. First, consistent with the asymptotic behavior in the small-deformation limit, $\mathcal{H}(\overline{I}_1, \overline{I}_2) \geq 0$ for $\widehat{\gamma}_0/2A\mu_m = 1.5882$ and $\mathcal{H}(\overline{I}_1, \overline{I}_2) \leq 0$ for $\widehat{\gamma}_0/2\mu_m A = 0.1985$ indicating that the presence of liquid inclusions leads to the stiffening (softening) of the material when the surface-tension-to-inclusion-size ratio $\widehat{\gamma}_0/2A$ is sufficiently large (small) relative to the elasticity of the underlying elastomeric matrix, even at finite deformations. Second, the proposed analytical approximation (69) is in good quantitative agreement with the numerical solution for $\mathcal{H}(\overline{I}_1, \overline{I}_2)$.

The fact that $\mathcal{H}(\overline{I}_1, \overline{I}_2) \geq 0$ for $\widehat{\gamma}_0/2\mu_m A = 1.5882 > 1$ and $\mathcal{H}(\overline{I}_1, \overline{I}_2) \leq 0$ for $\widehat{\gamma}_0/2\mu_m A = 0.1985 < 1$ prompts the question of whether the value $\widehat{\gamma}_0/2\mu_m A = 1$ leads to $\mathcal{H}(\overline{I}_1, \overline{I}_2) = 0$ for *all* deformations as it does in the small-deformation limit; see Remark 15. The numerical solution for $\mathcal{H}(\overline{I}_1, \overline{I}_2)$ for $\widehat{\gamma}_0/2\mu_m A = 1$ plotted in Fig. 5 reveals that the answer to this question is negative. Notwithstanding that the effective function $\mathcal{H}(\overline{I}_1, \overline{I}_2)$ does not remain identically zero at finite deformations when $\widehat{\gamma}_0/2\mu_m A = 1$, its magnitude $|\mathcal{H}(\overline{I}_1, \overline{I}_2)|$ is significantly smaller than that of the corresponding elastic energy $(\mu_m/2)[\overline{I}_1 - 3]$ of the elastomeric matrix and hence it is practically negligible. The construction of the simple approximation (69) for $\mathcal{H}(\overline{I}_1, \overline{I}_2)$ below exploits this very trait.

The deformation in and around the liquid inclusions. To gain further insight into the macroscopic response of dilute suspensions, Fig. 6(a) presents the numerical results obtained for the aspect ratio

$$\frac{a_1}{a_2} := \frac{\chi_1\left(\frac{\ell}{2} + A, \frac{\ell}{2}, \frac{\ell}{2}\right)}{\chi_2\left(\frac{\ell}{2}, \frac{\ell}{2} + A, \frac{\ell}{2}\right)} \tag{67}$$

of the inclusions in the deformed configuration when the applied macroscopic stretch $\overline{\lambda}_2 = 1.24 - 0.24\overline{\lambda}_1$ with $\overline{\lambda}_1 \geq 1$, which is roughly the loading for which Style et al. (2015a) reported experimental measurements in Fig. 2 of their work. The results are shown as a function of $\overline{\lambda}_1$ for the same two values of the dimensionless parameter $\widehat{\gamma}_0/2\mu_m A = 1.5882$ and 0.1985 considered in Fig. 4, as well as for the intermediate value $\widehat{\gamma}_0/2\mu_m A = 0.5294$. The figure includes the aforementioned experimental results (solid circles) of Style et al. (2015a) for ionic-liquid droplets of initial radii $A = 2, 6, 16$ μm embedded in a silicone elastomer, which correspond, respectively, to the values $\widehat{\gamma}_0/2\mu_m A = 1.5882, 0.5294, 0.1985$. To illustrate the importance of finite deformations, the figure also includes the asymptotic results (dotted lines) obtained from the linearized theory in the limit of small deformations as $\overline{\lambda}_1, \overline{\lambda}_2 \to 1$:

$$\frac{a_1}{a_2} = 1 + \frac{5\left(\overline{\lambda}_1 - \overline{\lambda}_2\right)}{3 + \frac{5\widehat{\gamma}_0}{2\mu_m A}} + O\left((\overline{\lambda}_1 - 1)^2\right) + O\left((\overline{\lambda}_1 - 1)(\overline{\lambda}_2 - 1)\right) + O\left((\overline{\lambda}_2 - 1)^2\right). \tag{68}$$

To further highlight the importance of finite deformations, Fig. 6(b) presents the contour plots in the deformed configuration of the component $F_{11}(\mathbf{X})$ of the local deformation gradient in the elastomer around the inclusions for the three values of the dimensionless parameter $\widehat{\gamma}_0/2\mu_m A = 1.5882, 0.5294, 0.1985$ at two applied macroscopic stretches, $\overline{\lambda}_1 = 1.2$ and 1.4. To aid the visualization of the deformation of the inclusions, the figure displays as well their undeformed shape when $\overline{\lambda}_1 = 1$.

Three observations are particularly noteworthy from Fig. 6. First, larger values of the dimensionless parameter $\widehat{\gamma}_0/2\mu_m A$ lead to smaller deformations of the inclusions. Stated differently, once more, inclusions with larger $\widehat{\gamma}_0/2\mu_m A$ pose a larger resistance to deformation and hence are bound to lead to stiffer macroscopic responses as indeed observed in Fig. 4. Second, the deformation of the elastomeric matrix around the inclusions can be significantly larger than the applied macroscopic deformation which, as expected, makes the accounting for finite kinematics essential. Third, the theoretical results for the aspect ratio a_1/a_2 of the inclusions are in good agreement with the experimental measurements of Style et al. (2015a) up to a macroscopic stretch of about $\overline{\lambda} = 1.1$. For larger stretches, the theory deviates from the reported measurements, more so for the two smaller values of $\widehat{\gamma}_0/2\mu_m A$. A possible explanation for this difference is that the surface tension at the silicone/ionic-liquid interfaces is *not* a constant – as assumed by the model (24) with $(64)_3$ used in the theoretical calculations – but rather a function of deformation. Since the deformation of the

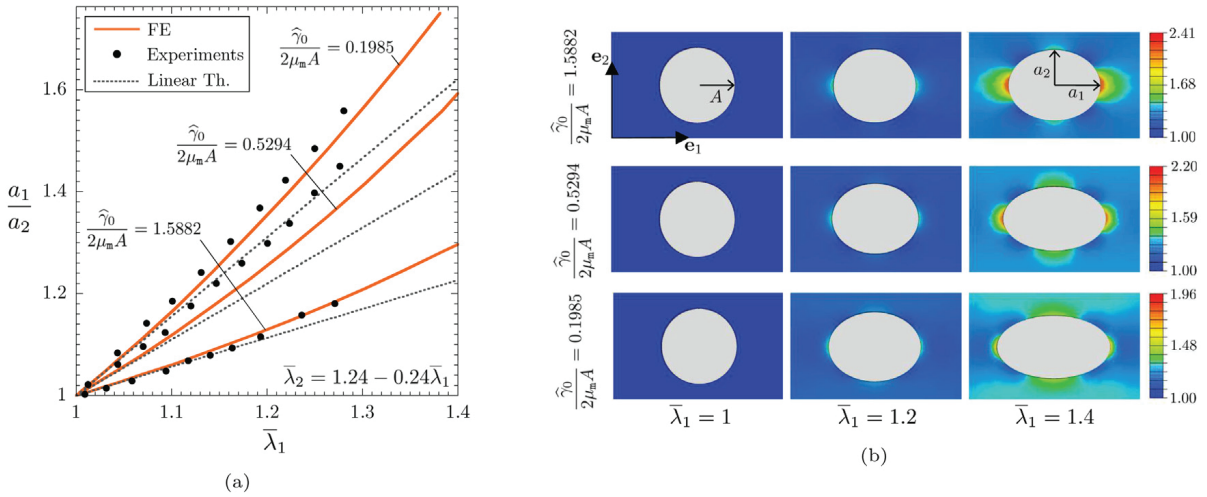

Fig. 6. The deformation in and around monodisperse spherical liquid inclusions in dilute suspensions, for three values of the dimensionless parameter $\widehat{\gamma}_0/2\mu_m A$, subjected to the macroscopic stretch $\overline{\lambda}_2 = 1.24 - 0.24\overline{\lambda}_1$ with $\overline{\lambda}_1 \geq 1$. (a) The aspect ratio (67) of the inclusions as a function of the applied macroscopic stretch $\overline{\lambda}_1$. For direct comparison, the experimental measurements (solid circles) of Style et al. (2015a) on ionic-liquid droplets of initial radii $A = 2, 6, 16$ μm embedded in a silicone elastomer – corresponding to $\widehat{\gamma}_0/2\mu_m A = 1.5882, 0.5294, 0.1985$ – are also plotted, as well as the asymptotic result (68) from the linearized small-deformation theory (dotted lines). (b) Contour plots (in the deformed configuration) of the component $F_{11}(\mathbf{X})$ of the local deformation gradient in the elastomer around the inclusions at two macroscopic stretches $\overline{\lambda}_1$.

elastomer around the inclusions is very significant, it is indeed likely that one has to account for a deformation-dependent surface tension in the theory to be able to explain the experimental observations of Style et al. (2015a). We will come back to this important point in the final section of the paper.

5.2. A simple explicit approximation

In general, the homogenized behavior of a hyperelastic heterogeneous solid without residual stresses and interfacial forces is characterized by an effective stored-energy function that is functionally very different from the stored-energy functions that describe the underlying hyperelastic constituents. Based on a wide range of analytical and numerical results that have appeared over the past two decades, as well as some new results, Lefèvre et al. (2022) have conjectured that the case of isotropic incompressible Neo-Hookean materials in 2D is a rare exception to this general rule. Precisely, these authors have conjectured that the homogenized behavior of an isotropic hyperelastic solid comprised of incompressible Neo-Hookean materials is itself *exactly* Neo-Hookean. From the work of Lopez-Pamies et al. (2013a) on suspensions of rigid inclusions in rubber, we know that the same conjecture cannot possibly hold in 3D. However, from the same and ensuing works (Goudarzi et al., 2015; Lefèvre and Lopez-Pamies, 2017a,b), we also know that in 3D the homogenized behavior of an isotropic hyperelastic solid comprised of incompressible Neo-Hookean materials is *approximately* Neo-Hookean— that is, the resulting effective stored-energy function is approximately linear in $\overline{I}_1$ and independent of $\overline{I}_2$. Interestingly, the same turns out to be true in the present more general setting of isotropic incompressible Neo-Hookean materials with residual stresses and interfacial forces wherein, again, the underlying bulk and interface stored-energy functions are given by (15) and (23) with $(64)_{2,3}$. To see this for the dilute suspensions of liquid inclusions of interest in the section, it suffices to plot $\mathcal{H}(\overline{I}_1, \overline{I}_2)$ as a function of the invariants $\overline{I}_1$ and $\overline{I}_2$. Fig. 7 presents representative examples of such plots for the case when $\widehat{\gamma}_0/2\mu_m A = 1.5882$. Specifically, Fig. 7(a) presents results for $\mathcal{H}(\overline{I}_1, \overline{I}_2)/\mu_m$ as a function of $\overline{I}_1$ for the two fixed values of $\overline{I}_2 = 3.5$ and 4, while Fig. 7(b) presents results for $\mathcal{H}(\overline{I}_1, \overline{I}_2)/\mu_m$ as a function of $\overline{I}_2$ for the four fixed values of $\overline{I}_1 = 3.5, 4, 4.5$. Clearly, $\mathcal{H}(\overline{I}_1, \overline{I}_2)$ is approximately linear in $\overline{I}_1$ and independent of $\overline{I}_2$.

In view of the above observation, heeding the small-deformation result $(56)_1$ for the effective shear modulus of dilute suspensions, we can readily identify

$$\mathcal{H}(\overline{I}_1, \overline{I}_2) = \frac{5\left(\frac{\widehat{\gamma}_0}{2A} - \mu_m\right)\mu_m}{2\left(3\mu_m + 5\frac{\widehat{\gamma}_0}{2A}\right)}\left[\overline{I}_1 - 3\right] \tag{69}$$

as a simple approximation (which neglects the small nonlinearity in $\overline{I}_1$ and the small dependence on $\overline{I}_2$ of the exact solution) for the effective function $\mathcal{H}(\overline{I}_1, \overline{I}_2)$ that has the merit of being exact to $O(\|\overline{\mathbf{F}} - \mathbf{I}\|^2)$ in the limit of small deformations as $\overline{\mathbf{F}} \to \mathbf{I}$. At finite deformations, while not exact beyond $O(\|\overline{\mathbf{F}} - \mathbf{I}\|^2)$, the comparisons with the numerical solutions in Figs. 4 and 7 illustrate that the approximation (69) remains fairly accurate. Given (69), the corresponding approximate solution for the effective stored-energy

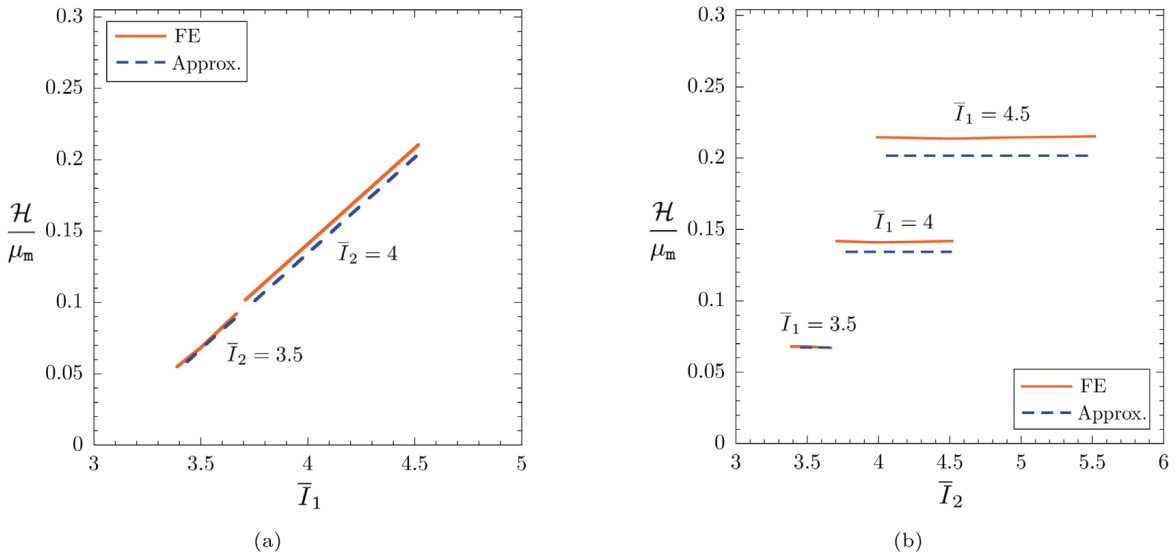

Fig. 7. The effective function $\mathcal{H}(\bar{I}_1, \bar{I}_2)$, normalized by the shear modulus of the elastomeric matrix μ_m, for dilute suspensions of monodisperse spherical liquid inclusions with the dimensionless parameter $\hat{\gamma}_0/2\mu_m A = 1.5882$. (a) $\mathcal{H}(\bar{I}_1, \bar{I}_2)/\mu_m$ as a function of $\bar{I}_1$ for two fixed values of $\bar{I}_2$. (b) $\mathcal{H}(\bar{I}_1, \bar{I}_2)/\mu_m$ as a function of $\bar{I}_2$ for three fixed values of $\bar{I}_1$. For direct comparison, the plots include the results (dashed lines) based on the approximation (69).

function (65) reads simply as

$$\overline{W}(\bar{\mathbf{F}}) = \begin{cases} \dfrac{\mu_m}{2}\left[\bar{I}_1 - 3\right] + \dfrac{5\left(\dfrac{\hat{\gamma}_0}{2A} - \mu_m\right)\mu_m}{2\left(3\mu_m + 5\dfrac{\hat{\gamma}_0}{2A}\right)}\left[\bar{I}_1 - 3\right]c + O(c^2) & \text{if } \det\bar{\mathbf{F}} = 1 \\ +\infty & \text{otherwise} \end{cases} . \tag{70}$$

6. Results for isotropic suspensions of monodisperse liquid inclusions at finite volume fractions

We proceed with the results for isotropic suspensions of monodisperse liquid inclusions at finite volume fractions. In the footstep of a now well-established practice in infinitesimal and finite elasticity alike (Gusev, 1997; Lopez-Pamies et al., 2013b), such suspensions can be efficiently described as infinite media made out of the periodic repetition of a unit cell containing a random distribution of a finite number $M^\sharp$ of inclusions that is sufficiently large so that the resulting macroscopic response is isotropic to within a high degree of accuracy. Obviously, a critical point in this approach is to determine what that sufficiently large number

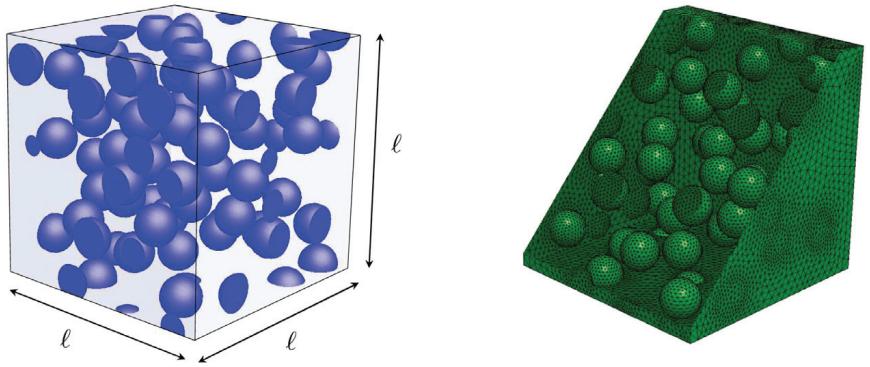

Fig. 8. Representative unit cell $\mathcal{Y}_0$ containing $M^\sharp = 30$ randomly distributed monodisperse spherical liquid inclusions at volume fraction $c = 0.15$ and its FE discretization ${}^h\mathcal{Y}_0$ with 609,061 elements.

$M^\sharp$ is. For the range $c \in [0, 0.25]$ of volume fractions of inclusions for which we present results in this section, a parametric study reveals that $M^\sharp = 30$ suffices.[10]

In order to construct unit cells $\mathcal{Y}_0$ with $M^\sharp = 30$ randomly distributed inclusions, we make use of the algorithm introduced by Lubachevsky et al. (1991). For their FE discretization, we employ the open-source mesh generator code NETGEN (Schöberl, 1997). Fig. 8 shows a representative unit cell at volume fraction $c = 0.15$ alongside its FE discretization with 609,061 elements; meshes with about 600,000 elements were checked to be refined enough to deliver accurate solutions for the problems at hand here, at least up to the deformations that we considered.

6.1. Numerical results

6.1.1. Results in the small-deformation limit

Focusing first on the initial response at small deformations, Fig. 9 presents results for the effective shear modulus of the suspensions in the small-deformation limit, as defined by the isotropic projection (see the Appendix in Spinelli et al., 2015)

$$\overline{\mu} = \frac{1}{10}\boldsymbol{\mathcal{K}} \cdot \overline{\mathbf{L}} = \mathcal{K}_{ijkl}\overline{L}_{ijkl} = \frac{1}{20}\left(\overline{L}_{ijij} + \overline{L}_{ijji} - \frac{2}{3}\overline{L}_{iijj}\right) \tag{71}$$

of the effective modulus of elasticity (52). While Fig. 9(a) shows the effective shear modulus (71), normalized by the shear modulus of the elastomeric matrix $\mu_{\rm m}$, as a function of the volume fraction c of inclusions for the three values of the dimensionless parameter $\widehat{\gamma}_0/2\mu_{\rm m}A = 7, 1, 0.2$, Fig. 9(b) shows $\overline{\mu}/\mu_{\rm m}$ as a function of $\widehat{\gamma}_0/2\mu_{\rm m}A$ for $c = 0.05, 0.15, 0.25$. These specific values are consistent with the experiments reported by Style et al. (2015a) – and included in both figures (solid circles) for direct comparison – on two silicone elastomers, with initial shear moduli $\mu_{\rm m} = 33$ kPa and 1 kPa, filled with glycerol droplets with initial radii of about $A = 1$ μm at volume fractions in the range $c \in [0.04, 0.2]$, and silicone/glycerol interfaces featuring an estimated initial surface tension of $\widehat{\gamma}_0 = 0.014$ N/m. Both figures also display the results (solid lines) for the effective shear modulus $(60)_1$.

As anticipated at the end of Remark 15, a quick glance suffices to recognize that the formula $(60)_1$ is in good agreement.[11] with all the numerical results presented in Fig. 9 Accordingly, the numerical results indicate that the presence of inclusions with dimensionless parameter $\widehat{\gamma}_0/2\mu_{\rm m}A = 0.2 < 1$ leads to softening, more so the larger the volume fraction c of inclusions. By the same token, the presence of inclusions with $\widehat{\gamma}_0/2\mu_{\rm m}A = 7 > 1$ leads to stiffening, more so the larger the value of c. Irrespectively of c, furthermore, the transition from softening to stiffening occurs at $\widehat{\gamma}_0/2\mu_{\rm m}A = 1$. It is also of note from Fig. 9 that there are some appreciable differences between the theoretical results and the experiments. These may be due to the fact that the reported value $\widehat{\gamma}_0 = 0.014$ N/m for the initial surface tension of the silicone/glycerol interfaces is just a rough estimate and/or that the size polydispersity of the inclusions in the specimens is not negligible.

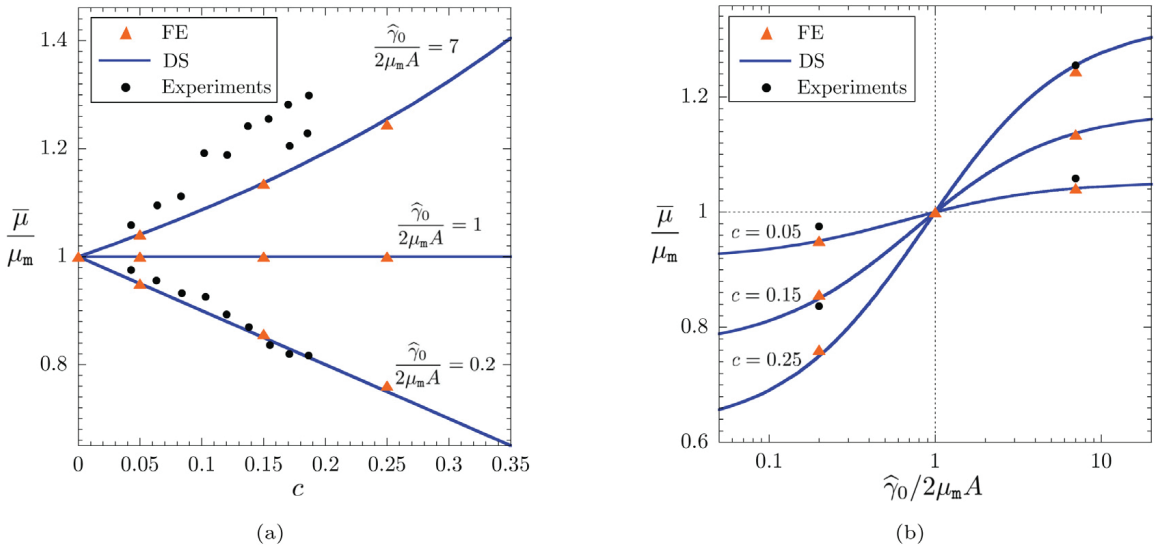

Fig. 9. The effective shear modulus $\overline{\mu}$, normalized by the shear modulus of the elastomeric matrix $\mu_{\rm m}$, for isotropic suspensions of monodisperse spherical liquid inclusions. (a) $\overline{\mu}/\mu_{\rm m}$ as a function of the volume fraction c of inclusions for three values of the dimensionless parameter $\widehat{\gamma}_0/2\mu_{\rm m}A$. (b) $\overline{\mu}/\mu_{\rm m}$ as a function of $\widehat{\gamma}_0/2\mu_{\rm m}A$ for three values of c. For direct comparison, the plots include the results (solid lines) for the effective shear modulus $(60)_1$, as well as the experiments (solid circles) of Style et al. (2015a) on two different silicone elastomers filled with glycerol droplets of initial radii $A \approx 1$ μm.

[10] We emphasize, nevertheless, that suspensions with volume fractions $c \geq 0.25$ and/or bulk and interface constitutive behaviors different from (17) and (24) may require significantly more than $M^\sharp = 30$ inclusions per unit cell to yield sufficiently isotropic responses; see Section 3 in Ghosh et al. (2022).

[11] This agreement should not be taken as a forgone outcome because, again, the effective shear modulus $(60)_1$ is an exact result not for isotropic suspensions of monodisperse spherical liquid inclusions but for isotropic suspensions of *polydisperse* spherical liquid inclusions with radii that are suitably scaled so that they all have the same initial elasto-capillary number $\widehat{\gamma}_0/2\mu_{\rm m}A$ as the inclusions in the monodisperse suspensions.

6.1.2. Results at finite deformations

We now turn to the response of the suspensions at finite deformations. Fig. 10 presents representative results for the macroscopic stress-deformation response (47) of suspensions, with the same three values of dimensionless parameter $\widehat{\gamma}_0/2\mu_{\rm m}A = 7, 1, 0.2$ considered in Fig. 9 and with volume fraction of inclusions $c = 0.15$, under *uniaxial tension* when

$$\overline{\mathbf{F}} = \overline{\lambda}_{un}\mathbf{e}_1 \otimes \mathbf{e}_1 + \overline{\lambda}_{un}^{-1/2}(\mathbf{e}_2 \otimes \mathbf{e}_2 + \mathbf{e}_3 \otimes \mathbf{e}_3) \quad \text{with} \quad \overline{\lambda}_{un} \geq 1 \quad \text{and} \quad \overline{\mathbf{S}} = \overline{S}_{un}\mathbf{e}_1 \otimes \mathbf{e}_1$$

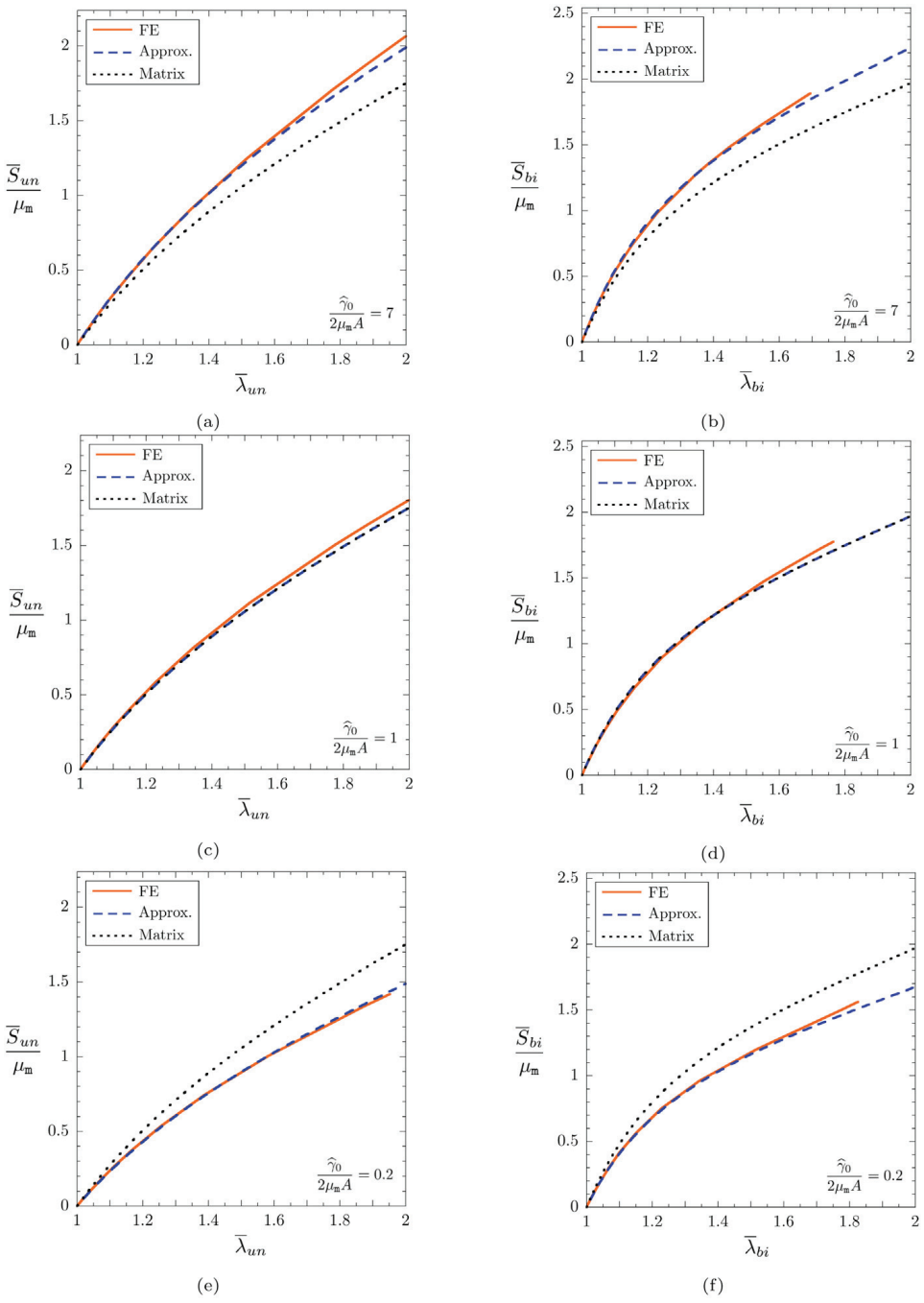

Fig. 10. Macroscopic stress-deformation response (47) of isotropic suspensions of monodisperse spherical liquid inclusions under: (a), (c), (e) uniaxial tension and (b), (d), (f) equibiaxial tension. Results are shown for the uniaxial $\overline{S}_{un}$ and biaxial $\overline{S}_{bi}$ nominal stresses, normalized by the shear modulus of the elastomeric matrix $\mu_{\rm m}$, as functions of the applied uniaxial $\overline{\lambda}_{un}$ and biaxial $\overline{\lambda}_{bi}$ stretches for volume fraction $c = 0.15$ of inclusions and three values of the dimensionless parameter $\widehat{\gamma}_0/2\mu_{\rm m}A$. For direct comparison, the plots include the results (dashed lines) based on the approximation (72) and those (dotted lines) for the elastomeric matrix itself without inclusions.

in parts (a), (c), (e), and under *equibiaxial tension* when

$$\overline{\mathbf{F}} = \overline{\lambda}_{bi}(\mathbf{e}_1 \otimes \mathbf{e}_1 + \mathbf{e}_2 \otimes \mathbf{e}_2) + \overline{\lambda}_{bi}^{-2}\mathbf{e}_3 \otimes \mathbf{e}_3 \quad \text{with} \quad \overline{\lambda}_{bi} \geq 1 \quad \text{and} \quad \overline{\mathbf{S}} = \overline{S}_{bi}(\mathbf{e}_1 \otimes \mathbf{e}_1 + \mathbf{e}_2 \otimes \mathbf{e}_2)$$

in parts (b), (d), (f). In terms of the effective stored-energy function (44), remark that the uniaxial $\overline{S}_{un}$ and biaxial $\overline{S}_{bi}$ nominal stresses are given by the relations $\overline{S}_{un} = \partial\overline{W}(\overline{\mathbf{F}})/\partial\overline{\lambda}_{un}$ and $\overline{S}_{bi} = (1/2)\partial\overline{W}(\overline{\mathbf{F}})/\partial\overline{\lambda}_{bi}$.

Specifically, Figs. 10(a), (c), (e) show results for the uniaxial nominal stress $\overline{S}_{un}$, normalized by the shear modulus of the elastomeric matrix μ_{m}, as a function of the applied uniaxial stretch $\overline{\lambda}_{un}$, while Figs. 10(b), (d), (f) show results for the normalized biaxial nominal stress $\overline{S}_{un}/\mu_{\mathrm{m}}$ as a function of the applied biaxial stretch $\overline{\lambda}_{bi}$. For direct comparison, all plots include (dashed lines) the results $\overline{S}_{un} = \partial\overline{W}(\overline{\mathbf{F}})/\partial\overline{\lambda}_{un} = \overline{\mu}\,(\overline{\lambda}_{un} - \overline{\lambda}_{un}^{-2})$ and $\overline{S}_{bi} = (1/2)\partial\overline{W}(\overline{\mathbf{F}})/\partial\overline{\lambda}_{bi} = \overline{\mu}\,(\overline{\lambda}_{bi} - \overline{\lambda}_{bi}^{-5})$ based on the approximation (72) introduced in the next subsection. All plots display (dotted lines) as well the corresponding results $\overline{S}_{un} = \partial W_{\mathrm{m}}(\overline{\mathbf{F}})/\partial\overline{\lambda}_{un} = \mu_{\mathrm{m}}(\overline{\lambda}_{un} - \overline{\lambda}_{un}^{-2})$ and $\overline{S}_{bi} = (1/2)\partial W_{\mathrm{m}}(\overline{\mathbf{F}})/\partial\overline{\lambda}_{bi} = \mu_{\mathrm{m}}(\overline{\lambda}_{bi} - \overline{\lambda}_{bi}^{-5})$ for the elastomeric matrix, when $c = 0$. Since Style et al. (2015a) restricted their study to small deformations, no experimental data is plotted in these figures.

Consistent with all the asymptotic results (in the limits of small volume fractions or small deformations) examined above in Figs. 4 and 9, it is plain from Fig. 10 that the suspension wherein the liquid inclusions feature a dimensionless parameter $\widehat{\gamma}_0/2\mu_{\mathrm{m}}A < 1$ exhibits a softer response than that of the elastomeric matrix, while the suspension wherein the liquid inclusions feature a dimensionless parameter $\widehat{\gamma}_0/2\mu_{\mathrm{m}}A > 1$ exhibits a stiffer response. What is more, even for the moderate values of dimensionless parameter $\widehat{\gamma}_0/2\mu_{\mathrm{m}}A = 7, 0.2$, volume fraction $c = 0.15$ of inclusions, and finite stretches $\overline{\lambda}_{un}$, $\overline{\lambda}_{bi} \in [1, 2]$ considered here, such softening and stiffening can be very significant. For instance, at the uniaxial stretch of $\overline{\lambda}_{un} = 2$, the uniaxial stress $\overline{S}_{un}/\mu_{\mathrm{m}} = 1.50$ for the suspension with $\widehat{\gamma}_0/2\mu_{\mathrm{m}}A = 0.2$, while $\overline{S}_{un}/\mu_{\mathrm{m}} = 2.00$ for the suspension with $\widehat{\gamma}_0/2\mu_{\mathrm{m}}A = 7$.

Consistent too with the above asymptotic results is the fact that the macroscopic response of the suspension wherein the liquid inclusions feature the dimensionless parameter $\widehat{\gamma}_0/2\mu_{\mathrm{m}}A = 1$ is essentially the same as that of the elastomeric matrix. That is, the presence of such inclusions – even at the volume fraction $c = 0.15$ and at finite stretches $\overline{\lambda}_{un}$, $\overline{\lambda}_{bi} \in [1, 2]$ – has little effect in the macroscopic response.

We close the discussion of Fig. 10 by noting that the results based on the proposed analytical approximation (72), which we take on next, are in good quantitative agreement with the numerical results.

6.2. A simple explicit approximation

As anticipated in Section 5.2, much like for isotropic hyperelastic solids comprised of incompressible Neo-Hookean materials without residual stresses and interfacial forces (Lopez-Pamies et al., 2013b; Goudarzi et al., 2015; Lefèvre and Lopez-Pamies, 2017a,b), all our numerical results indicate that the effective stored-energy function (44) for isotropic suspensions of monodisperse spherical liquid inclusions characterized by bulk and interface stored-energy functions (15) and (23) with $(64)_{2,3}$ is *approximately* Neo-Hookean.

By way of an example, Fig. 11 shows results for the effective stored-energy function $\overline{W}(\overline{\mathbf{F}})$, normalized by the shear modulus of the elastomeric matrix μ_{m}, for a suspension with dimensionless parameter $\widehat{\gamma}_0/2\mu_{\mathrm{m}}A = 0.2$ and volume fraction of inclusions $c = 0.15$ as a function of the invariants $\overline{I}_1$ and $\overline{I}_2$. Specifically, Fig. 11(a) presents results for $\overline{W}(\overline{\mathbf{F}})/\mu_{\mathrm{m}}$ as a function of $\overline{I}_1$ for the fixed values

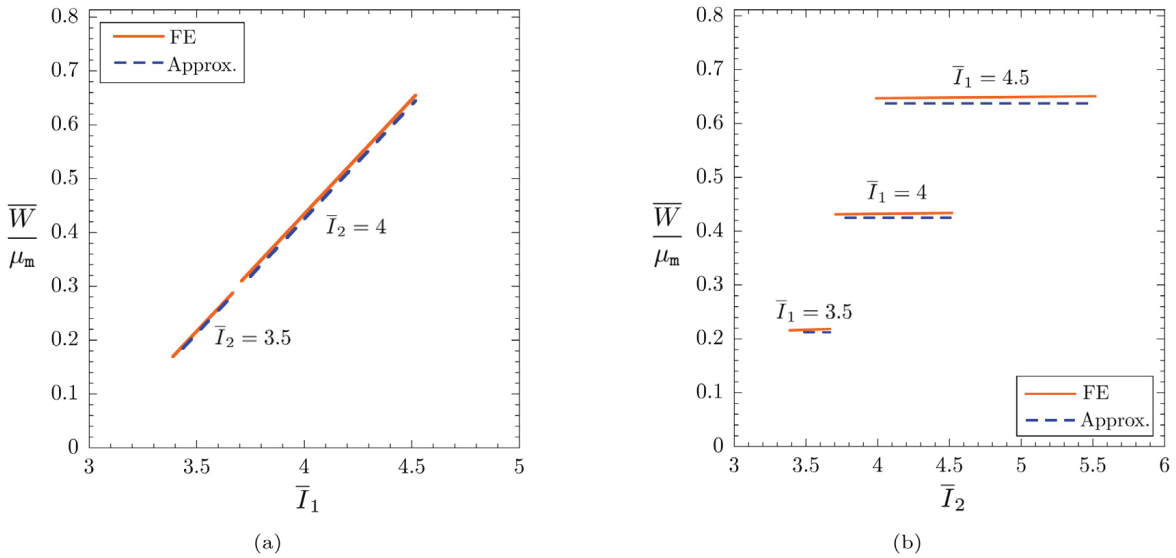

Fig. 11. The effective stored-energy function $\overline{W}(\overline{\mathbf{F}})$, normalized by the shear modulus of the elastomeric matrix μ_{m}, for an isotropic suspension of monodisperse spherical liquid inclusions at volume fraction $c = 0.15$ with dimensionless parameter $\widehat{\gamma}_0/2\mu_{\mathrm{m}}A = 0.2$. (a) $\overline{W}(\overline{\mathbf{F}})/\mu_{\mathrm{m}}$ for fixed values of $\overline{I}_2$ as a function of $\overline{I}_1$. (b) $\overline{W}(\overline{\mathbf{F}})/\mu_{\mathrm{m}}$ for fixed values of $\overline{I}_1$ as a function of $\overline{I}_2$. For direct comparison, the plots include the results (dashed lines) based on the approximation (72).

$\overline{I}_2 = 3.5$ and 4, while Fig. 11(a) presents results for $\overline{W}(\overline{\mathbf{F}})/\mu_{\rm m}$ as a function of $\overline{I}_2$ for fixed $\overline{I}_1 = 3.5$, 4, and 4.5. Clearly, $\overline{W}(\overline{\mathbf{F}})$ is approximately linear in $\overline{I}_1$ and independent of $\overline{I}_2$.

Ergo, neglecting its small nonlinearity in $\overline{I}_1$ and the small dependence on $\overline{I}_2$, the effective stored-energy function (44) for isotropic suspensions of monodisperse spherical liquid inclusions can be readily approximated by the effective Neo-Hookean stored-energy function

$$\overline{W}(\overline{\mathbf{F}}) = \begin{cases} \dfrac{\overline{\mu}}{2}\left[\overline{I}_1 - 3\right] & \text{if } \det\overline{\mathbf{F}} = 1 \\ +\infty & \text{otherwise} \end{cases},$$

where $\overline{\mu}$ is nothing more than the effective shear modulus (71) in the small-deformation limit. Now, as established in Section 6.1.1, the formula $(60)_1$ is accurately descriptive of the effective shear modulus (71) for suspensions with volume fractions of inclusions in the small-to-moderate range $c \in [0, 0.20]$. For those, we can then write the more explicit approximation

$$\overline{W}(\overline{\mathbf{F}}) = \begin{cases} \dfrac{\mu_{\rm m}}{2(1-c)^{\frac{5(eCa-1)}{3+5eCa}}}\left[\overline{I}_1 - 3\right] & \text{if } \det\overline{\mathbf{F}} = 1 \\ +\infty & \text{otherwise} \end{cases} \qquad \text{with} \qquad eCa = \frac{\widehat{\gamma}_0}{2\mu_{\rm m}A}. \tag{72}$$

This formula reduces to (70) in the dilute limit of inclusions as $c \searrow 0$. For finite volume fractions c, the comparisons with the numerical solutions in Figs. 10 and 11, and with others not included here for conciseness, indicate that the formula (72) remains a fairly accurate approximation.

7. Summary and final comments

In this paper, we have formulated the homogenization problem that describes the mechanical response of elastomers filled with liquid inclusions under finite quasistatic deformations. Specifically, neglecting dissipative phenomena, we have considered that the elastomer making up the matrix is a hyperelastic solid, that the liquid making up the inclusions is a hyperelastic fluid, that the interfaces separating the solid elastomer from the liquid inclusions are hyperelastic interfaces, possibly including initial interfacial forces such as surface tension, and that the inclusions are spherical in shape in their ground state.

We have then shown that the resulting macroscopic behavior of such filled elastomers is that of a hyperelastic solid – distinctly, one that depends directly on the size of the inclusions and the constitutive behavior of the interfaces – and hence that it is characterized by an effective stored-energy function $\overline{W}(\overline{\mathbf{F}})$ of the macroscopic deformation gradient $\overline{\mathbf{F}}$. For the case of filled elastomers with periodic microstructures, moreover, we have provided a formula – given by Eq. (44) – for $\overline{W}(\overline{\mathbf{F}})$.

The computation of $\overline{W}(\overline{\mathbf{F}})$ amounts to solving a super-cell problem, that defined by Eqs. (46), which exhibits two non-standard features: (*i*) residual stresses (in the inclusions) and (*ii*) a non-standard jump condition across material (matrix/inclusions) interfaces due to the presence of interfacial forces. These two features have profound implications not only on the mechanical response of the material, but also on the mathematical analysis of the problem. The most notable for the latter is that in the limit of small deformations, when the governing equations are linearized, the standard argument based on the Lax–Milgram theorem does not apply to prove existence of solution because of the lack of pointwise positive definiteness of the moduli of elasticity for the bulk (49) and the interfaces (28).

Strikingly, in spite of the fact that there are local residual stresses within the inclusions (due to the presence of initial interfacial forces), the resulting macroscopic behavior turns out to be free of residual stresses, that is, $\partial\overline{W}(\mathbf{I})/\partial\overline{\mathbf{F}} = \mathbf{0}$. What is more, in spite of the fact that the local moduli of elasticity in the bulk (49) and the interfaces (28) in the small-deformation limit do not possess minor symmetries (due to the presence of residual stresses and initial interfacial forces), the resulting effective modulus of elasticity (52) does posses the standard minor symmetries, that is, $\overline{L}_{ijkl} = \overline{L}_{jikl} = \overline{L}_{ijlk}$, where we recall that $\overline{L}_{ijkl} = \partial^2\overline{W}(\mathbf{I})/\partial\overline{F}_{ij}\partial\overline{F}_{kl}$.

To gain quantitative insight, we have also introduced and made use of a FE implementation of the proposed general formulation to work out numerical solutions for the macroscopic response of Neo-Hookean elastomers filled with random isotropic distributions of incompressible liquid inclusions of monodisperse size and interfaces featuring a constant surface tension, which is arguably the most basic class of elastomers filled with liquid inclusions. We have presented solutions both for elastomers filled with dilute volume fractions of inclusions and with finite volume fractions. All of them turn out to be well approximated by the explicit effective stored-energy function (72).

Notably, the solutions have shown that the presence of inclusions with large (small) surface-tension-to-inclusions-size ratio relative to the shear stiffness of the underlying elastomer can lead to very significant stiffening (softening) of the macroscopic response, more so the larger the volume fraction of inclusions and the larger the macroscopic deformation. This behavior – which confirms previous experimental and theoretical results centered on small deformations – is due to the fact that inclusions with a relatively surface-tension-to-inclusions-size ratio pose significant resistance to deformation and hence *de facto* behave like stiff inclusions.

The solutions have also shown that locally the deformations in and around the inclusions can be large, even when the macroscopic deformations are small. This, together with the comparisons of the solutions with the experimental measurements of Style et al. (2015a) on ionic-liquid droplets presented in Fig. 6(a), suggests that the surface tension at elastomer/liquid-inclusion interfaces should be assumed not to remain constant in general, but to be deformation dependent instead.

Accounting for a nonlinear surface tension. Indeed, preliminary results that make use of an interface stored-energy function of the form

$$\widehat{W}(\widehat{\mathbf{F}}) = \widehat{g}(\widehat{J}), \tag{73}$$

where $\widehat{g}(\widehat{J})$ is a non-negative function of the interface determinant $\widehat{J}$ satisfying the conditions $\widehat{g}(1) = \widehat{g}'(1) = \widehat{\gamma}_0$ and $\widehat{g}(\widehat{J}) < \widehat{\gamma}_0\widehat{J}$ for $\widehat{J} \gg 1$, indicate that it is possible to have excellent agreement with the experiments of Style et al. (2015a) reproduced in Fig. 6(a). The interface stored-energy function (73) is a natural generalization of the stored-energy function $\widehat{W}(\widehat{\mathbf{F}}) = \widehat{\gamma}_0\widehat{J}$ describing interfaces with constant surface tension $\widehat{\gamma}_0$. The associated interface first Piola–Kirchhoff and Cauchy stress tensors read

$$\widehat{\mathbf{S}} = \frac{\partial \widehat{W}}{\partial \widehat{\mathbf{F}}}(\widehat{\mathbf{F}}) = \widehat{g}'(\widehat{J})\widehat{J}\widehat{\mathbf{F}}^{-T} \qquad \text{and} \qquad \widehat{\mathbf{T}} = \widehat{J}^{-1}\widehat{\mathbf{S}}\widehat{\mathbf{F}}^{T} = \widehat{g}'(\widehat{J})\widehat{\mathbf{i}}$$

and so the derivative $\widehat{g}'(\widehat{J})$ represents a nonlinear surface tension. It would be interesting to carry out experiments on a variety of interfaces to gain insight into the physical implications and generality of models of the form (73).

Other generalizations. It would also be interesting to pursue several other generalizations of the analysis presented in this work, both for fundamental and practical reasons. A generalization that is clear-cut is that of accounting for the non-Gaussian elasticity of elastomers. Another straightforward one is that of considering spherical inclusions of polydisperse sizes. A far less straightforward generalization is that of considering inclusions of arbitrary initial shape. As elaborated in Section 2.4, the presence of liquid inclusions whose shapes do not have constant mean curvature entails residual stresses not only within the inclusions but also in the surrounding elastomeric matrix. This complicates the analysis significantly. The study of applications involving liquid–metal and/or ferrofluid inclusions requires extending the present analysis to the coupled realms of electro- and magneto-elastostatics. Another interesting generalization that may be needed for certain applications is that of accounting for viscous dissipation in the bulk and interfaces.

CRediT authorship contribution statement

Kamalendu Ghosh: Conceptualization, Methodology, Software, Writing – review & editing. **Oscar Lopez-Pamies:** Conceptualization, Methodology, Supervision, Writing – original draft, Writing – review & editing, Funding acquisition.

Declaration of competing interest

The authors declare that they have no known competing financial interests or personal relationships that could have appeared to influence the work reported in this paper.

Acknowledgments

Support for this work by the National Science Foundation through the Grant DMREF–1922371 is gratefully acknowledged.

Appendix A. The equilibrium Eqs. (9)–(10) in Lagrangian form

On substitution of the definitions $\mathbf{S} = J\mathbf{T}\mathbf{F}^{-T}$, $\widehat{\mathbf{S}} = \widehat{J}\widehat{\mathbf{T}}\widehat{\mathbf{F}}^{-T}$, and $\mathbf{B} = J\mathbf{b}$ in the Eulerian balance of linear momentum (7), we have

$$\begin{cases} \dfrac{\partial}{\partial x_j}\left[J^{-1}S_{ik}F_{jk}\right] + J^{-1}B_i = 0, & \mathbf{x} \in \Omega \setminus \Gamma \\ \dfrac{\partial}{\partial x_p}\left[\widehat{J}^{-1}\widehat{S}_{ik}\widehat{F}_{jk}\right]\widehat{i}_{pj} - [\![J^{-1}S_{ik}F_{jk}]\!]\widehat{n}_j = 0, & \mathbf{x} \in \Gamma \end{cases} . \tag{74}$$

Given that $\operatorname{div}\left[J^{-1}\mathbf{F}^T\right] = \widehat{\operatorname{div}}\left[\widehat{J}^{-1}\widehat{\mathbf{F}}^T\right] = \mathbf{0}$, Eqs. (74) simplify to

$$\begin{cases} J^{-1}\dfrac{\partial S_{ik}}{\partial x_j}F_{jk} + J^{-1}B_i = 0, & \mathbf{x} \in \Omega \setminus \Gamma \\ \widehat{J}^{-1}\dfrac{\partial \widehat{S}_{ik}}{\partial x_p}\widehat{i}_{pj}\widehat{F}_{jk} - [\![J^{-1}S_{ik}F_{jk}]\!]\widehat{n}_j = 0, & \mathbf{x} \in \Gamma \end{cases} .$$

By employing now the chain rule and the identities $\widehat{\mathbf{F}}^{-1} = \mathbf{F}^{-1}\widehat{\mathbf{i}}$ and $\widehat{\mathbf{n}} = \widehat{J}^{-1}J\mathbf{F}^{-T}\widehat{\mathbf{N}}$ together with the fact that $J^{\mathrm{i}}\mathbf{F}^{\mathrm{i}\,-T}\widehat{\mathbf{N}} = J^{\mathrm{m}}\mathbf{F}^{\mathrm{m}-T}\widehat{\mathbf{N}}$, we obtain

$$\begin{cases} \dfrac{\partial S_{ik}}{\partial X_p}F^{-1}_{pj}F_{jk} + B_i = 0, & \mathbf{X} \in \Omega_0 \setminus \Gamma_0 \\ \dfrac{\partial \widehat{S}_{ik}}{\partial X_q}\widehat{F}^{-1}_{qj}\widehat{F}_{jk} - [\![S_{ik}]\!]\widehat{N}_k = 0, & \mathbf{X} \in \Gamma_0 \end{cases} .$$

Finally, recognizing that $\widehat{\mathbf{F}}^{-1}\widehat{\mathbf{F}} = \widehat{\mathbf{I}}$, the balance of linear momentum in Lagrangian form (9) readily follows:

$$\begin{cases} \dfrac{\partial S_{ik}}{\partial X_k} + B_i = 0, & \mathbf{X} \in \Omega_0 \setminus \Gamma_0 \\ \dfrac{\partial \widehat{S}_{ik}}{\partial X_q}\widehat{I}_{qk} - [\![S_{ik}]\!]\widehat{N}_k = 0, & \mathbf{X} \in \Gamma_0 \end{cases}.$$

Given the definitions $\mathbf{S} = J\mathbf{T}\mathbf{F}^{-T}$ and $\widehat{\mathbf{S}} = \widehat{J}\widehat{\mathbf{T}}\widehat{\mathbf{F}}^{-T}$ of the bulk and interface first Piola–Kirchhoff stress tensors, it is trivial to deduce from the balance of angular momentum (8) in Eulerian form that the balance of angular momentum in Lagrangian form is given by (10).

Appendix B. The average identities (35) and (36)

Making use of the bulk divergence theorem and the continuity of the deformation field $\mathbf{y}$, it follows that

$$\begin{aligned} \frac{1}{|\Omega_0|}\int_{\partial\Omega_0} y_i N_j \, \mathrm{d}\mathbf{X} &= \frac{1}{|\Omega_0|}\left(\int_{\Omega_0} \frac{\partial y_i}{\partial X_j}\, \mathrm{d}\mathbf{X} - \int_{\Gamma_0} [\![y_i]\!]\, \widehat{N}_j \, \mathrm{d}\mathbf{X}\right) \\ &= \frac{1}{|\Omega_0|}\int_{\Omega_0} F_{ij}\, \mathrm{d}\mathbf{X}. \end{aligned}$$

Similarly, making use of the bulk and interface divergence theorems, the facts that the bulk and interface stresses $\mathbf{S}$ and $\widehat{\mathbf{S}}$ satisfy the balance of linear momentum (9) with zero body force $\mathbf{B} = \mathbf{0}$ and that $\widehat{\mathbf{S}}$ is a superficial tensor, it follows that

$$\begin{aligned} \frac{1}{|\Omega_0|}\int_{\partial\Omega_0} S_{in}N_n X_j \, \mathrm{d}\mathbf{X} &= \frac{1}{|\Omega_0|}\left(\int_{\Omega_0} \frac{\partial}{\partial X_n}\left(S_{in}X_j\right)\, \mathrm{d}\mathbf{X} - \int_{\Gamma_0} [\![S_{in}]\!]\, \widehat{N}_n X_j \, \mathrm{d}\mathbf{X}\right) \\ &= \frac{1}{|\Omega_0|}\left(\int_{\Omega_0} S_{ij}\, \mathrm{d}\mathbf{X} - \int_{\Gamma_0} \frac{\partial \widehat{S}_{in}}{\partial X_p}\widehat{I}_{pn} X_j \, \mathrm{d}\mathbf{X}\right) \\ &= \frac{1}{|\Omega_0|}\left(\int_{\Omega_0} S_{ij}\, \mathrm{d}\mathbf{X} - \int_{\Gamma_0} \frac{\partial}{\partial X_p}\left(\widehat{S}_{in}X_j\right)\widehat{I}_{pn}\, \mathrm{d}\mathbf{X} + \int_{\Gamma_0} \widehat{S}_{in}\widehat{I}_{pn}\frac{\partial X_j}{\partial X_p}\, \mathrm{d}\mathbf{X}\right) \\ &= \frac{1}{|\Omega_0|}\left(\int_{\Omega_0} S_{ij}\, \mathrm{d}\mathbf{X} + \int_{\Gamma_0} \widehat{S}_{ij}\, \mathrm{d}\mathbf{X}\right). \end{aligned}$$

Appendix C. The formulas (38) and (47) for the macroscopic constitutive response

Given the definition $(38)_2$ for $\overline{W}(\overline{\mathbf{F}})$, making use of the bulk and interface divergence theorems, the continuity of the deformation field $\mathbf{y}$, the affine boundary condition $\mathbf{y} = \overline{\mathbf{F}}\mathbf{X}$, $\mathbf{X} \in \partial\Omega_0$, and the facts that the bulk and interface stresses $\mathbf{S}$ and $\widehat{\mathbf{S}}$ satisfy the balance of linear momentum (9) with zero body force $\mathbf{B} = \mathbf{0}$, and that $\widehat{\mathbf{S}}$ is a superficial tensor, it follows that

$$\begin{aligned} \frac{\partial \overline{W}}{\partial \overline{F}_{ij}}(\overline{\mathbf{F}}) &= \frac{1}{|\Omega_0|}\left(\int_{\Omega_0} S_{mn}\frac{\partial^2 y_m}{\partial \overline{F}_{ij}\partial X_n}\, \mathrm{d}\mathbf{X} + \int_{\Gamma_0} \widehat{S}_{mn}\frac{\partial}{\partial \overline{F}_{ij}}\left(\frac{\partial y_m}{\partial X_p}\widehat{I}_{pn}\right)\, \mathrm{d}\mathbf{X}\right) \\ &= \frac{1}{|\Omega_0|}\left(\int_{\Omega_0} \frac{\partial}{\partial X_n}\left(S_{mn}\frac{\partial y_m}{\partial \overline{F}_{ij}}\right)\, \mathrm{d}\mathbf{X} - \int_{\Omega_0} \frac{\partial S_{mn}}{\partial X_n}\frac{\partial y_m}{\partial \overline{F}_{ij}}\, \mathrm{d}\mathbf{X} + \right. \\ &\qquad \left. \int_{\Gamma_0} \frac{\partial}{\partial X_p}\left(\widehat{S}_{mn}\frac{\partial y_m}{\partial \overline{F}_{ij}}\right)\widehat{I}_{pn}\, \mathrm{d}\mathbf{X} - \int_{\Gamma_0} \frac{\partial \widehat{S}_{mn}}{\partial X_p}\widehat{I}_{pn}\frac{\partial y_m}{\partial \overline{F}_{ij}}\, \mathrm{d}\mathbf{X}\right) \\ &= \frac{1}{|\Omega_0|}\left(\int_{\Omega_0} \frac{\partial}{\partial X_n}\left(S_{mn}\frac{\partial y_m}{\partial \overline{F}_{ij}}\right)\, \mathrm{d}\mathbf{X} - \int_{\Gamma_0} \frac{\partial \widehat{S}_{mn}}{\partial X_p}\widehat{I}_{pn}\frac{\partial y_m}{\partial \overline{F}_{ij}}\, \mathrm{d}\mathbf{X}\right) \\ &= \frac{1}{|\Omega_0|}\int_{\partial\Omega_0} S_{mn}N_n\frac{\partial y_m}{\partial \overline{F}_{ij}}\, \mathrm{d}\mathbf{X} \\ &= \frac{1}{|\Omega_0|}\int_{\partial\Omega_0} S_{in}N_n X_j \, \mathrm{d}\mathbf{X} \\ &= \frac{1}{|\Omega_0|}\left(\int_{\Omega_0} S_{ij}\, \mathrm{d}\mathbf{X} + \int_{\Gamma_0} \widehat{S}_{ij}\, \mathrm{d}\mathbf{X}\right). \end{aligned}$$

Similarly, given the definition (44) for $\overline{W}(\overline{\mathbf{F}})$, making use of the bulk and interface divergence theorems, the continuity of the deformation field χ and its form (45), and the facts that the bulk and interface stresses $\mathbf{S}^\sharp$ and $\widehat{\mathbf{S}}$ satisfy the super-cell problem (46), and that $\widehat{\mathbf{S}}$ is a superficial tensor, it follows that

$$\frac{\partial \overline{W}}{\partial \overline{F}_{ij}}(\overline{\mathbf{F}}) = \frac{1}{|\mathcal{Y}_0^{\mathbf{k}}|}\left(\int_{\mathcal{Y}_0^{\mathbf{k}}} S^\sharp_{mn}\frac{\partial^2 \chi_m}{\partial \overline{F}_{ij}\partial Y_n}\, \mathrm{d}\mathbf{Y} + \int_{\mathcal{C}_0^{\mathbf{k}}} \widehat{S}_{mn}\frac{\partial}{\partial \overline{F}_{ij}}\left(\frac{\partial \chi_m}{\partial Y_p}\widehat{I}_{pn}\right)\, \mathrm{d}\mathbf{Y}\right)$$

$$
\begin{aligned}
&= \frac{1}{|\mathcal{Y}_0^{\mathbf{k}}|}\left(\int_{\mathcal{Y}_0^{\mathbf{k}}} \frac{\partial}{\partial Y_n}\left(S^{\sharp}_{mn}\frac{\partial \chi_m}{\partial \overline{F}_{ij}}\right)\mathrm{d}\mathbf{Y} - \int_{\mathcal{Y}_0^{\mathbf{k}}} \frac{\partial S^{\sharp}_{mn}}{\partial Y_n}\frac{\partial \chi_m}{\partial \overline{F}_{ij}}\,\mathrm{d}\mathbf{Y} + \right.\\
&\qquad \left. \int_{\mathcal{C}_0^{\mathbf{k}}} \frac{\partial}{\partial Y_p}\left(\widehat{S}_{mn}\frac{\partial \chi_m}{\partial \overline{F}_{ij}}\right)\widehat{I}_{pn}\,\mathrm{d}\mathbf{Y} - \int_{\mathcal{C}_0^{\mathbf{k}}} \frac{\partial \widehat{S}_{mn}}{\partial Y_p}\widehat{I}_{pn}\frac{\partial \chi_m}{\partial \overline{F}_{ij}}\,\mathrm{d}\mathbf{Y}\right)\\
&= \frac{1}{|\mathcal{Y}_0^{\mathbf{k}}|}\left(\int_{\mathcal{Y}_0^{\mathbf{k}}} \frac{\partial}{\partial Y_n}\left(S^{\sharp}_{mn}\frac{\partial \chi_m}{\partial \overline{F}_{ij}}\right)\mathrm{d}\mathbf{Y} - \int_{\mathcal{C}_0^{\mathbf{k}}} \frac{\partial \widehat{S}_{mn}}{\partial Y_p}\widehat{I}_{pn}\frac{\partial \chi_m}{\partial \overline{F}_{ij}}\,\mathrm{d}\mathbf{Y}\right)\\
&= \frac{1}{|\mathcal{Y}_0^{\mathbf{k}}|}\int_{\partial\mathcal{Y}_0^{\mathbf{k}}} S^{\sharp}_{mn}N^{\mathbf{k}}_n\frac{\partial \chi_m}{\partial \overline{F}_{ij}}\,\mathrm{d}\mathbf{Y}\\
&= \frac{1}{|\mathcal{Y}_0^{\mathbf{k}}|}\left(\int_{\partial\mathcal{Y}_0^{\mathbf{k}}} S^{\sharp}_{in}N^{\mathbf{k}}_n Y_j\,\mathrm{d}\mathbf{Y} + \int_{\partial\mathcal{Y}_0^{\mathbf{k}}} S^{\sharp}_{mn}N^{\mathbf{k}}_n\frac{\partial u_m}{\partial \overline{F}_{ij}}\,\mathrm{d}\mathbf{Y}\right)\\
&= \frac{1}{|\mathcal{Y}_0^{\mathbf{k}}|}\int_{\partial\mathcal{Y}_0^{\mathbf{k}}} S^{\sharp}_{in}N^{\mathbf{k}}_n Y_j\,\mathrm{d}\mathbf{Y}\\
&= \frac{1}{|\mathcal{Y}_0^{\mathbf{k}}|}\left(\int_{\mathcal{Y}_0^{\mathbf{k}}} S^{\sharp}_{ij}\,\mathrm{d}\mathbf{Y} + \int_{\mathcal{C}_0^{\mathbf{k}}} \widehat{S}_{ij}\,\mathrm{d}\mathbf{Y}\right),
\end{aligned}
$$

where $\mathbf{N}^{\mathbf{k}}$ denotes the outward unit normal to the super-cell $\mathcal{Y}_0^{\mathbf{k}}$.

Appendix D. A derivation of the dilute solution (54) and (55)

In this appendix, we present the derivation of the effective shear modulus $\overline{\mu}^{\mathrm{dil}}$ and the effective first Lamé modulus $\overline{\Lambda}^{\mathrm{dil}}$ of an isotropic elastomer filled with a dilute volume fraction of spherical liquid inclusions of monodisperse radius A. For completeness, we do so for the general case when the bulk and interface moduli of elasticity are given by (20) and (28) and only at the end of the derivation we will choose $\Lambda_i = +\infty$, $\widehat{\mu} = \widehat{\Lambda} = 0$ to come to the expressions (54) and (55) given in the main body of the text.

In the footstep of a well-settled approach, we do not deal directly with the unit-cell problem (48) but, instead, consider the boundary-value problem of a body that occupies the spherical domain $\Omega_0 = \{\mathbf{X} : |\mathbf{X}| < B\}$, contains a single inclusion, and is subjected to the affine displacement boundary condition $\mathbf{u}(\mathbf{X}) = \overline{\mathbf{H}}\mathbf{X}$, $|\mathbf{X}| = B$. Precisely, the body is made of a single liquid inclusion of radius A whose center coincides with that of the body and is surrounded by the elastomer. In the notation of Section 2, the governing equations are thus given by

$$
\left\{\begin{array}{l}
\mathrm{Div}\left[\mu(\mathbf{X})(\nabla\mathbf{u}+\nabla\mathbf{u}^T) + \dfrac{2\widehat{\gamma}_0}{A}\theta_0^{\mathrm{i}}(\mathbf{X})\nabla\mathbf{u}^T + \left(\Lambda(\mathbf{X}) - \dfrac{2\widehat{\gamma}_0}{A}\theta_0^{\mathrm{i}}(\mathbf{X})\right)(\mathrm{tr}\,\nabla\mathbf{u})\mathbf{I}\right] = \mathbf{0}, \quad \mathbf{X}\in\Omega_0\setminus\Gamma_0\\
\widehat{\mathrm{Div}}\left[\widehat{\gamma}_0\widehat{\mathbf{I}} + \widehat{\gamma}_0\nabla\mathbf{u}\,\widehat{\mathbf{I}} + (\widehat{\mu}-\widehat{\gamma}_0)\left(\widehat{\mathbf{I}}\nabla\mathbf{u}\,\widehat{\mathbf{I}} + \widehat{\mathbf{I}}\nabla\mathbf{u}^T\widehat{\mathbf{I}}\right) + (\widehat{\Lambda}+\widehat{\gamma}_0)\mathrm{tr}\left(\widehat{\mathbf{I}}\nabla\mathbf{u}\,\widehat{\mathbf{I}}\right)\widehat{\mathbf{I}}\right] -\\
\left[\!\left[\mu(\mathbf{X})(\nabla\mathbf{u}+\nabla\mathbf{u}^T) + \dfrac{2\widehat{\gamma}_0}{A}\theta_0^{\mathrm{i}}(\mathbf{X})\nabla\mathbf{u}^T + \left(\Lambda(\mathbf{X}) - \dfrac{2\widehat{\gamma}_0}{A}\theta_0^{\mathrm{i}}(\mathbf{X})\right)(\mathrm{tr}\,\nabla\mathbf{u})\mathbf{I}\right]\!\right]\mathbf{X} = \mathbf{0}, \quad \mathbf{X}\in\Gamma_0\\
\mathbf{u}(\mathbf{X}) = \overline{\mathbf{H}}\mathbf{X}, \quad |\mathbf{X}| = B
\end{array}\right. ,
\tag{75}
$$

where $\Gamma_0 = \{\mathbf{X} : |\mathbf{X}| = A\}$ and $\theta_0^{\mathrm{i}}(\mathbf{X}) = 1$ if $|\mathbf{X}| < A$ and $\theta_0^{\mathrm{i}}(\mathbf{X}) = 0$ otherwise.

In the limit of separation of length scales as $c = A^3/B^3 \searrow 0$, the solution of the single-inclusion boundary-value problem (75) is expected to reduce (up to its periodic repetition) to the solution of the unit-cell problem (48) up to $O(c)$ and, in consequence, can be used to determine the effective modulus of elasticity $\overline{\mathbf{L}}$ of an isotropic elastomer filled with a dilute volume fraction of monodisperse spherical liquid inclusions up to $O(c)$; see, e.g., the works of Sanchez-Palencia (1985), Duerinckx and Gloria (2021), and references therein. The usefulness of the alternative problem (75) is that its solution can be expediently constructed in terms of spherical harmonics. The construction of the solution goes as follows.

Begin by noting that, thanks to the overall (geometric and constitutive) isotropy of the problem, it suffices to consider an affine "uniaxial strain", $\overline{\mathbf{H}} = \overline{H}_{33}\mathbf{e}_3\otimes\mathbf{e}_3$ say, and that for this boundary condition the displacement field

$$
\begin{aligned}
u_1(\mathbf{X}) &= \phi_1(|\mathbf{X}|)X_1 + \phi_3(|\mathbf{X}|)X_1X_3^2,\\
u_2(\mathbf{X}) &= \phi_1(|\mathbf{X}|)X_2 + \phi_3(|\mathbf{X}|)X_2X_3^2,\\
u_3(\mathbf{X}) &= \phi_2(|\mathbf{X}|)X_3 + \phi_3(|\mathbf{X}|)X_3^2
\end{aligned}
\tag{76}
$$

with

$$
\phi_1(|\mathbf{X}|) = \left\{\begin{array}{ll}
\dfrac{-3\alpha_1\Lambda_{\mathrm{m}}|\mathbf{X}|^5 - \alpha_3(5\mu_{\mathrm{m}}+3\Lambda_{\mathrm{m}}) + \alpha_6(\mu_{\mathrm{m}}+\Lambda_{\mathrm{m}})}{|\mathbf{X}|^3(\mu_{\mathrm{m}}+\Lambda_{\mathrm{m}})} - \alpha_2 + \dfrac{3\alpha_4}{2|\mathbf{X}|^5} + \alpha_5 & \text{if } \mathbf{X}\in\Omega_0^{\mathrm{m}}\\
-3\beta_1|\mathbf{X}|^2 - \beta_2 + \beta_5 & \text{if } \mathbf{X}\in\Omega_0^{\mathrm{i}}
\end{array}\right. ,
$$

$$
\phi_2(|\mathbf{X}|) = \left\{\begin{array}{ll}
\dfrac{3\alpha_1|\mathbf{X}|^5(7\mu_{\mathrm{m}}+4\Lambda_{\mathrm{m}}) + \alpha_3(\mu_{\mathrm{m}}-3\Lambda_{\mathrm{m}}) + \alpha_6(\mu_{\mathrm{m}}+\Lambda_{\mathrm{m}})}{|\mathbf{X}|^3(\mu_{\mathrm{m}}+\Lambda_{\mathrm{m}})} + 2\alpha_2 + \dfrac{9\alpha_4}{2|\mathbf{X}|^5} + \alpha_5 & \text{if } \mathbf{X}\in\Omega_0^{\mathrm{m}}\\
12\beta_1|\mathbf{X}|^2 + 2\beta_2 + \beta_5 & \text{if } \mathbf{X}\in\Omega_0^{\mathrm{i}}
\end{array}\right. ,
$$

$$\phi_3(|\mathbf{X}|)=\begin{cases}\dfrac{3}{2}\left(-\dfrac{2\alpha_1(7\mu_m+2\Lambda_m)}{\mu_m+\Lambda_m}+\dfrac{6\alpha_3}{|\mathbf{X}|^5}-\dfrac{5\alpha_4}{|\mathbf{X}|^7}\right) & \text{if } \mathbf{X}\in\Omega_0^m\\ -6\beta_1 & \text{if } \mathbf{X}\in\Omega_0^i\end{cases},$$

where α_1, α_2, α_3, α_4, α_5, α_6, β_1, β_2, β_5 are constants, satisfies automatically the equilibrium equation $(75)_1$.

Since the displacement field (76) must be continuous – that is, $[\![\mathbf{u}(\mathbf{X})]\!]=0$, $\mathbf{X}\in\Gamma_0$ – the constants α_1, α_2, α_3, α_4, α_5, α_6, β_1, β_2, β_5 are not independent from one another but satisfy the algebraic relations

$$\begin{cases}\frac{3\alpha_4}{A^5}+\frac{-\frac{4\alpha_3\mu_m}{\mu_m+\Lambda_m}-6\alpha_3+2\alpha_6}{A^3}+A^2\left(6\beta_1-\frac{6\alpha_1\Lambda_m}{\mu_m+\Lambda_m}\right)-2\alpha_2+2(\alpha_5+\beta_2-\beta_5)=0\\ -\frac{15\alpha_4}{A^7}+\frac{18\alpha_3}{A^5}+6\alpha_1\left(-\frac{5\mu_m}{\mu_m+\Lambda_m}-2\right)+12\beta_1=0\\ \frac{9\alpha_4}{A^5}+\frac{2(\alpha_3(\mu_m-3\Lambda_m)+\alpha_6(\mu_m+\Lambda_m))}{A^3(\mu_m+\Lambda_m)}+6A^2\left(\alpha_1\left(\frac{3\mu_m}{\mu_m+\Lambda_m}+4\right)-4\beta_1\right)+4\alpha_2+2\alpha_5-4\beta_2-2\beta_5=0\end{cases}. \tag{77}$$

Substitution of the displacement field (76) in the jump $(75)_2$ and boundary $(75)_3$ conditions yields the additional algebraic equations:

$$\begin{cases}-3A^7\alpha_1\mu_m\Lambda_m-6A^6\beta_1(\mu_m+\Lambda_m)(2\widehat{\gamma}_0-3(\widehat{\mu}+\widehat{\Lambda}))+A^5(\mu_m+\Lambda_m)(2\alpha_2\mu_m-2\alpha_5\mu_m-3\alpha_5\Lambda_m+3\beta_5\Lambda_1)-\\ 2A^4(\mu_m+\Lambda_m)(\beta_2(2\widehat{\gamma}_0-\widehat{\mu}-\widehat{\Lambda})+\beta_5(\widehat{\gamma}_0-2(\widehat{\mu}+\widehat{\Lambda})))+2A^2\mu_m(2\alpha_6(\mu_m+\Lambda_m)-\alpha_3(10\mu_m+9\Lambda_m))+\\ 12\alpha_4\mu_m(\mu_m+\Lambda_m)=0\\ A^7\alpha_1\mu_m(14\mu_m+19\Lambda_m)+4A^6\beta_1(\mu_m+\Lambda_m)(3\widehat{\gamma}_0-14\widehat{\mu}-9\widehat{\Lambda})-20\alpha_4\mu_m(\mu_m+\Lambda_m)+\\ 4A^4\beta_2(\mu_m+\Lambda_m)(\widehat{\gamma}_0-2\widehat{\mu}-\widehat{\Lambda})+24\alpha_3\mu_m(\mu_m+\Lambda_m)=0\\ -3A^7\alpha_1\mu_m(14\mu_m+17\Lambda_m)-12A^6\beta_1(\mu_m+\Lambda_m)(\widehat{\gamma}_0-11\widehat{\mu}-6\widehat{\Lambda})-A^5(\mu_m+\Lambda_m)(4\alpha_2\mu_m+2\alpha_5\mu_m+\\ 3\alpha_5\Lambda_m-3\beta_5\Lambda_i)-2A^4(\mu_m+\Lambda_m)(2\beta_2(\widehat{\gamma}_0-5\widehat{\mu}-2\widehat{\Lambda})+\beta_5(\widehat{\gamma}_0-2(\widehat{\mu}+\widehat{\Lambda})))+4A^2\mu_m(\alpha_6(\mu_m+\Lambda_m)-\\ \alpha_3(8\mu_m+9\Lambda_m))+36\alpha_4\mu_m(\mu_m+\Lambda_m)=0\\ \frac{-3\alpha_1B^5\Lambda_m-\alpha_3(5\mu_m+3\Lambda_m)+\alpha_6(\mu_m+\Lambda_m)}{B^3(\mu_m+\Lambda_m)}-\alpha_2+\frac{3\alpha_4}{2B^5}+\alpha_5=0\\ \alpha_1\left(-\frac{10\mu_m}{\mu_m+\Lambda_m}-4\right)+\frac{6\alpha_3}{B^5}-\frac{5\alpha_4}{B^7}=0\\ \frac{3\alpha_1B^5(7\mu_m+4\Lambda_m)+\alpha_3(\mu_m-3\Lambda_m)+\alpha_6(\mu_m+\Lambda_m)}{B^3(\mu_m+\Lambda_m)}+2\alpha_2+\frac{9\alpha_4}{2B^5}+\alpha_5-\overline{H}_{33}=0\end{cases}. \tag{78}$$

Combined, Eqs. (77) and (78) constitute a system of nine linear algebraic equations for the nine constants α_1, α_2, α_3, α_4, α_5, α_6, β_1, β_2, β_5, which can be readily solved in closed form; due to their bulkiness, we do not report their explicit solution here. These last results establish then that the displacement field (76) with the constants defined uniquely by the system of linear algebraic Eqs. (77)–(78) is the solution of the single-inclusion boundary-value problem (75).

Now, a standard calculation shows that the macroscopic stress (33) specializes in this case to

$$\overline{\mathbf{S}}=\overline{S}_{\text{lat}}(\mathbf{e}_1\otimes\mathbf{e}_1+\mathbf{e}_2\otimes\mathbf{e}_2)+\overline{S}\,\mathbf{e}_3\otimes\mathbf{e}_3$$

with

$$\overline{S}_{\text{lat}}=-\frac{42}{5}\alpha_1B^2\mu_m-2\alpha_2\mu_m+\alpha_3\left(\frac{2\mu_m^2}{B^3(\mu_m+\Lambda_m)}+\frac{18\mu_m}{5B^3}\right)+\alpha_5(2\mu_m+3\Lambda_m)-\frac{4\alpha_6\mu_m}{B^3}$$

and

$$\overline{S}=\frac{84}{5}\alpha_1B^2\mu_m+4\alpha_2\mu_m-\frac{4\alpha_3\mu_m(14\mu_m+9\Lambda_m)}{5B^3(\mu_m+\Lambda_m)}+\frac{\alpha_5\left(10B^3\mu_m+15B^3\Lambda_m\right)}{5B^3}-\frac{4\alpha_6\mu_m}{B^3}.$$

Since we also have

$$\overline{\mathbf{S}}=\overline{\mu}^{\text{dil}}\left(\overline{\mathbf{H}}+\overline{\mathbf{H}}^T\right)+\overline{\Lambda}^{\text{dil}}(\text{tr}\,\overline{\mathbf{H}})\mathbf{I}+O(c^2)$$

in the limit as $c=A^3/B^3\searrow 0$, we can finally deduce that

$$\overline{\mu}^{\text{dil}}=\frac{\overline{S}-\overline{S}_{\text{lat}}}{2\overline{H}_{33}}\qquad\text{and}\qquad\overline{\Lambda}^{\text{dil}}=\frac{\overline{S}_{\text{lat}}}{\overline{H}_{33}}$$

to $O(c)$ in the limit as $c\searrow 0$. For the basic case when $\Lambda_i=+\infty$, $\widehat{\mu}=\widehat{\Lambda}=0$, these equations yield the expressions (54) and (55) given in the main body of the text.

Appendix E. The hybrid set of governing equations (61)

The derivation of the hybrid Eqs. (61) goes as follows. Introduce the function

$$\Psi(\mathbf{X},\mathbf{F},\mathfrak{J})=W(\mathbf{X},\mathbf{F})\quad\text{when}\quad\mathfrak{J}=J=\det\mathbf{F}$$

alongside its partial Legendre transform

$$\Psi^\star(\mathbf{X},\mathbf{F},p)=\sup_{\mathfrak{J}}\left\{p(\mathfrak{J}-1)-\Psi(\mathbf{X},\mathbf{F},\mathfrak{J})\right\}. \tag{79}$$

Since $\Psi(\mathbf{X},\mathbf{F},\mathfrak{J})$ is convex in its third argument, it follows that

$$W(\mathbf{X},\mathbf{F})=\left(\Psi^\star\right)^\star(\mathbf{X},\mathbf{F},J)=\sup_{p}\left\{p(J-1)-\Psi^\star(\mathbf{X},\mathbf{F},p)\right\}.$$

It turn, it follows that the first Piola–Kirchhoff stress tensor (17) in the bulk can be rewritten in terms of the dual function (79) as

$$\mathbf{S}(\mathbf{X})=\frac{\partial W}{\partial\mathbf{F}}(\mathbf{X},\mathbf{F})=-\frac{\partial\Psi^\star}{\partial\mathbf{F}}(\mathbf{X},\mathbf{F},p)+pJ\mathbf{F}^{-T}\quad\text{with}\quad J-1-\frac{\partial\Psi^\star}{\partial p}(\mathbf{X},\mathbf{F},p)=0. \tag{80}$$

Making explicit use of the pointwise stored-energy function (15), we have that

$$\begin{aligned}\Psi^\star(\mathbf{X},\mathbf{F},p)=&-\frac{\mu(\mathbf{X})}{2}\left[\mathbf{F}\cdot\mathbf{F}-3\right]+\mu(\mathbf{X})\ln\left[\frac{\Lambda(\mathbf{X})-r_{\rm i}(\mathbf{X})+p+\sqrt{4\Lambda(\mathbf{X})\mu(\mathbf{X})+(\Lambda(\mathbf{X})-r_{\rm i}(\mathbf{X})+p)^2}}{2\Lambda(\mathbf{X})}\right]-\\&\frac{r_{\rm i}(\mathbf{X})+\mu(\mathbf{X})}{2}-\frac{1}{4}\left(\Lambda(\mathbf{X})+2p-\sqrt{\Lambda^2(\mathbf{X})+2\Lambda(\mathbf{X})(2\mu(\mathbf{X})-r_{\rm i}(\mathbf{X})+p)+(p-r_{\rm i}(\mathbf{X}))^2}\right)+\\&\frac{p-r_{\rm i}(\mathbf{X})}{4\Lambda(\mathbf{X})}\left(p-r_{\rm i}(\mathbf{X})+\sqrt{\Lambda^2(\mathbf{X})+2\Lambda(\mathbf{X})(2\mu(\mathbf{X})-r_{\rm i}(\mathbf{X})+p)+(p-r_{\rm i}(\mathbf{X}))^2}\right)\end{aligned}$$

and hence that (80) specializes to

$$\mathbf{S}(\mathbf{X})=\mu(\mathbf{X})\mathbf{F}+pJ\mathbf{F}^{-T}\quad\text{with}\quad J-1+\frac{\Lambda(\mathbf{X})+r_{\rm i}(\mathbf{X})-p-\sqrt{4\Lambda(\mathbf{X})\mu(\mathbf{X})+(\Lambda(\mathbf{X})-r_{\rm i}(\mathbf{X})+p)^2}}{2\Lambda(\mathbf{X})}=0.$$

Given this last result, the governing equations (61) characterizing the macroscopic response of filled elastomers with periodic microstructures are readily obtained.

References

Andreotti, B., Bäumchen, O., Boulogne, F., Daniels, K.E., Dufresne, E.R., Perrin, H., Salez, T., Snoeijer, J.H., Style, R.W., 2016. Solid capillarity: When and how does surface tension deform soft solids? Soft Matter 12, 2993–2996.

Avellaneda, M., 1987. Iterated homogenization, differential effective medium theory and applications. Comm. Pure Appl. Math. 40, 527–554.

Bartlett, M.D., Kazem, N., Powell-Palm, M.J., Huang, X., Sun, W., Malen, J.A., Majidi, C., 2017. High thermal conductivity in soft elastomers with elongated liquid metal inclusions. Proc. Natl. Acad. Sci. 114, 2143–2148.

Bensoussan, A., Lions, J.L., Papanicolau, G., 2011. Asymptotic Analysis for Periodic Structures. AMS Chelsea, Providence.

Bico, J., Reyssat, E., Roman, B., 2018. Elastocapillarity: When surface tension deforms elastic solids. Annu. Rev. Fluid Mech. 50, 629–659.

Boffi, D., Brezzi, F., Fortin, M., 2012. Mixed Finite Element Methods and Applications. Springer, New York.

Braides, A., 1985. Homogenization of some almost periodic coercive functional. Rend. Accad. Naz. Sci. XL Mem. Mat. Appl. (5) 103, 313–322.

Brinkman, H.C., 1952. The viscosity of concentrated suspensions and solutions. J. Chem. Phys. 20, 571–573.

Bruggeman, D.A.G., 1935. Berechnung verschiedener physikalischer konstanten von heterogenen substanzen. I. Dielektrizitätskonstanten und leitfähigkeiten der mischkörper aus isotropen substanzen [Calculation of various physical constants in heterogeneous substances. I. Dielectric constants and conductivity of composites from isotropic substances]. Ann. Physics 416, 636–664.

do Carmo, M.P., 2016. Differential Geometry of Curves and Surfaces. Dover.

Christensen, R.M., Lo, K.M., 1979. Solutions for effective shear properties in three-phase sphere and cylinder models. J. Mech. Phys. Solids 27, 315–330.

Duan, H.L., Wang, J., Huang, Z.P., Karihaloo, B.L., 2005a. Eshelby formalism for nano-inhomogeneities. Proc. R. Soc. Lond. Ser. A Math. Phys. Eng. Sci. 461, 3335–3353.

Duan, H.L., Wang, J., Huang, Z.P., Karihaloo, B.L., 2005b. Size-dependent effective elastic constants of solids containing nano-inhomogeneities with interface stress. J. Mech. Phys. Solids 53, 1574–1596.

Duerinckx, M., Gloria, A., 2021. On Einstein's effective viscosity formula. arXiv:2008.03837.

Geymonat, G., Müller, S., Triantafyllidis, N., 1993. Homogenization of nonlinearly elastic materials, microscopic bifurcation and macroscopic loss of rank-one convexity. Arch. Ration. Mech. Anal. 122, 231–290.

Ghosh, K., Lefèvre, V., Lopez-Pamies, O., 2022 Homogenization of elastomers filled with liquid inclusions: The small-deformation limit. (submitted for publication).

Girault, V., Raviart, P.-A., 1986. Finite Element Methods for Navier–Stokes Equations. Theory and Algorithms. Berlin.

Goudarzi, T., Spring, D.W., Paulino, G.H., Lopez-Pamies, O., 2015. Filled elastomers: A theory of filler reinforcement based on hydrodynamic and interphasial effects. J. Mech. Phys. Solids 80, 37–67.

Gurtin, M.E., Murdoch, A.I., 1975a. Addenda to our paper a continuum theory of elastic material surfaces. Arch. Ration. Mech. Anal. 59, 1–2.

Gurtin, M.E., Murdoch, A.I., 1975b. A continuum theory of elastic material surfaces. Arch. Ration. Mech. Anal. 57, 291–323.

Gurtin, M.E., Weissmüller, J., Larché, F., 1998. A general theory of curved deformable interfaces in solids at equilibrium. Phil. Mag. A 78, 1093–1109.

Gusev, A.A., 1997. Representative volume element size for elastic composites: A numerical study. J. Mech. Phys. Solids 45, 1449–1459.

Healey, T.J., Simpson, H.C., 1998. Global continuation in nonlinear elasticity. Arch. Ration. Mech. Anal. 143, 1–28.

Hill, R., 1972. On constitutive macrovariables for heterogeneous solids at finite strain. Proc. R. Soc. Lond. Ser. A Math. Phys. Eng. Sci. 326, 131–147.

Javili, A., McBride, A., Steinmann, P., 2013. Thermomechanics of solids with lower-dimensional energetics: On the importance of surface, interface, and curve structures at the nanoscale. A unifying review. Appl. Mech. Rev. 65, 010802.

Kenmotsu, K., 2003. Surfaces with Constant Mean Curvature. American Mathematical Society, Providence.

Krichen, S., Liu, L., Sharma, P., 2019. Liquid inclusions in soft materials: Capillary effect, mechanical stiffening and enhanced electromechanical response. J. Mech. Phys. Solids 127, 332–357.

Lefèvre, V., Danas, K., Lopez-Pamies, O., 2017. A general result for the magnetoelastic response of isotropic suspensions of iron and ferrofluid particles in rubber, with applications to spherical and cylindrical specimens. J. Mech. Phys. Solids 107, 343–364.

Lefèvre, V., Francfort, G.A., Lopez-Pamies, O., 2022 The curious case of 2D isotropic incompressible Neo-Hookean composites. (submitted for publication).

Lefèvre, V., Lopez-Pamies, O., 2017a. Nonlinear electroelastic deformations of dielectric elastomer composites: I — Ideal elastic dielectrics. J. Mech. Phys. Solids 99, 409–437.
Lefèvre, V., Lopez-Pamies, O., 2017b. Nonlinear electroelastic deformations of dielectric elastomer composites: II — Non-Gaussian elastic dielectrics. J. Mech. Phys. Solids 99, 438–470.
Lefèvre, V., Lopez-Pamies, O., 2022 The effective shear modulus of a random isotropic suspension of monodisperse rigid n-spheres: From the dilute limit to the percolation threshold. (submitted for publication).
Lopez-Pamies, O., 2014. Elastic dielectric composites: Theory and application to particle-filled ideal dielectrics. J. Mech. Phys. Solids 64, 61–82.
Lopez-Pamies, O., Goudarzi, T., Danas, K., 2013a. The nonlinear elastic response of suspensions of rigid inclusions in rubber: II — A simple explicit approximation for finite-concentration suspensions. J. Mech. Phys. Solids 61, 19–37.
Lopez-Pamies, O., Goudarzi, T., Nakamura, T., 2013b. The nonlinear elastic response of suspensions of rigid inclusions in rubber: I — An exact result for dilute suspensions. J. Mech. Phys. Solids 61, 1–18.
Lubachevsky, B.D., Stillinger, F.H., Pinson, E.N., 1991. Disks vs. spheres: Contrasting properties of random packings. J. Stat. Phys. 64, 501–523.
Mancarella, F., Style, R.W., Wettlaufer, J.S., 2016. Interfacial tension and a three-phase generalized self-consistent theory of non-dilute soft composite solids. Soft Matter 12, 2744–2750.
Michel, J.C., Lopez-Pamies, O., Ponte Castañeda, P., Triantafyllidis, N., 2010. Microscopic and macroscopic instabilities in finitely strained fiber-reinforced elastomers. J. Mech. Phys. Solids 58, 1776–1803.
Müller, S., 1987. Homogenization of nonconvex integral functionals and cellular elastic materials. Arch. Ration. Mech. Anal. 99, 189–212.
Norris, A., 1985. A differential scheme for the effective moduli of composites. Mech. Mater. 4, 1–16.
Ogden, R.W., 1974. On the overall moduli of non-linear elastic composite materials. J. Mech. Phys. Solids 22, 541–553.
Popinet, S., 2018. Numerical models of surface tension. Annu. Rev. Fluid Mech. 50, 49–75.
Roscoe, R., 1952. The viscosity of suspensions of rigid spheres. Br. J. Appl. Phys. 3, 267–269.
Roscoe, R., 1973. Isotropic composites with elastic or viscoelastic phases: General bounds for the moduli and solutions for special geometries. Rheol. Acta 12, 404–411.
Sanchez-Palencia, E., 1985. Einstein-like approximation for homogenization with small concentration. I — Elliptic problems. Nonlinear Anal. 9, 1243–1254.
Schöberl, J., 1997. NETGEN an advancing front 2D/3D-mesh generator based on abstract rules. Comput. Vis. Sci. 1, 41–52.
Scott, G.D., 1960. Packing of spheres: Packing of equal spheres. Nature 188, 908–909.
Sharma, P., Ganti, S., 2004. Size-dependent Eshelby's tensor for embedded nano-inclusions incorporating surface/interface energies. J. Appl. Mech. 71, 663–671.
Sharma, P., Ganti, S., Bhate, N., 2003. Effect of surfaces on the size-dependent elastic state of nano-inhomogeneities. Appl. Phys. Lett. 82, 535–537.
Spinelli, S.A., Lefèvre, V., Lopez-Pamies, O., 2015. Dielectric elastomer composites: A general closed-form solution in the small-deformation limit. J. Mech. Phys. Solids 83, 263–284.
Style, R.W., Boltyanskiy, R., Benjamin, A., Jensen, K.E., Foote, H.P., Wettlaufer, J.S., Dufresne, E.R., 2015a. Stiffening solids with liquid inclusions. Nat. Phys. 11, 82–87.
Style, R.W., Wettlaufer, J.S., Dufresne, E.R., 2015b. Surface tension and the mechanics of liquid inclusions in compliant solids. Soft Matter 11, 672–679.
Wang, Y., Henann, D.L., 2016. Finite-element modeling of soft solids with liquid inclusions. Extreme Mech. Lett. 9, 147–157.
Wang, C.-C., Truesdell, C., 1973. Introduction to Rational Elasticity. Noordhoff International, Leyden.
Weatherburn, C.E., 2016. Differential Geometry of Three Dimensions. Cambridge University Press.
Yavari, A., Golgoon, A., 2019. Nonlinear and linear elastodynamic transformation cloaking. Arch. Ration. Mech. Anal. 234, 211–316.
Yun, G., Tang, S.Y., Sun, S., Yuan, D., Zhao, Q., Deng, L., Yan, S., Du, H., Dickey, M.D., Li, W., 2019. Liquid metal-filled magnetorheological elastomer with positive piezoconductivity. Nature Commun. 10, 1300.
Zafar, M.R., Basu, S., 2022. Stiffness and toughness of soft, liquid reinforced composites. J. Mech. Phys. Solids 159, 104714.